

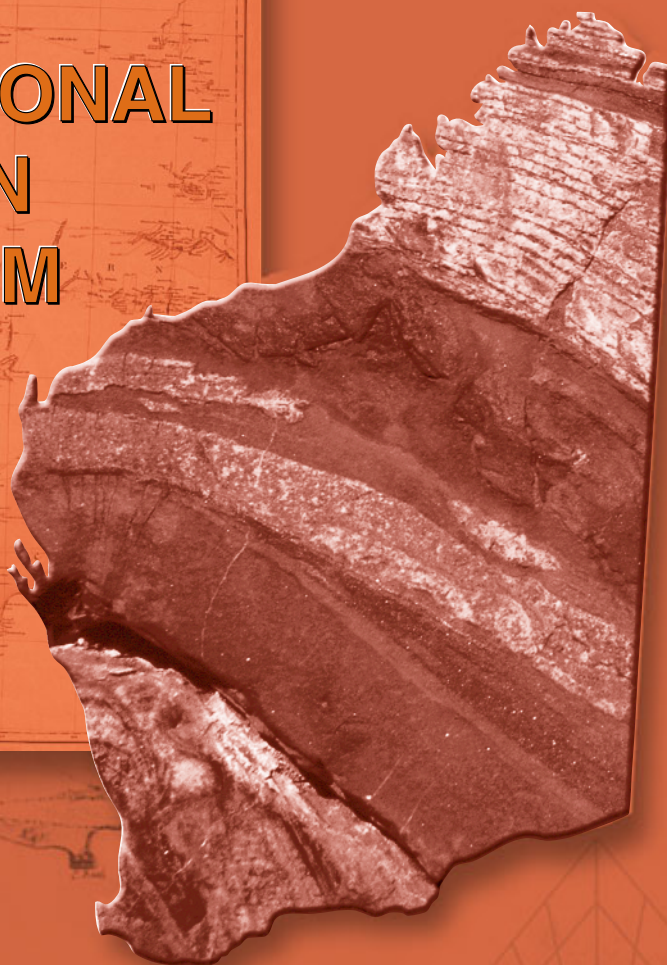
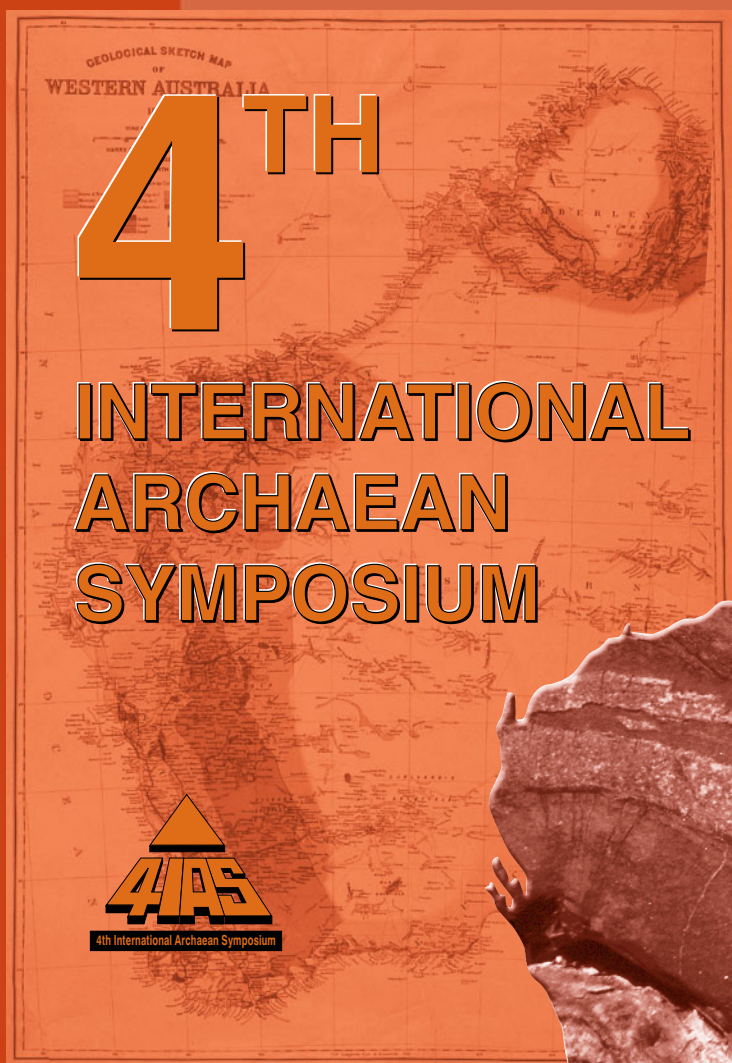


Department of Mineral and
Petroleum Resources

**RECORD
2001/11**

METALLOGENESIS OF THE NORTH PILBARA GRANITE–GREENSTONES WESTERN AUSTRALIA— A FIELD GUIDE

**by D. L. Huston, R. S. Blewett, M. Sweetapple, C. Brauhart,
H. Cornelius, and P. L. F. Collins**



Geological Survey of Western Australia



GEOLOGICAL SURVEY OF WESTERN AUSTRALIA

Record 2001/11

METALLOGENESIS OF THE NORTH PILBARA GRANITE–GREENSTONES, WESTERN AUSTRALIA — A FIELD GUIDE

by

**D. L. Huston¹, R. S. Blewett¹, M. Sweetapple², C. Brauhart³,
H. Cornelius⁴, and P. L. F. Collins²**

¹ AGSO – Geoscience Australia

² Mineral Deposits and Exploration Research Group, School of Applied Geology,
Curtin University of Technology, Western Australia

³ Sipa–Gaia Resources Ltd

⁴ Sons of Gwalia Ltd

Perth 2001

MINISTER FOR STATE DEVELOPMENT
Hon. Clive Brown MLA

DIRECTOR GENERAL
DEPARTMENT OF MINERAL AND PETROLEUM RESOURCES
Jim Limerick

DIRECTOR, GEOLOGICAL SURVEY OF WESTERN AUSTRALIA
Tim Griffin

Notice to users of this guide:

This field guide is one of a series published by the Geological Survey of Western Australia (GSWA) for excursions conducted as part of the 4th International Archaean Symposium, held in Perth on 24–28 September 2001. Authorship of these guides included contributors from AGSO, CSIRO, tertiary academic institutions, and mineral exploration companies, as well as GSWA. Editing of manuscripts was restricted to bringing them into GSWA house style. The scientific content of each guide, and the drafting of the figures, was the responsibility of the authors.

REFERENCE

The recommended reference for this publication is:

HUSTON, D. L., BLEWETT, R. S., SWEETAPPLE, M., BRAUHART, C., CORNELIUS, H., and COLLINS, P. L. F., 2001, Metallogensis of the north Pilbara granite–greenstones, Western Australia — a field guide: Western Australia Geological Survey, Record 2001/11, 87p.

National Library of Australia Card Number and ISBN 0 7307 5699 8

Grid references in this publication refer to either the Geocentric Datum of Australia 1994 (GDA94), with locations referenced using Map Grid Australia (MGA) coordinates, Zone 50, or the Australian Geodetic Datum 1966 (AGD66), with locations referenced using Australian Map Grid (AMG) coordinates, Zones 50 and 51. All locations are quoted to at least the nearest 100 m.

Printed by Image Source, Perth, Western Australia

Published 2001 by Geological Survey of Western Australia

Copies available from:

Information Centre
Department of Mineral and Petroleum Resources
100 Plain Street
EAST PERTH, WESTERN AUSTRALIA 6004
Telephone: (08) 9222 3459 Facsimile: (08) 9222 3444

This and other publications of the Geological Survey of Western Australia are available online through dme.bookshop at www.dme.wa.gov.au

Contents

Introduction	1
Geology of the north Pilbara granite–greenstones	2
The East Pilbara Granite–Greenstone Terrane	2
The West Pilbara Granite–Greenstone Terrane	5
The Central Pilbara Tectonic Zone	5
The Fortescue Group	6
Mineralizing events affecting the north Pilbara granite–greenstones	6
The East Pilbara Granite–Greenstone Terrane	6
The West Pilbara Granite–Greenstone Terrane	8
The Central Pilbara Tectonic Zone	9
The Fortescue Group	9
Part one: Deposits of the West Pilbara Granite–Greenstone Terrane	10
Geology of the West Pilbara Granite–Greenstone Terrane	10
The Roebourne Group	10
The Whundo Group	10
Granitoids	10
Layered mafic intrusions	12
Structure	12
The Radio Hill deposit	12
The Whundo deposit	15
The Elizabeth Hill deposit	16
Excursion localities	16
Locality 1.1: Radio Hill layered intrusion	16
Locality 1.2: Radio Hill mine	18
Locality 1.3: Structure of the Yanerry Hill copper deposit	18
Locality 1.4: The Whundo copper–zinc deposit	18
Locality 1.5: The Elizabeth Hill silver deposit	19
Part two: The Mons Cupri copper–zinc–lead and Balla Balla vanadium–titanium deposits	20
Geology of the Whim Creek greenstone belt and Caines Well Granitoid Complex	20
Geology of the Mons Cupri deposit	22
Mons Cupri Volcanics	22
Cistern Formation	22
Lower Cistern conglomerate	22
Upper Cistern arkose	22
Rushall Slate	24
Local structure	24
Base metal mineralization	25
Excursion localities	27
Locality 2.1: Caines Well Granitoid Complex	27
Locality 2.2: Traverse through Warambie Basalt and Mount Brown Rhyolite Member	27
Locality 2.3: Cistern Formation	28
Locality 2.4: Silicified Mons Cupri epiclastic rocks with disseminated sulfide	28
Locality 2.5: Altered Mount Brown Rhyolite Member	28
Locality 2.6: Mons Cupri deposit	28
Locality 2.7: Alteration of the Comstock Member	29
Locality 2.8: Traverse through Cistern Formation north of the graben-bounding fault	29
Locality 2.9: ‘Northwest Pits’ prospect	30
Locality 2.10: The Balla Balla vanadium deposit	30
Part three: Lode-gold–antimony and epithermal deposits of the Indee district	31
Geology of the Indee district	31
Structural history	32
aD_1 deformation	32
aD_2 deformation	32
aD_3 deformation	32
aD_4 deformation	32
Extension	33
aD_5 deformation	33
Faults	33
Mineral deposits	33
Withnell deposit	33
Peawah deposit	35
Becher deposit	35

Excursion localities	35
Locality 3.1: Mallina Shear Zone at Peawah River crossing	35
Locality 3.2: Peawah prospect	37
Locality 3.3: Roberts Hill	39
Locality 3.4: Hill south of Withnell prospect	39
Locality 3.5: Becher prospect	39
Locality 3.6: Drillcore inspection	40
Part four: The Wodgina tantalum–tin pegmatite district	41
Introduction	41
Exploration and mining history of the area	41
Production and resources since 1988	44
Mining operations	45
Geological setting	45
Wodgina greenstone belt	45
Host rocks and structure of the Wodgina pegmatite district	45
The Wodgina main-lode pegmatite	46
Geological overview	46
Mineralization	46
The Mount Cassiterite pegmatite group	47
Geological overview	47
Mineralization	53
Discussion	53
Excursion localities	54
Locality 4.1A: Wodgina South pit	54
Locality 4.1B: Wodgina North pit, east wall of ramp	55
Locality 4.2A: Mount Cassiterite pit lookout	55
Locality 4.2B: Mount Cassiterite pit floor	56
Locality 4.2C: Core shed	56
Locality 4.3: Processing plant	58
Locality 4.4: Unconformity at Strelley Pool	58
Part five: The Panorama volcanic-hosted massive sulfide district	59
Introduction	59
Regional hydrothermal alteration system	59
Volcanic-hosted massive sulfide deposits	63
Excursion localities	67
Locality 5.1: Sulphur Springs gossan, footwall dacite, and marker chert	67
Locality 5.2: Feldspar–sericite–quartz-altered andesite–basalt	67
Locality 5.3: Background and chlorite–quartz-altered andesite–basalt	67
Locality 5.4: Reaction zone	67
Locality 5.5: Subvolcanic intrusion	69
Locality 5.6: Granite-hosted semi-massive sulfide vein	69
Locality 5.7: Sulphur Springs Creek	69
Locality 5.8: Drillcore inspection	69
Part six (Option A): The Warrawoona lode-gold district	70
Structural geology and models of Archaean tectonics	70
Alternative tectonic model	73
Excursion localities	74
Locality 6A.1: Gauntlet mine	74
Locality 6A.2: Mullan zone adit	75
Locality 6A.3: Klondyke Queen mine	75
Part six (Option B): The Lennons Find volcanic-hosted massive sulfide district	76
Local stratigraphy	76
Mineralization	76
The Hammerhead zone	78
Alteration	78
Excursion localities	78
Locality 6B.1: Contact between Mount Edgar Batholith and felsic schists at base of Duffer Formation	78
Locality 6B.2: Metasedimentary rocks	79
Locality 6B.3: Hammerhead zone	79
Locality 6B.4: Tiger zone and Apex Basalt	79
Locality 6B.5: Grey Nurse zone	80
Locality 6B.6: Barite lens at the contact between the Duffer Formation and Apex Basalt	80
Acknowledgements	81
References	82

Appendix

Rare-metal minerals in pegmatites of the Wodgina district	87
---	----

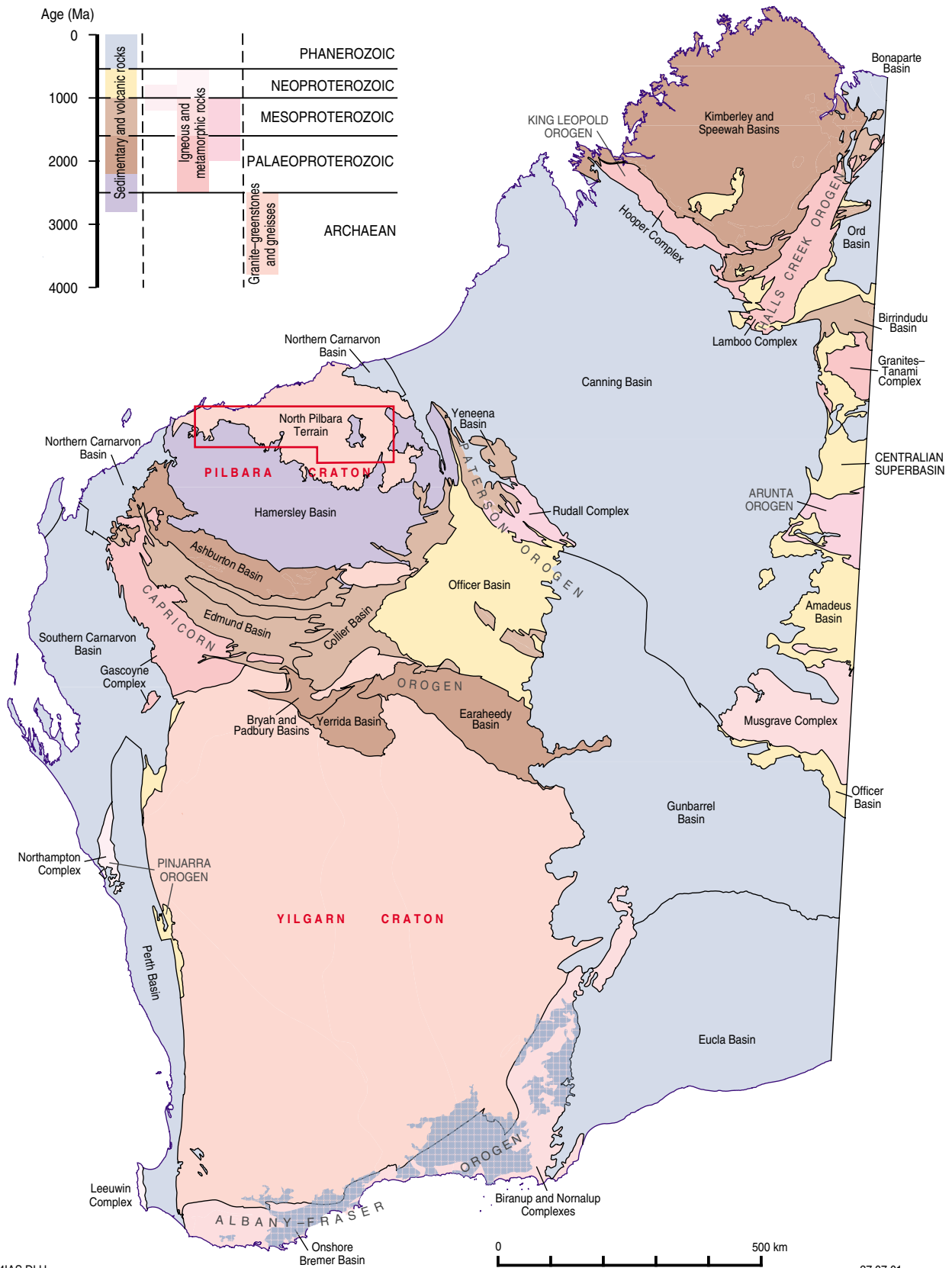
Figures

1.	Solid geology of the north Pilbara granite–greenstones showing the location of areas visited	3
2.	Geological history and mineralizing events affecting the constituent parts of the Pilbara Craton	7
3.	Geology of the West Pilbara Granite–Greenstone Terrane	11
4.	Geology of the southeastern part of the West Pilbara Granite–Greenstone Terrane showing the location of the Radio Hill, Whundo, and Elizabeth Hill deposits	13
5.	Surface geology of the Radio Hill nickel–copper–PGE deposit showing excursion localities	14
6.	Cross section through the Radio Hill deposit showing relationships to the Radio Hill complex and host rocks	15
7.	Surface geology of the Whundo copper–zinc deposit	17
8.	Geology of part of the Central Pilbara Tectonic Zone showing the locations of the Mons Cupri, Balla Balla, Peawah, Withnell, and Becher deposits	21
9.	Geology of the Mons Cupri area showing excursion localities	23
10.	Rock relationships and textures in the Mons Cupri area	24
11.	Cross section of the Mons Cupri deposit	25
12.	Graphical log of diamond drillhole MSD005 illustrating variations in lithology, alteration facies, and mineralization	26
13.	Geology of part of the Central Pilbara Tectonic Zone showing the location of excursion localities	31
14.	Rocks of the Indee district	34
15.	Graphical log of drillhole INDD003, Withnell deposit	36
16.	Geology of the Becher deposit	38
17.	Geological map of the Wodgina greenstone belt showing distribution of pegmatite fields or groups	42
18.	Geological plan of the Wodgina pegmatite district showing the location of opencuts	43
19.	Cross section 10930N (looking north) at Wodgina pit	48
20.	Representative stratigraphic column of rocks exposed in the Wodgina South pit	50
21.	Long section of the upper and main sheets of the Mount Cassiterite pegmatite along 10780E, showing RC drillhole intercepts	51
22.	Cross section showing the outline of the upper, main, and basal sheets of the Mount Cassiterite pegmatite group along 20500N, together with drillhole traces	52
23.	Schematic stratigraphic column showing the textural and compositional nature of the uppermost pegmatite sheet in the west wall of the Mount Cassiterite pit	57
24.	Geology of the Panorama volcanic-hosted massive sulfide district	60
25.	Distribution of alteration facies at the Panorama volcanic-hosted massive sulfide district	61
26.	Variations in mass changes of copper and zinc in the Panorama volcanic-hosted massive sulfide district	62
27.	Panorama volcanic-hosted massive sulfide district	64
28.	Cross section of the Sulphur Springs volcanic-hosted massive sulfide deposit	65
29.	Plan and cross section of the Kangaroo Caves volcanic-hosted massive sulfide deposit	66
30.	Geological map of the Sulphur Springs area showing excursion localities	68
31.	Simplified geological map of the Warrawoona district and location of the Klondyke deposit	71
32.	Structures developed in the Warrawoona belt	72
33.	Geology of the Lennons Find area showing excursion localities	77

Tables

1.	Summary structural correlation table for the east, central, and west Pilbara	4
2.	Correlation of local deformation histories with regional framework	5
3.	Gold production and resources of the north Pilbara granite–greenstones based on host rock	8
4.	Tantalum indicated resources and proven and probable reserves within the Mount Cassiterite pegmatite group	41
5.	Production figures from the Wodgina and Mount Cassiterite orebodies to June 1998	44
6.	Tantalum–tin–niobium mineral assemblages observed in different pegmatite groups	47
7.	Mineralogical units within the Wodgina main-lode pegmatite	55

Record 2001/11
North Pilbara Metallogeny Excursion



Metallogenesis of the north Pilbara granite–greenstones, Western Australia — a field guide

by

**D. L. Huston¹, R. S. Blewett¹, M. Sweetapple², C. Brauhart³,
H. Cornelius⁴, and P. L. F. Collins²**

Introduction

Compared with the Yilgarn Craton to the south, the north Pilbara granite–greenstones in northwestern Western Australia are not well mineralized. However, based on diversity and age of the mineral deposits, these granite–greenstones are unparalleled by any other Archaean craton. The north Pilbara granite–greenstones contain the oldest ore deposit known in the world. Paradoxically, this deposit, with an age of around 3490 Ma, is a barite deposit, a type more typical of Phanerozoic than Archaean terranes.

In addition to this deposit, the north Pilbara granite–greenstones also contain the oldest volcanic-hosted massive sulfide (VHMS; 3470 Ma), lode-gold (3420 Ma), porphyry copper–molybdenum (3320 Ma), komatitite-hosted nickel–copper (3270 Ma), iron (3200–3000 Ma), layered mafic-intrusion-hosted nickel–copper–PGE (platinum group element; 2920 Ma), tantalum–tin pegmatite (2880 Ma), and epithermal (2750 Ma) deposits in the world. Many of the deposit types present in the north Pilbara granite–greenstones are rare in other Archaean terranes, and even the more common deposits have unusual characteristics for the Archaean (e.g. barite and lead in the VHMS deposits). In fact, many of the deposits and characteristics observed in the Pilbara are more characteristic of Phanerozoic terranes.

The purpose of this six-day excursion is to illustrate the variety of deposits in the northern Pilbara and to discuss their important regional and temporal controls. Deposits to be visited include layered mafic-intrusion-hosted nickel–copper–PGE and vanadium–titanium deposits, a silver–PGE vein deposit, VHMS and other stratabound copper–zinc–lead deposits, lode-gold(–antimony) deposits, an epithermal deposit, and a tantalum–tin pegmatite deposit. Many of the deposits visited are the oldest known examples of their type.

¹ AGSO – Geoscience Australia, GPO Box 378, Canberra, A.C.T. 2601.

² Mineral Deposits and Exploration Research Group, School of Applied Geology, Curtin University of Technology, GPO Box U 1987, Perth, W.A. 6845.

³ Sipa–Gaia Resources Ltd, PO Box 1183, West Perth, W.A. 6872.

⁴ Sons of Gwalia Ltd, PMB 16, West Perth, W.A. 6872.

Geology of the north Pilbara granite–greenstones

The north Pilbara granite–greenstones have had a long and active geological history; the oldest supracrustal rock being older than 3515 Ma and the youngest granitoid 2765 Ma (Nelson et al., 1999). Xenocrystic and detrital zircons older than 3700 Ma are also known (Thorpe et al., 1992a; Nelson, 1999), suggesting a much longer history. Hickman (1999) subdivided the north Pilbara granite–greenstones into three lithotectonic elements, each having separate geological histories that partly overlap, particularly after 2900 Ma:

1. The East Pilbara Granite–Greenstone Terrane (EPGGT);
2. The Central Pilbara Tectonic Zone (CPTZ);
3. The West Pilbara Granite–Greenstone Terrane (WPGGT; Fig. 1).

The north Pilbara granite–greenstones are covered by regional geophysical datasets. Magnetic, gravity, terrain, and gamma-ray spectrometric images, along with interpretation maps and plots of mineral deposits provide a critical view of this most fascinating province (Blewett et al., 2000). Low resolution images of these datasets are available for viewing and printing on the Australian Geological Survey Organisation (AGSO) website (www.agso.gov.au/minerals/pilbara/atlas).

The following description draws on data presented by Hickman (1983, 1984, 1997), Pidgeon (1984), Williams and Collins (1990), Arndt et al. (1991), Buick et al. (1995, in press), Nelson (1997, 1998, 1999, 2000), Barley et al. (1998), Smith et al. (1998), Sun and Hickman (1999), Van Kranendonk and Morant (1998), Witt et al. (1998), Smithies et al. (1999), Nelson et al. (1999), Blewett (2000a,b), Blewett et al. (2000), Sweetapple (2000), and Pike and Cas (in press).

Table 1 is a summary structural correlation for granite–greenstone terranes of the east, central, and west Pilbara based on the interpretations of Blewett (2000a). In the discussion about local areas, their local deformation histories are described. These are prefixed with an *italic* letter (e.g. *hD*₁ for the first deformation of the rocks in the Whundo Group). Table 2 facilitates the correlation of the local deformation histories with the regional framework of Blewett (2000a). Van Kranendonk (2000) and Hickman (2001) presented alternative interpretations of the structural history of selected parts of the north Pilbara granite–greenstones.

The East Pilbara Granite–Greenstone Terrane

The EPGGT has the longest and most diverse history of the north Pilbara granite–greenstones. The oldest preserved unit is the c. 3515 Ma Coonterunah Group, which consists mainly of mafic volcanic and mafic-derived volcanoclastic rocks. The Coonterunah Group is unconformably overlain by mafic and local felsic volcanic rocks of the 3480–3410 Ma Warrawoona Group. The Warrawoona Group is overlain by felsic volcanic rocks and intrusions of the 3330–3310 Ma Wyman Formation. Younger units form the 3240 Ma Sulphur Springs Group, which contains ultramafic to felsic volcanic rocks. This unit is overlain by the Gorge Creek Group, a mainly turbiditic succession with a probable age slightly younger than the Sulphur Springs Group. Aside from the 3020 Ma Cleaverville Formation along the western margin, and the 2950 Ma De Grey Group (including the Mosquito Creek Group in the far southeast), the Gorge Creek Group is the youngest major supracrustal unit in the EPGGT.

The EPGGT contains large (up to 100 km diameter) polyphase granitoid domes, with the supracrustal rocks forming synclines between the domes (Fig. 1). Emplacement of these plutonic bodies commonly extended over several hundred million years, with most intrusive phases corresponding to active volcanism in the supracrustal rocks. The

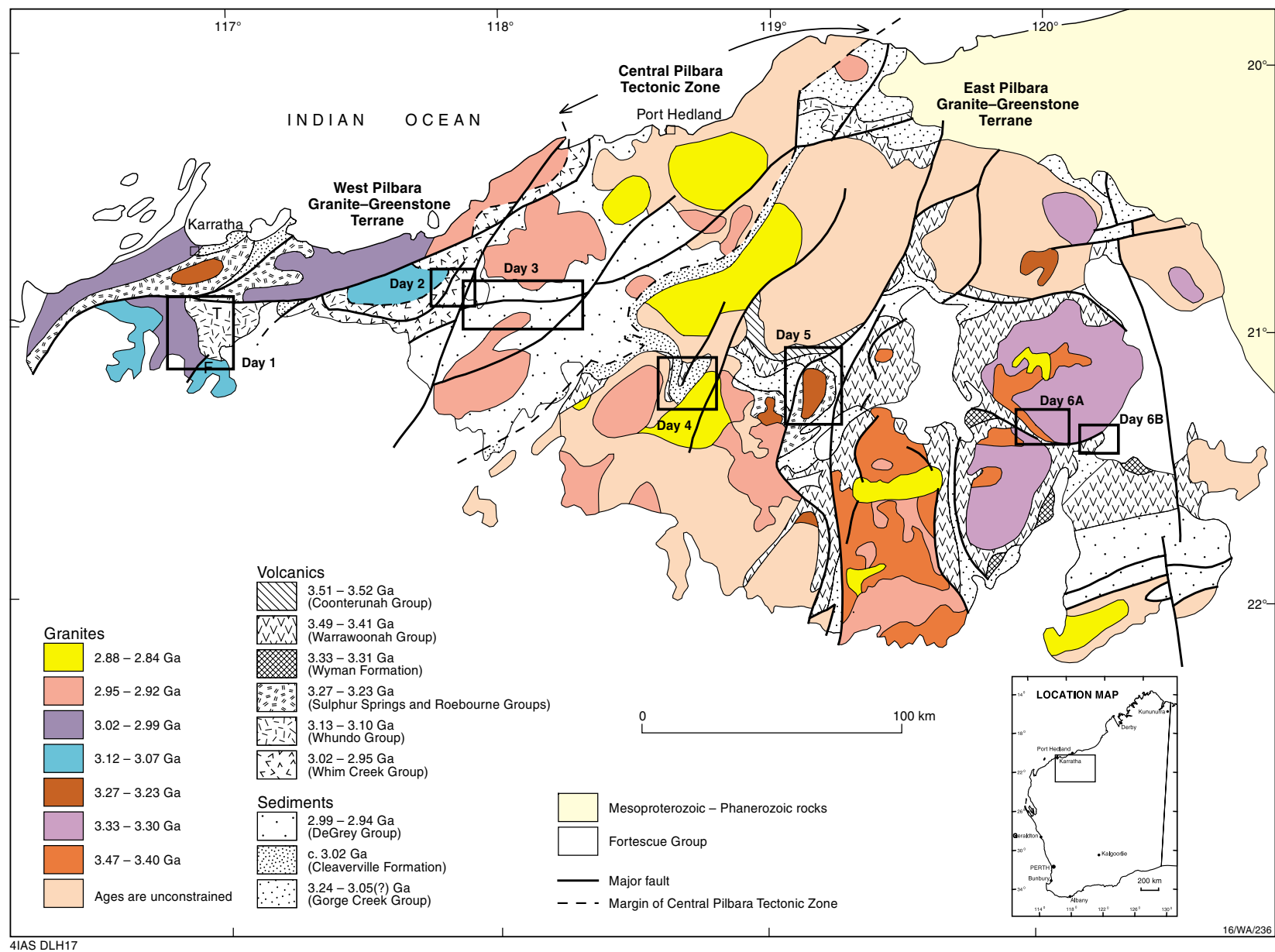


Figure 1. Solid geology of the north Pilbara granite–greenstones showing the location of areas visited

Table 1. Summary structural correlation table for the east, central, and west Pilbara (after Blewett, 2000a)

<i>Deformation event</i>	<i>Timing (Ma)</i>	<i>West and central Pilbara</i>	<i>East Pilbara</i>
D ₁	3515–3471	Basement not exposed	Tight folds and axial-planar schistosity, steep E dip (pre-refolding) in Coonterunnah Group; bedding-parallel fabric in Talga–Talga
D _{2a}	?3445–3380	Basement not exposed	Main schistose fabric and isoclinal folds in Warrawoona Group, variable trends now envelopes post-D _{2a} granitoid complexes; E-striking foliation in later crenulation (S _{2b}); Talga–Talga anticline
D _{2b}	3380 – >3330	Basement not exposed	Shear zones West Coongan Belt; Southern Mount Edgar Belt mylonites; thrusting Coppin Gap; N-striking crenulation cleavage in Warrawoona Belt
D _{2c}	c. 3325	Basement not exposed	Main shear fabric in Warrawoona Belt; metamorphic zircon in Mount Edgar
D _{2d}	3260	Isoclinal and rootless S-verging folds; E-NE plunging folds cut by Harding Granite (3260 Ma); S-directed thrusts	Not known
D _{3a}	c. ?3200	Lower amphibolite metamorphism, Roebourne Group; horizontal asymmetrical layer-parallel faults; ‘doming’ of Karratha Granodiorite	NNE to NE folds and fabric in Wodgina, NORTH SHAW; Tambourah Dome folds; folding; isoclinal folds (Yarrie); NE-trending crenulations and folds in older groups
D _{3b}	c. ?3100	Earliest fabric preserved in microlithons of later fabrics; 3107 Ma metamorphism	Not known
D _{3c}	c. 3015	NNW–SSE folds; sinistral transtension on Sholl SZ; early melange development in Cleaverville Formation. Main NW-trending greenschist to amphibolite schistosity to crenulation cleavage in Whundo Group	NW-trending steeply dipping crenulation in Wodgina and Pilgangoora Belts; NW-plunging folds at Yarrie
D _{4a} progressive	c. 3000–2950	NE-plunging tight upright folds that verge south, crenulation cleavage; S-directed thrusting Sholl SZ. NE-plunging tight upright folds & crenulation cleavage (Whundo); ENE folds with N-dipping cleavage (Mallina)	E–W crenulations; sinistral N–S-oriented shear zones (e.g. West Wodgina); reworking main fabric to a crenulation or shear bands; Mosquito Creek ENE plunging S-verging folds
D _{4b}	<2950	Normal sinistral shear on Sholl SZ, NW plunging lineations; NNE crenulations; sinistral shear zones; NNW folds and crenulation (Whundo); N–S upright folds and steep slaty cleavage; pencil-cleavage intersection (Mallina)	N–S crenulations of D ₄ shear zones (Wodgina); N–S upright folds (Pilgangoora); sinistral N–S shear (Pilgangoora); dextral shear zones (E–W) Mosquito Creek belt, Kurrana SZ
D _{4c}	2935–2880	Dextral shear on Sholl SZ (40 km) with gentle E-NE-plunging lineations; NE to ENE tight folds, steeply inclined with SE-dipping axial surface; reworked composite fabric (ENE trend) in Mallina Basin	ENE-trending moderate N-dipping crenulations; sinistral shear zones reworking west Pilgangoora; Mulgandinnah SZ; NNW-verging folds and thrusts in Mosquito Creek Belt controlling Au mineralization; open E-plunging folds at Yarrie
D _{4d}	c. ?2850	Shallow-dipping S-directed thrusts and open folds; conjugate fault arrays along Sholl SZ; NW thrusting on steep faults (e.g. ?Loudens Fault)	Weak E–W steep-dipping crenulations with E-plunging fold hinges; weak to moderate E–W foliation in 2950 Ma Sn granites
Extension	2780	Hamersley Basin initiated; normal N-down Mallina Fault; Loudens Fault	Hamersley Basin initiated
D _{5a}	2765	Epithermal Au in NNW-trending dextral faults Hardey and Kylena Formations	E-plunging closed anticlines in Mount Roe Basalt, unconformably overlain by
D _{5b}	<2765	NW- to N-trending folds, crenulations, kinks; gentle upright subhorizontal folds trending NW	N- to NW-trending open folds and crenulations
D ₆₊	?2100 to Neoproterozoic	Western margin reworking —east-directed thrusting in Cape Preston (?Ophthalmia Orogeny); elevated Ar temperatures on Sholl SZ	Eastern margin reworking (Paterson Orogen) —thrusting, NNW-trending strike-slip faults, NW–SE folds, metamorphism (6 phases of post-Archaean deformation in the Rudall Complex)

Table 2. Correlation of local deformation histories with regional framework (after Blewett, 2000a)

<i>Regional events^(a)</i>	<i>Regional events^(b)</i>	<i>Whundo (h)</i>	<i>Mallina Basin (a)</i>	<i>Warrawoona Belt (w)</i>
D ₁	D ₁	–	–	–
D _{2a}	D ₂	–	–	wD ₁
D _{2b}	D ₂	–	–	wD ₂
D _{2c}	D ₂	–	–	wD ₃
D _{2d}	D ₂	–	–	–
D _{3a}	D ₂	–	–	wD ₄
D _{3b}	D ₂	hD ₁	–	–
D _{3c}	D ₂	hD ₂	–	–
D _{4a}	D ₂	hD ₃	aD ₁	–
D _{4b}	D ₂	hD ₄	aD ₂	wD ₅
D _{4c}	?D ₃	–	aD ₃	–
D _{4d}	?D ₃	–	aD ₄	–
D _{5a}	D ₄	–	–	–
D _{5b}	D ₄	–	–	–

SOURCES: (a) Blewett (2000a)
(b) Hickman (1983)

main exceptions to this trend are 2950–2930 Ma granitoids along the western margin that are associated with development of the CPTZ, and evolved 2840–2880 Ma post-orogenic granitoids associated with tin–tantalum mineralization.

Four deformation events are unique to the EPGGT, due to its age (Table 1). In addition to these events, the western and southwestern parts of the EPGGT have experienced the deformation events characteristic of the CPTZ, as discussed below.

The West Pilbara Granite–Greenstone Terrane

Although neodymium model ages and xenocrystic zircon populations indicate the presence of old source rocks, the oldest known supracrustal rock in the WPGGT are greenstones at the base of the Roebourne Group, which has been intruded by the c. 3270 Ma Karratha Granodiorite. The Roebourne Group consists mainly of basalt and partly overlaps in time with the Sulphur Springs Group of the EPGGT. The Roebourne Group is juxtaposed against the 3120 Ma Whundo Group by the regionally significant Sholl Shear Zone. The Whundo Group comprises mainly mafic and felsic volcanic rocks. The youngest unit within the WPGGT is the Cleaverville Formation, which mainly comprises sedimentary rocks with some banded iron-formation (BIF). This unit is the oldest that can be confidently correlated between the EPGGT and WPGGT.

In addition to the Karratha Granodiorite, the WPGGT was intruded by granitoids between 3120 and 2940 Ma. Another important magmatic (and metallogenic) event in the WPGGT is the intrusion of layered mafic bodies and some granitoids at c. 2920 Ma.

At least eight penetrative deformation events are recognized in the WPGGT, with the earliest predating intrusion of the Karratha Granodiorite (Blewett, 2000a). Several of the later events also affected the CPTZ and are described below.

The Central Pilbara Tectonic Zone

The EPGGT and WPGGT are separated by the CPTZ, which was defined by Hickman (1999) to effectively contain rocks of the Whim Creek and Mallina Basins. This zone is bounded by fault–shear zones and unconformities with older units, mainly the Cleaverville Formation. Units within the CPTZ include felsic to mafic volcanic rocks

and associated sedimentary units of the 3010–2950 Ma Whim Creek greenstone belt, and turbidites of the 2980–2940 Ma De Grey Group. Correlatives of the De Grey Group are also exposed in various areas of the EPGGT, including the Mosquito Creek Formation.

One of the characteristics of the CPTZ is the presence of several discrete granitoid intrusion events between 2950 and 2920 Ma. The earliest event is the intrusion of 2950 Ma sanukitoids (high-magnesium granodiorites), followed by intrusion of monzogranite at c. 2930 Ma and granite at 2920 Ma. The later event may be related to intrusion of layered mafic intrusions as in the WPGGT.

Three major deformation events are recognized in the CPTZ:

1. an event that produced easterly to east-northeasterly trending folds and a steeply dipping axial-planar fabric prior to 2950 Ma;
2. an event that produced north-trending folds and a steeply dipping axial-planar fabric at 2950 Ma;
3. an event that produced east to east-northeast folds and a steeply dipping fabric sometime between 2930 and 2880 Ma.

The main fabric observed in the rocks is a composite between the first and third fabric. A fourth, minor crenulation event, with a northwest orientation is developed locally. All these structures are also observed in the Mosquito Creek Formation in the southeastern part of the EPGGT, as well as in parts of the EPGGT and WPGGT adjacent to the CPTZ (Table 1).

The Fortescue Group

All three lithotectonic terranes of the north Pilbara granite–greenstones are overlain unconformably by the Fortescue Group, which forms the base of the Mount Bruce Supergroup to the south. The Fortescue Group comprises mainly mafic lavas with lesser felsic volcanic and sedimentary rocks. Deposition of the Fortescue Group commenced at about 2770 Ma and continued, possibly in two major pulses, to 2680 Ma. Unlike the north Pilbara granite–greenstones, most of the Fortescue Group is relatively undeformed and flat lying.

Mineralizing events affecting the north Pilbara granite–greenstones

Due to the extended period of time over which the north Pilbara granite–greenstones evolved, the mineralizing history of this area is also extensive. Moreover, it has involved a large number of discrete events, producing a wide variety of mineral deposits. As with the geological evolution, each lithotectonic terrane had separate histories of mineralization, with some overlap in the younger events (Fig. 2).

The East Pilbara Granite–Greenstone Terrane

Unlike the Coonterunah Group, which is weakly mineralized, the overlying Warrawoona Group is well mineralized, hosting significant VHMS (including stratiform barite) and lode-gold deposits. Lead-isotope model ages and zircon U–Pb ages of host units indicate that the syngenetic deposits formed at c. 3490 Ma (Dresser barite) and c. 3470 Ma (Big Stubby and Lennons Find; Thorpe et al., 1992b). The VHMS deposits, which are hosted by felsic volcanic rocks of the Duffer Formation, are lead rich and contain



Figure 2. Geological history and mineralizing events affecting the constituent parts of the Pilbara Craton

Table 3. Gold production and resources of the north Pilbara granite–greenstones based on host rock

<i>Host rocks</i>	<i>Production (tonnes)</i>	<i>Inferred resource (tonnes)</i>	<i>Total (tonnes)</i>	<i>Portion of total (%)</i>
Ultramafic–mafic volcanic rocks				
East Pilbara (3420 Ma event)	18.76	13.00	31.76	36.7
East Pilbara (2900 Ma event)	3.82	0.18	4.00	4.6
West Pilbara	0.18	0.74	0.92	1.1
Turbiditic rocks	5.11	36.83	41.95	48.4
Palaeoplacers	0.50	3.68	4.18	4.8
Felsic volcanic rocks – granitoids	0.43	1.18	1.62	1.9
Other	2.16	0.00	2.16	2.5
Total	30.96	55.62	86.59	–

SOURCES: Gifford (1990); Hickman (1983); Register of Australian Mining, (1997–98, 1999–2000, 2001–02); Woodall (1990)

significant barite, characteristics typical of Phanerozoic, but atypical of Archaean, VHMS deposits.

Lead-isotope model ages, although complex, indicate that the lode-gold deposits formed prior to 3400 Ma, probably at around 3420 Ma (Thorpe et al., 1992b; D. Huston and A. Hickman, unpublished data). These deposits, which account for about 32 t of gold (combined production and pre-mining inferred, indicated, and measured resources), constitute 37% of the total for the north Pilbara granite–greenstones (Table 3). These vein deposits are hosted by mafic and ultramafic volcanic rocks in association with quartz–sericite, quartz–fuchsite and talc–carbonate alteration assemblages (e.g. Zegers, 1996).

Porphyry copper–molybdenum and related deposits formed during deposition of the Warrawoona Group and the Wyman Formation. The 3450 Ma Miralga Creek deposit, which is associated with felsic stocks, consists of stockwork chalcopyrite–pyrite veins overprinted by later sphalerite–galena–pyrite veins (Geollnicht et al., 1988). Porphyry-style mineralization is also associated with a 3315 Ma stock at the Coppins Gap deposit (Thorpe et al., 1992a). This deposit is the oldest significant porphyry copper–molybdenum deposit known.

The youngest hydrothermal deposits associated with deposition of supracrustal rocks within the EPGGT are VHMS deposits, hosted by the 3240 Ma Sulphur Springs Group. These deposits are described in detail later.

Iron-ore deposits at Shay Gap, Nimingarra, Mount Goldworthy, and Yarrie are hosted by the Gorge Creek Group, which is constrained by geological relationships at between 3240 and 3020 Ma (Williams, 1999; Hickman, A., 2001, pers. comm.). Podmore (1990) interpreted the deposits at Shay Gap and Nimingarra to have formed by supergene enrichment of jaspillite and BIF.

Although younger mineral deposits are present in the EPGGT, these deposits are probably associated with the development of the CPTZ or the deposition of the Fortescue Group, or both, and are discussed later.

The West Pilbara Granite–Greenstone Terrane

The oldest known deposit in the WPGGT is the Ruth Well volcanic–peridotite-associated nickel–copper deposit (Marston, 1984), which is hosted by the Ruth Well Formation with an age in excess of 3270 Ma. The 3120 Ma Whundo Group hosts several VHMS deposits, the largest of which, the Whundo deposit, is described later.

The most significant mineralizing event in the WPGGT was the intrusion of a number of large layered mafic intrusions at 2920–2900 Ma (Hoatson et al., 1992). These intrusions host significant nickel–copper–PGE deposits at Radio Hill and Mount Sholl, and vanadium–titanium deposits at Balla Balla, and are related to the development of the CPTZ.

The Central Pilbara Tectonic Zone

The period between 2950 and 2840 Ma, during which the CPTZ developed, is the most significant period of mineralization in the north Pilbara granite–greenstones. This rich period of mineralization is inferred to relate to the opening and closing of the Mallina – Whim Creek Basin, a period during which three major deformation events (>2950, 2950, and 2930–2880 Ma; Smithies, 1998; Blewett, 2000a), three major felsic intrusive events (2950, 2930, and 2880–2840 Ma), and a major mafic intrusive event (2920–2900 Ma) occurred.

Deposits formed not only in the CPTZ, but also in the margins of the EPGGT and WPGGT adjacent to this zone, and in and adjacent to the similarly aged Mosquito Creek Basin. Deposits formed during this period include probable VHMS deposits (e.g. Whim Creek and Salt Creek, 2950 Ma), epigenetic copper–zinc–lead deposits (e.g. Mons Cupri and Comstock, 2920 Ma; Huston et al., 2000), layered mafic-intrusion-hosted nickel–copper and vanadium–titanium deposits (see above), lode-gold deposits (e.g. Withnell and Lynas Find – Mount York; 2890–2910 Ma; Neumayr et al., 1998, D. Huston, unpublished data), and pegmatite tantalum–tin deposits (e.g. Wodgina; 2880–2840 Ma; Kinny, 2000). Lode-gold (e.g. Nullagine district) and epigenetic copper–zinc–lead deposits (e.g. Coondamar Creek) deposits of similar ages as those in the CPTZ are also known in the Mosquito Creek Group in the southeastern part of the EPGGT (Thorpe et al., 1992b).

The Fortescue Group

Basaltic rocks from the base of the Fortescue Group contain a number of vein-lead–silver and fluorite deposits, the most important of which are the Braeside district and the Meentheena deposit. Lead-isotope model ages and geological relationships indicate that these deposits formed at 2750–2670 Ma (Richards et al., 1981; Richards and Blockley, 1984; Richards, 1986). Small quartz–galena–fluorite veins, with similar lead-isotope model ages are also scattered throughout the north Pilbara granite–greenstones. In addition, a number of quartz(–fluorite) vein deposits with distinct epithermal textures are also present. Geological relationships and mineralogical similarities to the deposits hosted by the Fortescue Group suggest that these deposits also formed at 2750–2670 Ma during a period of extensive volcanism within the Fortescue Group. This mineralizing event was the last significant event in the north Pilbara granite–greenstones.

Part one: Deposits of the West Pilbara Granite–Greenstone Terrane

by D. L. Huston and R. S. Blewett

The WPGGT has been the site of three relatively recently or currently active mining operations:

1. the Radio Hill layered mafic-intrusion-hosted nickel–copper–PGE deposit;
2. the Whundo VHMS copper–zinc deposit;
3. the Elizabeth Hill vein-silver deposit.

The purpose of the first day of this excursion is to illustrate the diversity in mineralization styles of the WPGGT by visiting these three deposits.

Geology of the West Pilbara Granite–Greenstone Terrane

Hickman et al. (2000) has subdivided rocks of the WPGGT (Fig. 3) into three units: the Roebourne and Whundo Groups, which are separated by the Sholl Shear Zone, and the Cleaverville Formation. Both the Roebourne and the Whundo Groups are overlain by the 3020–3015 Ma Cleaverville Formation, which is the oldest unit that can be correlated from the WPGGT to the EPGGT.

The Roebourne Group

The Roebourne Group, which is exposed north of the Sholl Shear Zone (Fig. 3), is divided into three formations. The basal Ruth Well Formation consists of basalt, peridotite, and chert and has been intruded by the c. 3270 Ma Karratha Granodiorite. The overlying Nickol River Formation contains banded chert, iron formation, clastic sedimentary rocks, and felsic volcanic rocks. Rhyolite within the Nickol River Formation has been dated at c. 3251 Ma. The Regal Formation, which is dominated by peridotitic komatiite and pillow basalt, has not been dated but is constrained by geological relationships at between 3250 and 3050 Ma (Hickman et al., 2000). The Ruth Well Formation hosts the Ruth Well komatiite-hosted nickel–copper deposit, the oldest known example of this deposit type.

The Whundo Group

The Whundo Group, which lies south of the Sholl Shear Zone (Fig. 3), hosts the three deposits we will visit. It has been divided into four formations: the basal Nallana Formation, the Tozer Formation, the Bradley Basalt, and the uppermost Woodbruck Formation. Ages range from 3125 to 3115 Ma (Hickman et al., 2000). The Nallana Formation and Bradley Basalt comprise mainly basalt with minor felsic volcanic units, ultramafic units (Nallana Formation), and chert (Bradley Basalt). The Tozer Formation, which hosts the Whundo and Yannery Hills deposits, comprises calc-alkaline volcanic rocks of various compositions, and the Woodbrook Formation comprises mainly felsic volcanoclastic rocks with minor basalt and BIF (Hickman et al., 2000).

Granitoids

The WPGGT is intruded by tonalite, granodiorite, monzogranite, and granite of the Dampier, Cherratta, Harding, and Caines Well Granitoid Complexes. The ages of intrusions vary greatly both within the WPGGT and within individual granitoid complexes. Ages, as determined by sensitive high-resolution ion microprobe (SHRIMP) U–Pb zircon analyses, range from 3270 to 2920 Ma (Smith et al., 1998; Nelson, 1997,

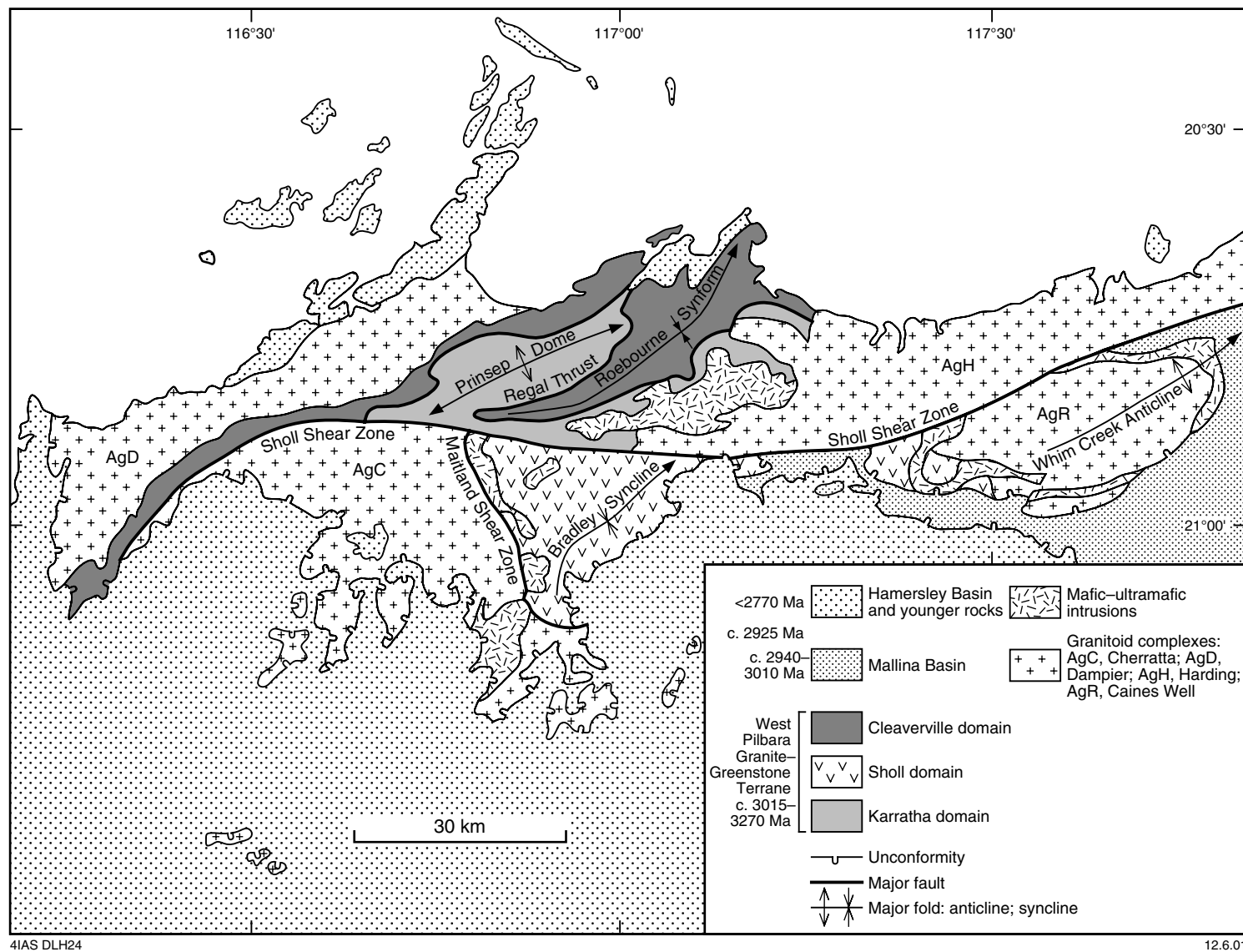


Figure 3. Geology of the West Pilbara Granite–Greenstone Terrane (after Hickman et al., 2000)

1998, 1999). Hickman et al. (2000) noted that in many cases the ages of granitoid intrusion corresponds to felsic volcanism in nearby supracrustal rocks.

Layered mafic intrusions

The WPGGT has been intruded by a number of c. 2920 Ma layered mafic–ultramafic complexes (Fig. 3), including the Balla Balla, Dingo, Maitland, Mount Sholl, Munni Munni, Radio Hill, and Sherlock Bay Complexes (Hoatson et al., 1992). These complexes host some of the most significant mineral deposits in the West Pilbara, including copper–nickel–PGE deposits at Radio Hill and Mount Sholl, PGE deposits at Munni Munni, and vanadium–titanium deposits at Balla Balla. In addition, nickel–copper mineralization is hosted in banded quartz–magnetite–amphibole schist adjacent to the Sherlock Bay Complex (Hoatson et al., 1992). Recent dating of an intrusive granite suggests that the age of the Andover Complex, which hosts vanadium–titanium deposits, is more than 3016 Ma (Hickman, A., 2001, pers. comm.).

Structure

At least four phases of deformation developed after c. 3125 Ma (Blewett, 2000a). The earliest observed penetrative fabric is present in the microlithons of a well-developed crenulation cleavage (hS_2). The hS_2 fabric is the first regionally extensive penetrative fabric in the Whundo Group and strikes northwest where unfolded. The hS_2 fabric ranges from a schistosity to crenulation cleavage of the earlier hS_1 fabric to a fracture cleavage in the east.

The hS_3 fabric is a regional crenulation cleavage or schistosity throughout the Whundo Group. At the Whundo mine it is subhorizontal (folded) and associated with easterly plunging hL_3 lineations.

Tight hF_4 folds plunge north-northwest and have steep east- to east-northeasterly striking axial surfaces. A fine-spaced hS_4 crenulation cleavage is developed in the axial regions of the hF_4 folds and in the more pelitic rock type. A regional hF_4 fold axis through the Whundo Group just west of the Yannery copper mine folds the main hS_2 fabric into a subhorizontal attitude.

The Radio Hill deposit

The Radio Hill deposit was discovered in 1982 by the Karratha Joint Venture (Teck Explorations Ltd and Samin Australia Pty Ltd) through drilling SIROTEM anomalies in an area with previously coincident aeromagnetic and weak nickel–copper soil anomalies (Peters and de Angelis, 1987). This deposit had pre-mining and combined measured and indicated resources estimated at 0.837 Mt grading 3.32% Ni, 2.03% Cu, 0.17% Co, and an inferred resource estimated at 1.223 Mt grading 0.73% Ni, 0.85% Cu, and 0.06% Co (as at June 1999; Register of Australian Mining, 1999–2000).

The deposit is hosted by the Radio Hill Intrusion, which intruded mainly mafic volcanic rocks of the Nallana Formation (Hickman, 1997; Hickman et al., 2000; Fig. 4). Hoatson et al. (1992) divided the Radio Hill Intrusion into two subzones; a basal ultramafic zone, which comprises mainly lherzolite, dunite, and websterite, and an overlying gabbroic zone. They subdivided the ultramafic zone into seven subzones, the most important of which is the basal subzone, which hosts the massive sulfide lenses at or near the contact with the Nallana Formation (Figs 5 and 6). This basal subzone (A) consists of chilled gabbro, gabbro-norite, and plagioclase websterite, containing massive, disseminated, veined, and brecciated pyrrhotite and pentlandite–chalcopyrite–magnetite (Hoatson et al., 1992).

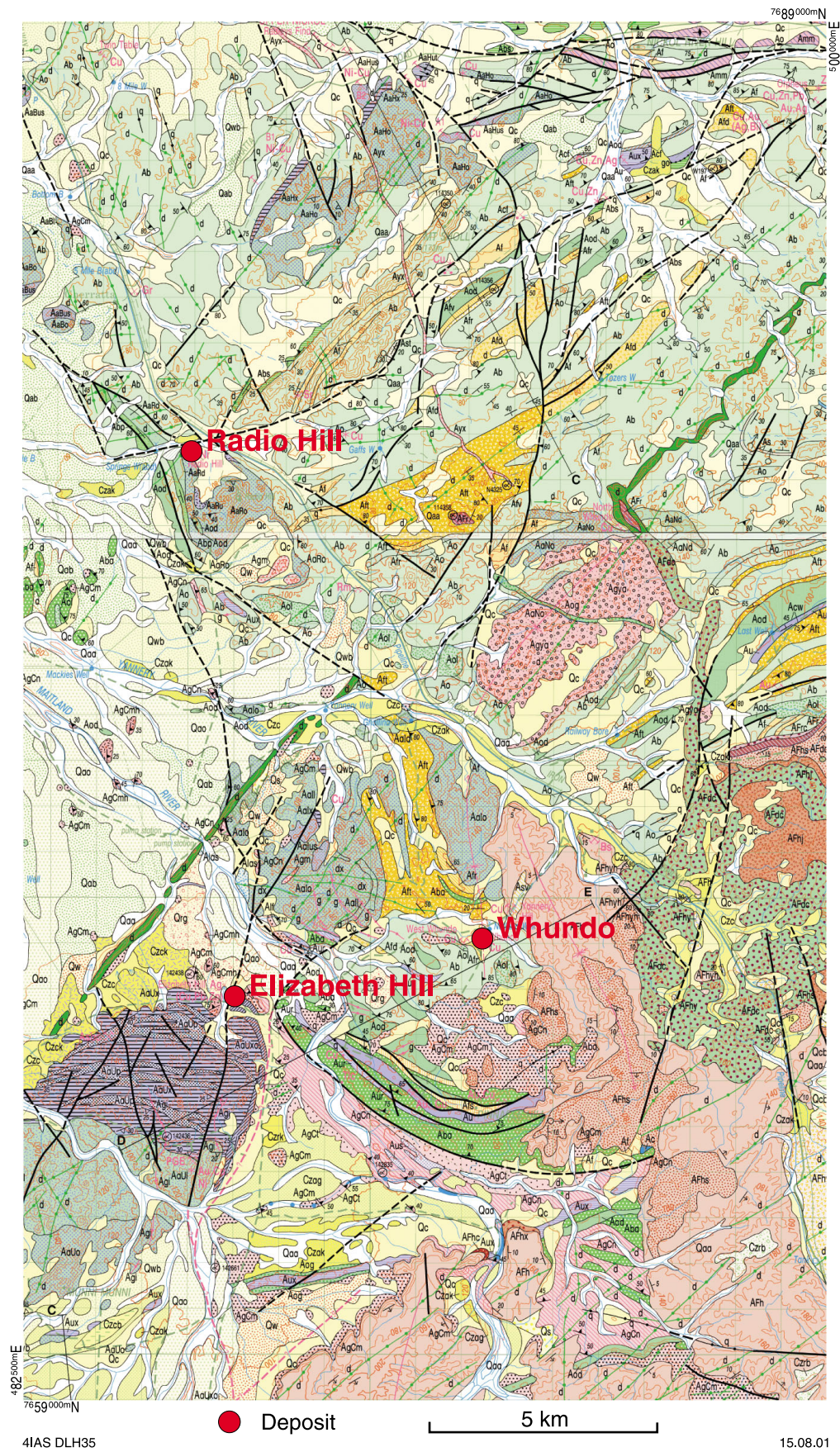
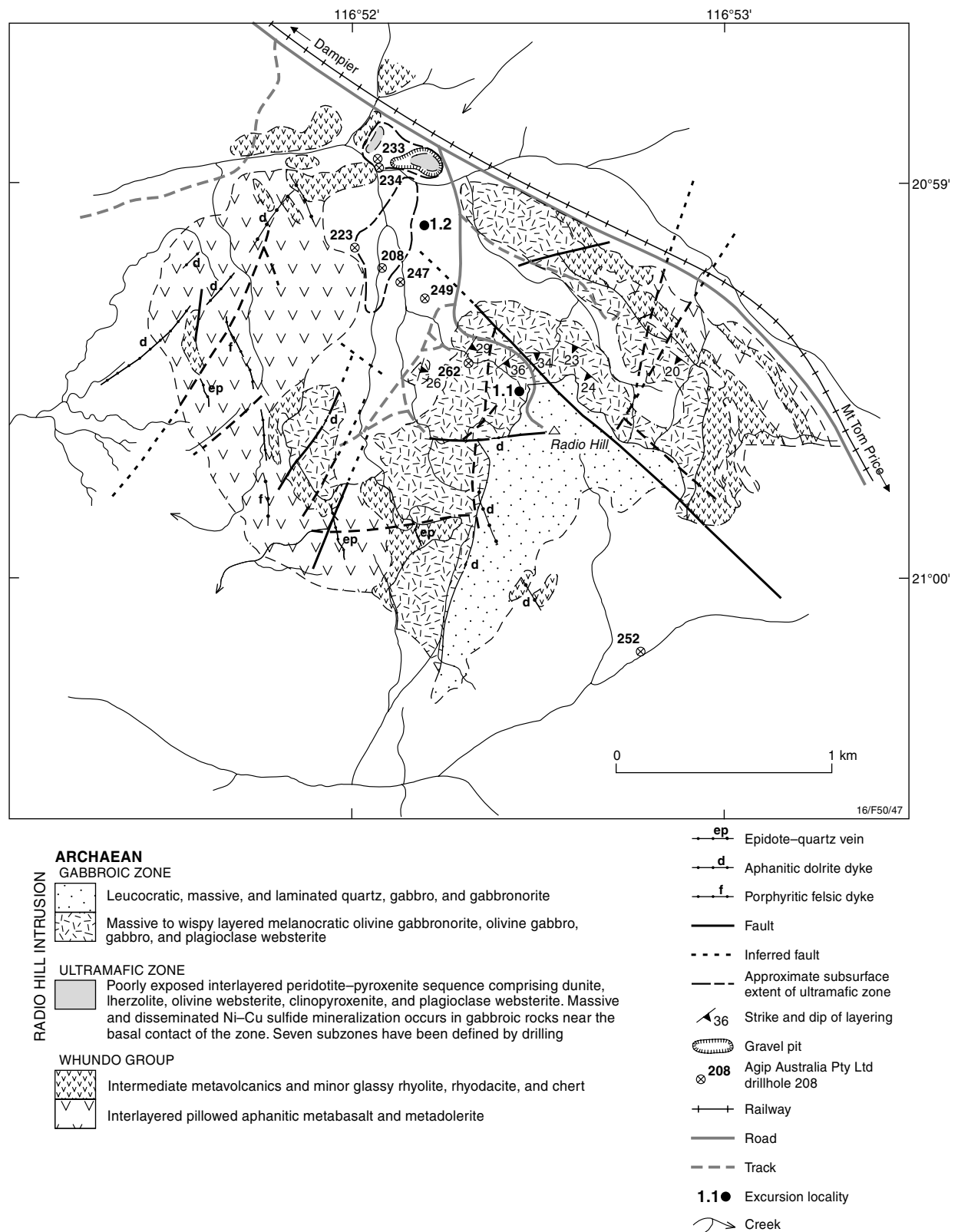


Figure 4. Geology of the southeastern part of the West Pilbara Granite–Greenstone Terrane showing the location of the Radio Hill, Whundo, and Elizabeth Hill deposits (modified from Hickman, 1996; and Kojan and Hickman, 2000)



4IAS DLH8

30.07.01

Figure 5. Surface geology of the Radio Hill nickel-copper-PGE deposit showing excursion localities (modified from Hoatson et al., 1992)

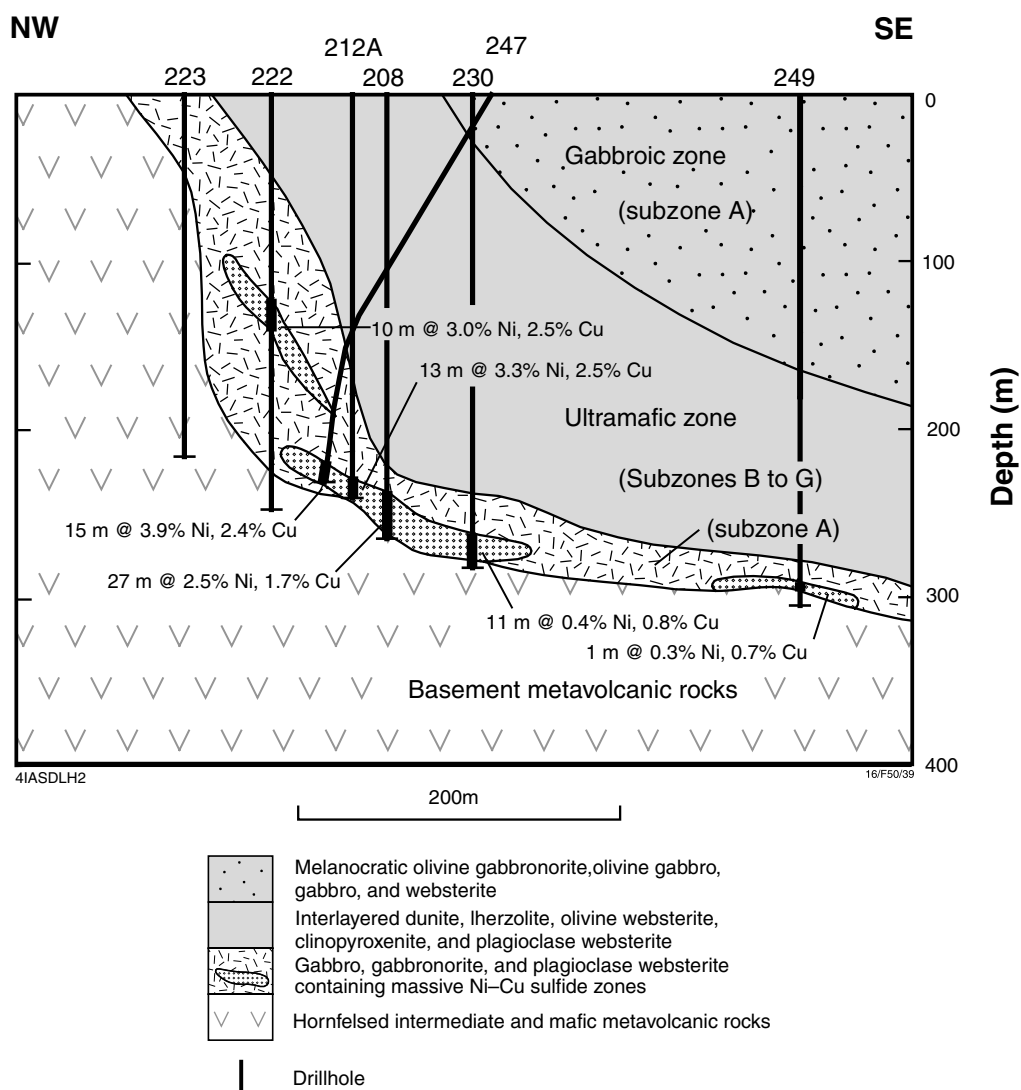


Figure 6. Cross section through the Radio Hill deposit showing relationships to the Radio Hill complex and host rocks (modified from Hoatson et al., 1992)

Mineralogically the ores are predominantly (mainly hexagonal) pyrrhotite with interstitial chalcopyrite and pentlandite. Magnetite is commonly associated with the massive sulfides. Minor and trace minerals include lead, bismuth, and lead tellurides, gersdorffite, and native tin. Palladium is presently a significant byproduct, with 4550 oz produced (as at June 1999; Register of Australian Mining, 1999–2000).

The Whundo deposit

Copper has been mined in the Whundo area intermittently since 1911, with the most recent operations ceasing in 1976. Total production from this area was 12 000 t of supergene ore grading 22.3% Cu, with a remaining inferred resource at the Whundo deposit estimated at 2.0 Mt grading 1.3% Zn, 2.0% Co, and 11 g/t Ag (Collins and Marshall, 1999a). The main production was from the Whundo and nearby Yannery Hill deposits.

The Whundo deposit is hosted within the Whundo Group at the contact between mafic volcanic rocks of the Nallana Formation and the overlying, mainly felsic, calc-

alkaline volcanic and volcanogenic rocks of the c. 3120 Ma Tozer Formation. The Yannery Hill deposit is hosted by the Tozer Formation (Hickman et al., 2000).

In detail the Whundo deposit is spatially associated with a 1 km-long, 200 m-thick amphibolite sill that is mainly stratigraphically above, but also partially engulfing, the deposit (Fig. 7; Collins and Marshall, 1999a). The deposit has two ore zones, Whundo and West Whundo. These deposits are hosted by altered basalt with minor quartz-phyric felsic rocks of the Nallana Formation, which is overlain by massive felsic to intermediate volcanic rocks of the Tozer Formation (Collins and Marshall, 1999a).

Rocks at and below the ore position have been altered to quartz–sericite–chlorite and quartz–chlorite schists (Fig. 7), with andalusite present in the former unit. Most of the known sulfide zones are confined to these altered units, which can be traced 1 km along strike. The sulfide mineralization is apparently confined to one stratigraphic position, but it is segmented into discrete ore shoots that plunge to the northwest. Primary ores are characterized by pyrrhotite, pyrite, sphalerite, chalcopryite, and magnetite (Collins and Marshall, 1999a).

The Elizabeth Hill deposit

The Elizabeth Hill deposit, which lies at the northern margin of the Munni Munni Intrusion, is an unusual vein deposit, rich in silver and platinum group elements and with minor nickel, lead, zinc, and copper. The deposit was discovered by Agip Australia Pty Ltd in 1987 during a search of lineaments near Karratha for hydrothermal mineralization (de Angelis et al., 1988). The vein strikes north and is near-vertical. Several ore pods plunge shallowly to the south and are 20–80 m long and 5–15 m wide (Marshall, 2000). The pre-mining measured resource is estimated to contain 24.1 kt grading 0.42% Ag in an upper pod, and 22.7 kt grading 0.12% Ag in a lower pod (Register of Australian Mining, 1999–2000).

The vein consists of carbonate–quartz breccia with clasts of pyroxenite and granite. The wallrocks are silicified, carbonated, and chloritized, with anastomosing quartz–carbonate–sulfide stringers. The ores are complex, with native silver, silver sulfides, and sulfosalts being the main ore minerals (Barnes, 1995).

Excursion localities

All deposits visited are on active mining leases and therefore permission is required prior to entry. The Radio Hill (Titan Resources NL) and Elizabeth Hill (East Coast Minerals NL and Legend Mining Ltd) deposits are presently being mined. The railway access roads are private roads of Hamersley Iron Pty Ltd and permission is required to use them. **Safety regulations and directions of the lease holders and Hamersley Iron must be complied with when on their respective properties.**

Locality 1.1: Radio Hill layered intrusion (DAMPIER*, AMG 869786†)

From the entrance to the Karratha airport, proceed south towards Karratha for 3.5 km past the Seven Mile facility. Turn right onto the Hamersley Iron railway access road. Drive along this road for 6.3 km until the Great Northern Highway is reached. Use this highway to cross the railway. Continue along the railway access road (along the western

* Capitalized names refer to standard 1:100 000 map sheets, unless otherwise indicated.

† Localities are specified by the Australian Map Grid (AMG) standard six-figure reference system whereby the first group of three figures (eastings) and the second group of three figures (northings) together uniquely define position, on this sheet, to within 100 m.

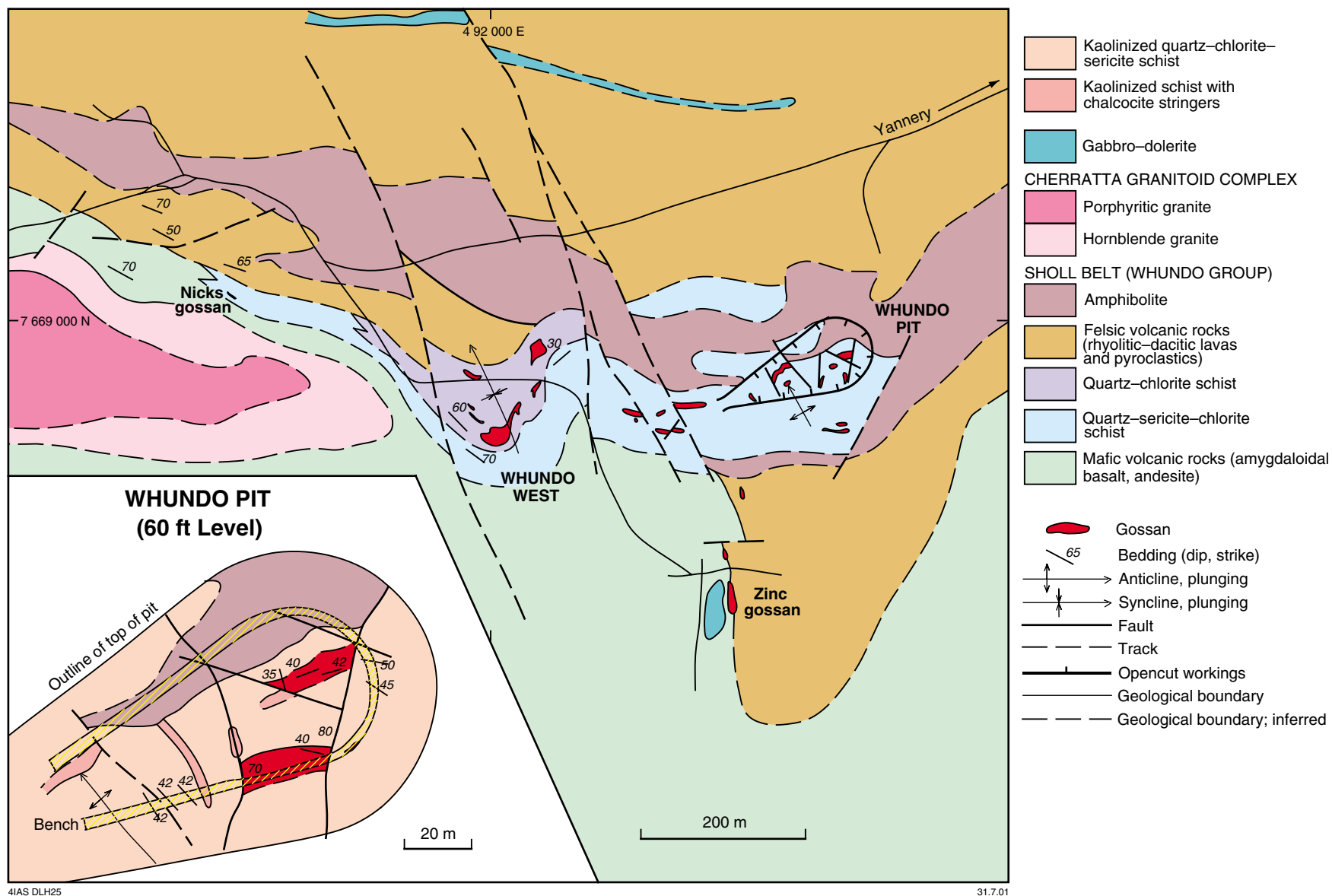


Figure 7. Surface geology of the Whundo copper-zinc deposit (after Collins and Marshall, 1999a)

side of the railway) for 25 km to the turnoff to Radio Hill on the right. Drive 1.5 km to the repeater station at the top of the hill.

At the top of the hill, layered mafic–ultramafic intrusions are visible at Munni Munni to the south and Mount Sholl (Fig. 3) to the north. The Munni Munni Intrusion hosts one of the most significant deposits of platinum group elements in Australia — the Munni Munni deposit. It contains an inferred resource estimated at 20–30 Mt at 2.9 g/t combined Pt, Pd, and Au, 0.2% Ni, and 0.3% Cu (Hoatson et al., 1992). The Mount Sholl Intrusion hosts an inferred resource estimated at 4.26 Mt grading 0.73% Ni and 0.87% Cu (Register of Australian Mining, 1999–2000). Both these deposits and the Radio Hill deposits are orthomagmatic deposits, associated with layered mafic intrusions in the WPGGT at about 2920 Ma.

Rocks of the gabbroic zone, which forms the upper part of the Radio Hill Intrusion, are exposed along the track down the hill. The contact between a leucocratic subzone and a melanocratic subzone is exposed approximately 200 m along the track from the repeater station. The leucocratic subzone is characterized by quartz gabbro, gabbro, and gabbro-norite, whereas the underlying melanocratic zone is characterized by olivine gabbro-norite, olivine gabbro, gabbro, and plagioclase websterite.

Rocks of the ultramafic zone, which forms the lower part of the Radio Hill Intrusion and host the nickel–copper–PGE ore lens, are not well exposed on this track, but are visible in drillcore and underground.

Locality 1.2: Radio Hill mine (DAMPIER, AMG 864791)

Drive back down the hill for 0.6 km to the entrance of Radio Hill mine. Proceed to the mine office.

The ore zone and host rocks will be observed underground and in drillcore. We will be shown around this locality by Titan Resources NL geologists whose instructions must be followed.

Locality 1.3: Structure of the Yanerry Hill copper deposit (PINDERI HILLS, AMG 931697)

Return to the railway access road, turn left and head south for 12 km where a track forks off to the right. Drive approximately 3 km along this track, parking about 100 m below the crest of a hill. The old Yanerry Hill copper workings are located to the right of the track.

Four phases of deformation are visible at this site. The main penetrative fabric is a crenulation cleavage, with a weak earlier fabric visible in the low-strain domains (microlithons). The main hS_2 fabric dips steeply to the northeast and is cut by a subhorizontal hS_3 crenulation cleavage and associated shallowly easterly plunging intersection lineation. Early quartz veins are folded (hF_2) and faulted (west-directed thrusts). Later hF_4 folds are upright and plunge to the north-northwest. These hF_4 folds and associated hS_4 crenulations overprint quartz veins and copper mineralization.

Locality 1.4: The Whundo copper–zinc deposit (PINDERI HILLS, AMG 924692)

Drive another 0.6 km southwest along this track to a fork on the left. Proceed south down this fork for 200 m and park.

The Whundo deposit is exposed in an opencut to the south (Fig. 7). Two ore shoots are exposed as well as kaolinitized quartz–chlorite–sericite schist, which is locally andalusite bearing. The amphibolite is exposed in the north-northwestern wall.

Locality 1.5: The Elizabeth Hill silver deposit (PINDERI HILLS, AMG 869678)

Return to the main track and drive 5 km southwest to a powerline. Turn right, towards the northwest, and travel along the powerline for 1 km to the Elizabeth Hill silver deposit.

The Elizabeth Hills mine was an underground mine that operated between 1997 and 2000, with full-scale mining carried out in 2000. Currently the tailings are being treated, with the intention of additional exploration after completion.

Return to the railway access road and drive north until the intersection with the Great Northern Highway. Turn right and head east to the Whim Creek Hotel caravan park.

Part two: The Mons Cupri copper–zinc–lead and Balla Balla vanadium–titanium deposits

by D. L. Huston

The CPTZ is perhaps the most richly mineralized part of the north Pilbara granite–greenstones. Deposits associated with this zone include probable VHMS deposits (e.g. Whim Creek and Salt Creek), lode-gold–antimony deposits (e.g. Mallina district), layered mafic-intrusion-hosted vanadium–titanium deposits (e.g. Balla Balla), and probable epigenetic base-metal deposits (e.g. Mons Cupri and Comstock). The purpose of this second excursion day is to visit the Mons Cupri and Balla Balla deposits, two significant deposits near the Whim Creek Hotel.

Geology of the Whim Creek greenstone belt and Caines Well Granitoid Complex

The local geology is dominated by the Whim Creek greenstone belt and the Caines Well Granitoid Complex. The main phase of the Caines Well Granitoid Complex, which has been dated at 3093 ± 4 Ma (Nelson, 1997), is unconformably overlain by the 3016–2940 Ma (Nelson, 1998, 2000) Whim Creek greenstone belt (Fig. 8). This unconformity is defined by the Geological Survey of Western Australia as the boundary between the WPGGT and the CPTZ (Fig. 1; Hickman A. H., 1999, pers. comm.).

Recently, the Whim Creek greenstone belt has been divided into two groups: the redefined Whim Creek Group, with an age of 3016–2970 Ma, and the Bookingarra Group, with an age of 2965–2942 Ma (Smithies et al., 2001). The redefined Whim Creek Group contains the Warambie Basalt and the Mons Cupri Volcanics, which contains the Mount Brown Rhyolite Member. The Warambie Basalt, which contains coherent lavas and volcanoclastic rocks, is commonly in unconformable contact with the older phase of the Caines Well Granitoid Complex; granite clasts are commonly included at its base. The Mons Cupri Volcanics consists of felsic epiclastic rocks that overlie, or are intruded by, the Mount Brown Rhyolite. The Mount Brown Rhyolite Member, a massive to spherulitic feldspar-phyric rhyolite, is an extensive subvolcanic sill (Pike G., 1999, pers. comm.).

The Bookingarra Group, which unconformably overlies the Mons Cupri Volcanics, consists from base to top of the Cistern Formation, Rushall Slate, Loudon Volcanics, and Mount Negri Volcanics. Detrital zircons from the Cistern Formation indicate a maximum age of 2965 Ma for the Bookingarra Group (data from Nelson, 2000). The minimum age is 2943 ± 7 Ma. This is the age of a young zircon population from the Kialrah Rhyolite (Nelson, 1998), which unconformably overlies the Bookingarra Group. Units of the Bookingarra Group contain all significant mineral deposits in the Whim Creek greenstone belt.

The Cistern Formation, which hosts the Mons Cupri deposit, contains a complex assemblage of rock types, including conglomerate, sandstone, and felsic volcanic rocks. The overlying Rushall Slate, which hosts the Whim Creek deposit, contains mainly slate and fine-grained sandstone, but locally contains mafic volcanic sills and dykes with a composition similar to the overlying Loudon Volcanics. The Loudon Volcanics comprise mainly high-magnesium basalt and komatiite, whereas the overlying Mount Negri Volcanics comprise mainly variolitic basalt (Hickman et al., 2000).

The Caines Well Granitoid Complex, although dominated by 3093 ± 4 Ma monzogranite, also contains the 2925 ± 4 Ma (Nelson, 1997) Bookingarra Granite.

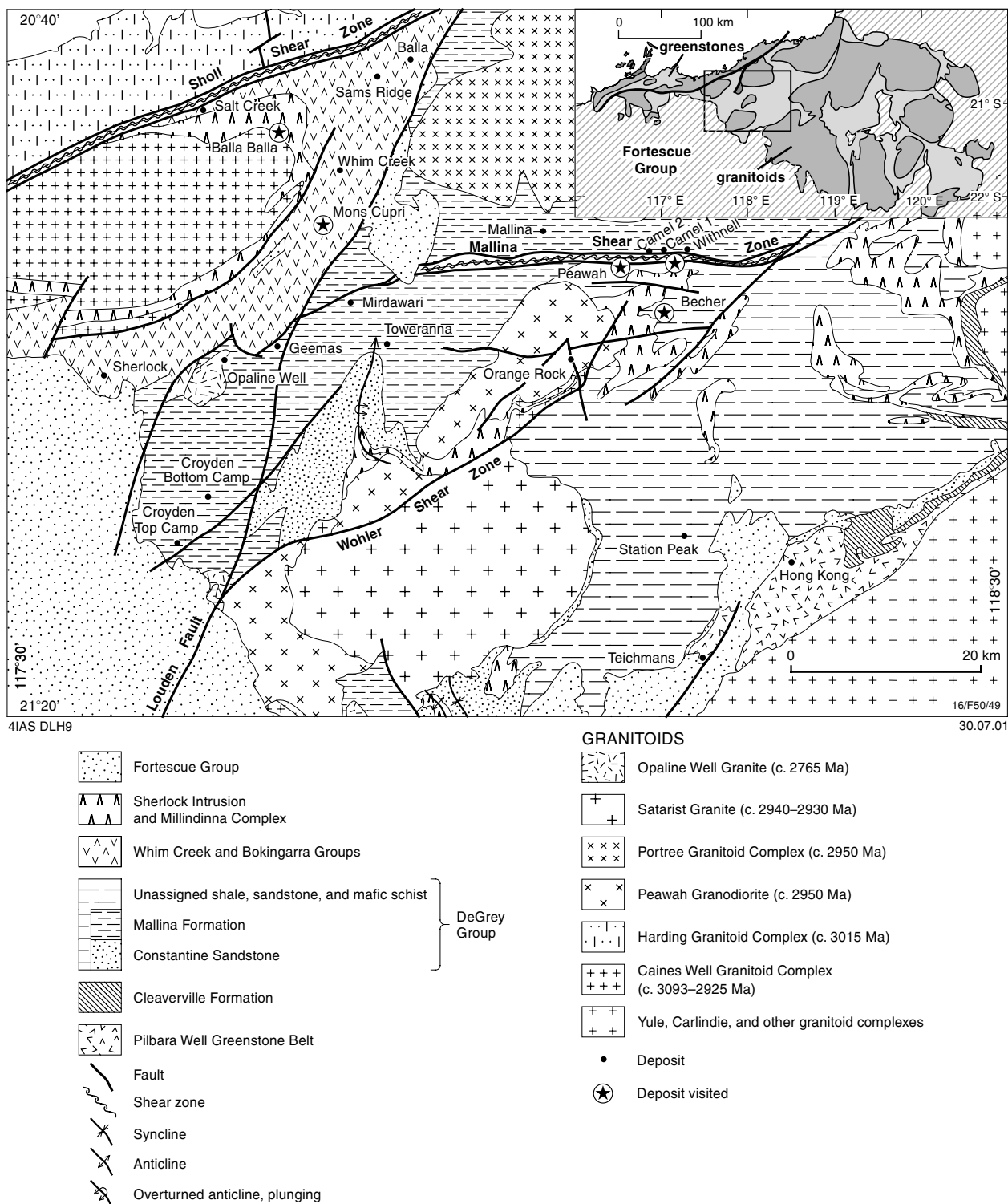


Figure 8. Geology of part of the Central Pilbara Tectonic Zone showing the locations of the Mons Cupri, Balla Balla, Peawah, Withnell, and Becher deposits (modified from Smithies, 1997, 1998, 1999)

The Caines Well Granitoid Complex was also intruded by the Balla Balla layered mafic complex probably at about this time (Hoatson et al., 1992).

Geology of the Mons Cupri deposit

With the exception of the Loudon and Mount Negri Volcanics, all units of the Whim Creek Group are present in the vicinity of the Mons Cupri deposit (Fig. 9). Of these units, the Mons Cupri Volcanics, the Cistern Formation, and the Rushall Slate are most closely related to the deposit and are described below.

Mons Cupri Volcanics

The Mons Cupri Volcanics, which is dominated by the Mount Brown Rhyolite Member, is most extensively exposed to the north and east of the Mons Cupri deposit. Other exposures include the thin rhyolite between the Warambie Basalt and the Cistern Formation and probable Mount Brown Rhyolite Member, 500 m south of this thin unit. The Mount Brown Rhyolite Member consists of massive to locally flow banded, aphyric to feldspar-phyric rhyolite or rhyodacite that is locally abundantly spherulitic. Fresh, apparently unaltered examples of this unit typically weather in a rounded outcrop pattern (Fig. 10a), whereas sericitic examples typically have a blocky outcrop pattern (Fig. 10b).

To the north and east of Mons Cupri, the Mount Brown Rhyolite Member is overlain by poorly bedded to massive, feldspathic volcanogenic sandstone, with subordinate volcanic breccia. These volcanoclastic rocks also contain small feldspar-phyric to aphyric rhyolitic dykes or flows.

Cistern Formation

The Cistern Formation, which hosts the Mons Cupri deposit, can be subdivided into two units informally called the lower Cistern conglomerate (Fig. 10c) and the upper Cistern arkose. The Cistern Formation has major thickness changes along its strike. The thickest development, with a true thickness of at least 400 m, is present in a northeast-trending corridor (Fig. 9), which contains the Mons Cupri deposit. To the north of this corridor the true thickness of the Cistern Formation decreases to less than 100 m, and to the east the true thickness is 50–200 m.

Lower Cistern conglomerate

The lower Cistern conglomerate, which constitutes the bulk of the Cistern Formation at Mons Cupri, consists of polymictic conglomerate, sandy conglomerate, and conglomeratic sandstone. The clasts, which are subangular to locally rounded, range in size from pebbles to blocks 10 m across, of mainly rhyolite, granite, and lesser basalt. In drillcore the matrix of some conglomeratic units contains juvenile rhyolitic clasts, which suggests coeval rhyolitic volcanism during deposition.

Additional evidence of coeval felsic volcanism is indicated by the presence of crosscutting rhyolitic dykes and the ‘domal rhyolite’ — a 100 × 500 m exposure of massive to feldspar-phyric rhyolite, 100–200 m south of Mons Cupri. Although this unit is typically massive, local brecciated zones (Fig. 10d) are also present.

Upper Cistern arkose

The upper part of the Cistern Formation consists of massive to weakly bedded volcanoclastic sandstone. The thickness of this unit is also quite variable, with the

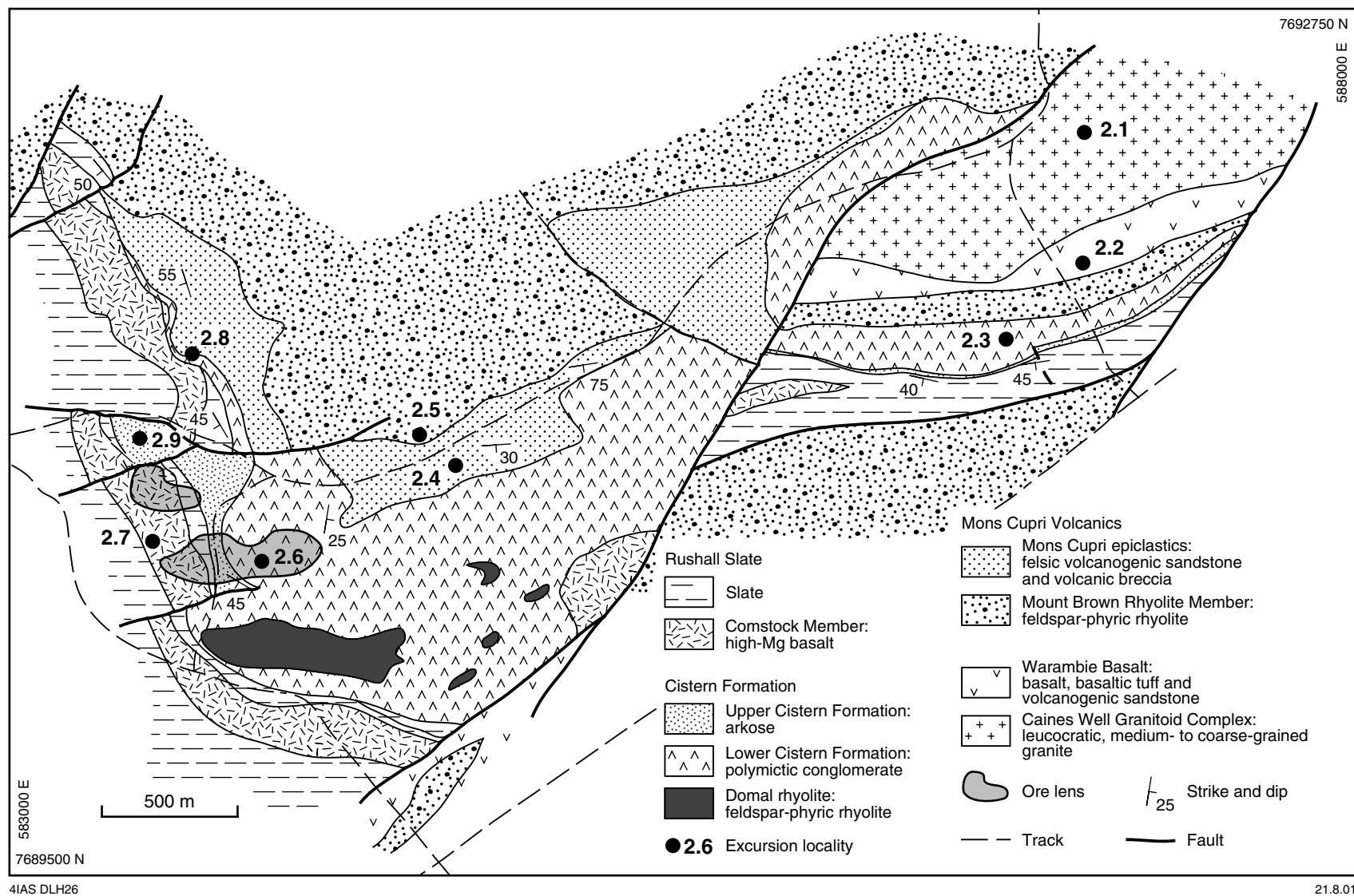


Figure 9. Geology of the Mons Cupri area showing excursion localities (modified from Hickman et al., 2000)

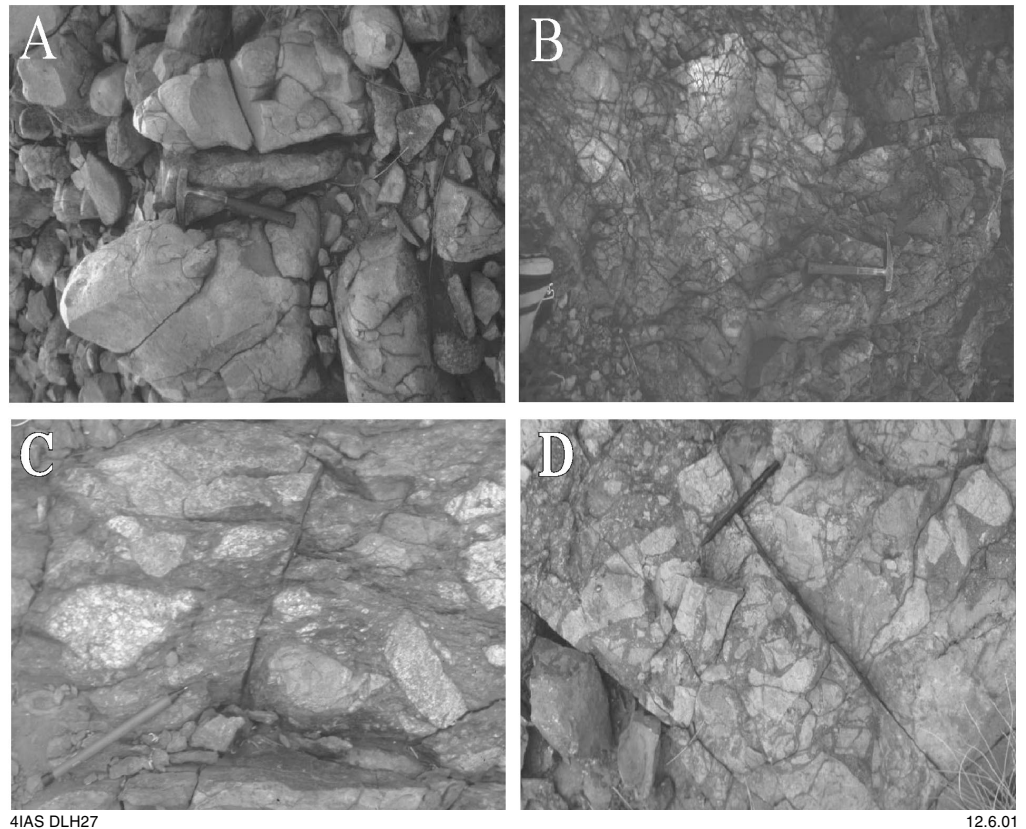


Figure 10. Rock relationships and textures in the Mons Cupri area: a) rounded outcrop pattern in the Mount Brown Rhyolite Member; b) blocky outcrop pattern in the Mount Brown Rhyolite Member; c) conglomeratic facies of the Cistern Formation; d) hydrothermal breccia within Domal Rhyolite

maximum true thickness of approximately 50 m developed against the northern bounding fault of the thickened Cistern corridor. The Mons Cupri ore lenses are closely associated with this thicker zone.

Rushall Slate

The Cistern Formation is overlain conformably by the Rushall Slate, which consists of variably cleaved shale and slate. About 4 km to the north-northeast, the Rushall Slate hosts the Whim Creek deposit. In the Mons Cupri area, the lower part of the Rushall Slate contains a 30–100 m-thick unit of high-magnesium basalt, formerly called the Comstock Andesite (Miller and Gair, 1975; Fig. 9). This unit is commonly weakly to moderately chloritized and has a blocky to flaggy outcrop pattern. Less-altered examples preserve a pyroxene-spinifex texture and have a more rounded outcrop pattern than the chloritized rocks.

Local structure

Changes in the thickness of the Cistern Formation and the extent of the Comstock Member (Fig. 9), suggest that the distribution of these units is controlled by synvolcanic faults, with the Mons Cupri deposit localized along the northern margin of a northeast-trending graben. Where present, bedding dips shallowly to moderately toward the south and southeast. Apart from the open fold defined by the south to southeast change in

dips, no other major folds are present. The Mount Brown Rhyolite Member is in faulted contact with the Rushall Slate in the eastern part of the area (Fig. 9).

Base metal mineralization

The Lower Cistern conglomerate hosts two lenses of base metal mineralization approximately 5–20 m below its contact with sandstone of the upper Cistern arkose (Fig. 11). The main lens consists of a stratiform 5–10 m-thick zone of zinc–lead-rich semi-massive to massive sulfide overlying a discordant, funnel-shaped, copper-rich stringer zone. Although the zinc–lead-rich lens is stratiform, textural evidence suggests that most or all of this zone is epigenetic.

Drillcore data (Fig. 12) suggests that the copper-rich stringer zone is associated with intense chloritic alteration, which grades into a peripheral silicified and carbonate-altered zone. The peripheral zones are commonly weakly zinc–lead mineralized. The stratiform zinc–lead-rich orebody is closely associated with carbonate alteration (Fig. 12).

The timing of mineralization at Mons Cupri is controversial. Although the deposit has many characteristics similar to syngenetic VHMS deposits (e.g. Miller and Gair, 1975), such as the form of the ore zones and metal ratios, textural evidence indicates the mineralization is epigenetic. Collins and Marshall (1999b) also noted this and suggested that the deposit formed by subseafloor replacement shortly after deposition of the host units.

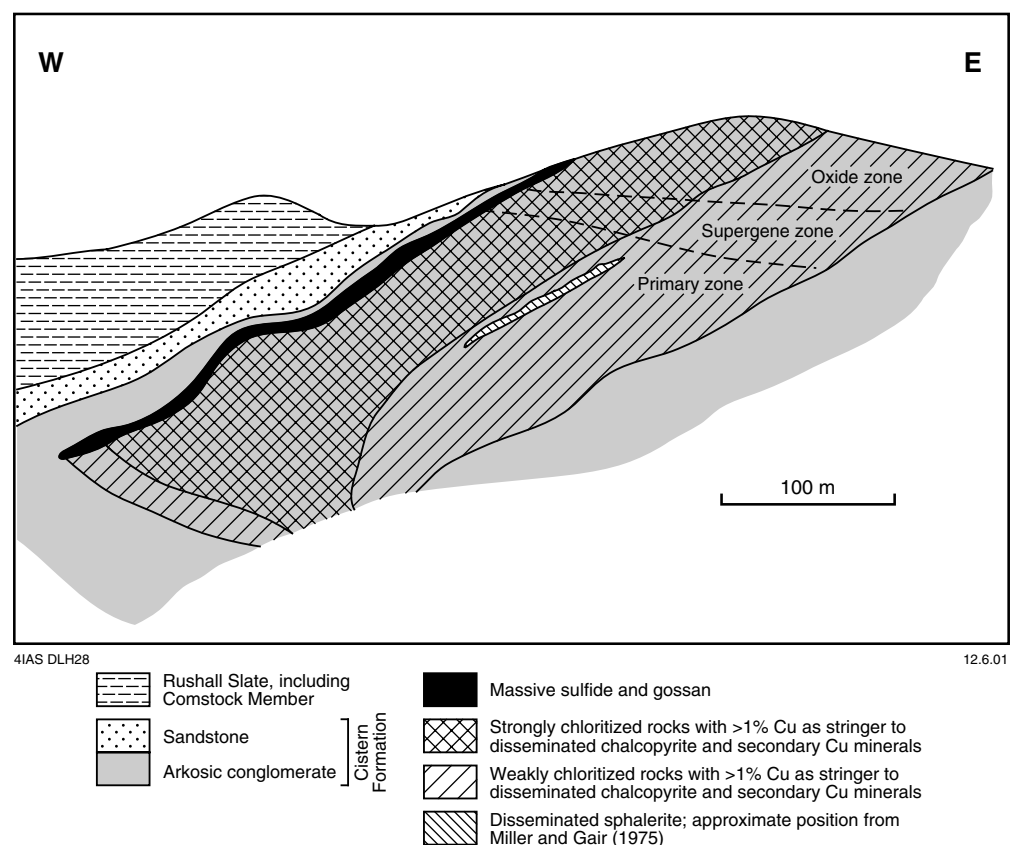
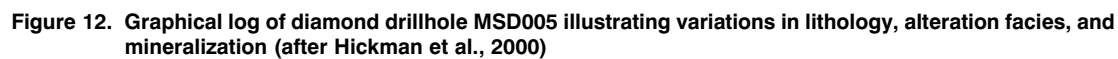


Figure 11. Cross section of the Mons Cupri deposit (after Hickman et al., 2000)



Alternatively, Huston et al. (2000) used lead-isotope model ages (model of Thorpe et al., 1992b) to suggest that the Mons Cupri deposit formed significantly after deposition of its host rocks. The model age is about 2920 Ma, similar to that of the nearby, clearly epigenetic, Comstock vein deposit, and significantly younger than the Whim Creek deposit (c. 2950 Ma) and the host unit. Owing to the inherent uncertainty of lead-isotope model ages, these absolute ages must be considered suspect. More convincing evidence of an epigenetic timing lies in the relative ages of the Whim Creek and Mons Cupri deposits. Although the Whim Creek deposit is only 4 km away and within the overlying Rushall Slate, its model age is 30 m.y. *younger* than the Mons Cupri deposit. This temporal anomaly can be explained in one of two ways: either the Mons Cupri deposit is younger than the Whim Creek deposit, or the source of lead for the two deposits is very different. Given the epigenetic character of the Mons Cupri deposit and the closeness of the two deposits, it is most likely that the Mons Cupri deposit is epigenetic and formed 30–40 m.y. after deposition of its host.

Excursion localities

With the exception of Balla Balla, localities described below are shown on Figure 9. At the time of writing, all localities described below were within active mining leases and therefore permission to enter is required.

Locality 2.1: Caines Well Granitoid Complex (SHERLOCK, AMG 869924)

From the Whim Creek Hotel proceed through the caravan park to a locked gate. Pass through this gate and proceed towards the Whim Creek mine for about 0.5 km until a junction is reached. Take the left fork through some abandoned buildings. Proceed along this road for 2.5 km until a second junction is reached. Three relatively small exposures of Caines Well Granitoid Complex are present in the plain to the south and east.

This medium- to coarse-grained leucocratic monzogranite, which is the older phase of the Caines Well Granitoid Complex, contains 0.2 – 1 m-long, fine-grained melanocratic inclusions. It is also cut by 0.1 – 0.2 m-thick pegmatite dykes and quartz and chlorite veins. This granitoid is interpreted as the basement to the Whim Creek Group because similar clasts are abundant in the Warambie Basalt and lower Cistern conglomerate.

Locality 2.2: Traverse through Warambie Basalt and Mount Brown Rhyolite Member (SHERLOCK, AMG 870918)

Return to the junction and take the left fork. Proceed down this track for 0.7 km. The Warambie Basalt is exposed in a low outcrop approximately 200 m east of the track across a small creek. The Mount Brown Rhyolite Member is exposed, albeit poorly, in the first low rise that the track crosses.

This stop briefly examines exposures of the Warambie Basalt and the overlying Mount Brown Rhyolite Member. At this locality the Warambie Basalt consists of quartz–feldspar-phyric amygdaloidal basalt, volcanogenic sandstone, and flaggy schistose and chloritic basaltic tuff. Granitoid clasts are preserved locally at the base of the Warambie Basalt (i.e. on the northern end of this low ridge). The Mount Brown Rhyolite Member consists of massive rhyolite with 10–15% feldspar phenocrysts (2–5 mm long) in low rounded outcrops.

Locality 2.3: Cistern Formation (SHERLOCK, AMG 868915)

From the exposure of Mount Brown Rhyolite Member at Locality 2.2, a large exposure of rock is visible on the western side of a gully about 350 m to the southwest. Proceed to this exposure.

A large well-exposed outcrop illustrates the characteristics of the lower part of the Cistern Formation. This unit consists of polymictic conglomerate with 50–60% subrounded to subangular clasts of granite, granodiorite, feldspar-phyric rhyolite, and basalt, ranging in size from 1 to 100 cm, in a fine-grained ‘dirty’ and weakly chloritic sandy matrix (Fig. 10c). Some granite clasts have a similar texture and composition to the Caines Well Granitoid Complex at Locality 2.1. A thin lens of sericitic upper Cistern arkose is in contact with Rushall Slate to the south of this large exposure. At this locality, small (<1 m) lenses of the Comstock Member are present within the slate. It should be noted that the thickness of this section of Cistern Formation is only about 100 m, which contrasts the 400 m of this unit around the Mons Cupri deposit.

Locality 2.4: Silicified Mons Cupri epiclastic rocks with disseminated sulfide (SHERLOCK, AMG 848911)

Return to the junction and turn left so that you are heading west-southwest on the main track. Proceed 2.2 km and park about 200 m west of the last creek crossing. Walk down into this creek and then up it for 50–100 m where you will find a siliceous ledge crossing the creek.

Volcanogenic sandstone of the Mons Cupri epiclastic rocks are well exposed along the creekbed. The silicified ledge is an example of small silicified zones within this unit. This ledge contains several percent disseminated pyrite. Other small silicified zones within the Mons Cupri epiclastic rocks contain up to 1% disseminated sphalerite as well as pyrite.

Locality 2.5: Altered Mount Brown Rhyolite Member (SHERLOCK, AMG 846912)

Return to vehicle and walk a further 100 m west until you reach a gully draining the massif to the north.

Two textural varieties of Mount Brown Rhyolite Member are exposed within this gully. The first, least altered variety, weathers to a rounded outcrop pattern and contains visible feldspar phenocrysts. The second variety is characterized by a blocky outcrop pattern and appears to be more sericitic. Whole-rock geochemical analyses indicate that the blocky variety has lost iron, magnesium, calcium, and fluorine, but gained lead and arsenic relative to the rounded variety.

Locality 2.6: Mons Cupri deposit (SHERLOCK, AMG 839907)

Return to vehicle and drive 0.7 km until you reach a fork in the track. Turn left and drive 0.4 km up towards a saddle along the ridge. The hill to the left is Mons Cupri. Stop at the saddle and walk up the hill.

As you walk up the hill you will be passing down through the stratigraphic succession that hosts the Mons Cupri deposit. The base of the Rushall Slate is exposed in the road cutting near the saddle where it is locally strongly silicified. This is underlain by sericitized sandstone of the upper Cistern arkose. The thickest development of the upper Cistern Formation is to the north of the saddle.

The underlying lower Cistern conglomerate is exposed further up the hill. This unit hosts the Mons Cupri deposit, which makes up most of this hill (Mons Cupri is Latin for 'mountain of copper'). In the vicinity of the deposit, the lower Cistern conglomerate is several hundred metres thick, chloritically altered, and contains abundant secondary copper minerals in veins and along fractures. A stratiform zinc–lead-rich zone is exposed in a cut on the western side of the hill. From the very top of the hill the narrow extension of the chloritic alteration zone to the east is visible, relative to the surrounding sericitic conglomerate.

Locality 2.7: Alteration of the Comstock Member (SHERLOCK, AMG 835907)

Return to the saddle and continue to the west along a drilling track (the main track continues down a gully to the south). The drilling track skirts the eastern ridge, first going south and then north. Walk down the first spur on the eastern side of this ridge. You will pass a large cut that forms part of a lower drilling track. About 50–100 m below this track you will come to several low rounded outcrops.

The Comstock Member of the Rushall Slate, which equates to the Comstock Andesite of Miller and Gair (1975), consists of high-magnesium basalt and can be traced for more than 4 km, 10–20 m above the basal contact of the Rushall Slate. It may be a sill related to high-magnesium basalt of the Loudon Volcanics, to which it is texturally and compositionally similar (Smithies R. H., 1998, pers. comm.). Sills and dykes of this rock type are abundant in the Rushall Slate overlying the Comstock Member.

This traverse illustrates the variety of alteration observed in the Comstock Member. The most common variety has a blocky outcrop pattern. Small exposures of highly weathered basalt with a flaggy outcrop pattern are present along the track, and fresh rounded outcrops are present near the base of the spur. The rounded outcrops have variably developed pyroxene-spinifex texture. These rocks are the least-altered known examples of the Comstock Member and contain amphibole (after pyroxene) and plagioclase.

Relative to the least-altered Comstock Member, the blocky and flaggy varieties have lost magnesium, manganese, calcium, sodium, and strontium, but have gained zinc. The flaggy variety is more intensely altered. Both altered varieties are characterized by chlorite and quartz.

Locality 2.8: Traverse through Cistern Formation north of the graben-bounding fault (SHERLOCK, AMG 837914)

Return to vehicle and drive back along the track to the junction. Turn left at the fork and drive west for 0.3 km. Cross the creek and walk up to the top of, and along, the ridge to the north for 300 m.

Along the top of the ridge the Cistern Formation is very narrow (<10 m wide) and consists only of the conglomeratic facies. The Cistern Formation is underlain by volcanic sandstone and breccia of the Mons Cupri epiclastic rocks and overlain by the Rushall Slate. This traverse is north of an inferred growth fault that bounds the graben hosting the Mons Cupri deposit to the south. Further to the north the Cistern Formation and the Mons Cupri epiclastic rocks pinch out entirely, leaving the Mount Brown Rhyolite Member in direct contact with the Rushall Slate. The very narrow width of the lower Cistern conglomerate contrasts with its thick development at the Mons Cupri deposit.

Locality 2.9: ‘Northwest Pits’ prospect (SHERLOCK, AMG 834911)

Return to vehicle and drive a further 0.3 km west along the track. To the south of the track are the old workings called the ‘Northwest Pits’.

At this prospect, which is hosted by the upper Cistern arkose, workings expose extensive copper staining, typically along joints. In addition, a small pit exposes a zinc-rich gossan characterized by dark-coloured smithsonite. To the west of this prospect the Comstock Member of the Rushall Slate is strongly silicified and contains minor disseminated pyrite.

Locality 2.10: The Balla Balla vanadium deposit (SHERLOCK, AMG 803035)

Return to Whim Creek Hotel and then to the Northwest Coastal Highway. Turn left and travel east for 1.5 km to the Balla Balla turnoff on the left. Drive along the Balla Balla road for 10 km to a track veering off to the left. Drive north along this track for about 1 km and then head southwestward towards a low rise (about 0.5 km), crossing a small drainage. This is the outcrop of the Balla Balla vanadium deposit.

The Balla Balla deposit, with inferred resources estimated at 84.5 Mt grading 0.78% V₂O₅, is one of the largest vanadium deposits in Australia. The deposit is in a shallowly dipping, 18–35 m-thick, vanadiferous, tabular, massive magnetite layer, within the Sherlock layered mafic intrusion. Three individual lenses, Western, Central, and Eastern, were formed by the faulting of a single tabular magnetite body that extended over 7 km. The Central lens, which is 2 km long and dips 25° to the northeast, is located along this hill. The magnetite body is located near the base of the intrusion, at the contact between a lower unit of anorthositic gabbro, anorthosite, norite and pyroxenite, and an upper unit of granophyre and leucogabbro (Starkey, 1994; Register of Australian Mining, 1999–2000).

Return to Whim Creek Hotel caravan park for the night.

Part three: Lode-gold–antimony and epithermal deposits of the Indee district

by D. L. Huston and R. S. Blewett

In 1997, Resolute Ltd commenced exploration in the Indee area. Although small antimony–gold deposits were known at Mallina and Peawah (Finucane and Telford, 1939), the discovery of deposits in the Indee district was the result of grassroots exploration. An inferred resource estimated at 4.96 Mt at 2.08 g/t Au has been defined for the Withnell, Camel 1, and Camel 2 deposits. Today we will examine the regional geology of the Indee district, with emphasis on defining structural elements and their control on mineralization. We will also examine the different styles of mineralization, both on the surface and in drillcore.

Geology of the Indee district

The Indee district lies within turbiditic sedimentary rocks near the northwestern margin of the Mallina Basin, about 20 km east-southeast of Whim Creek (Fig. 13). The host rocks are part of the c. 2940–3000 Ma De Grey Group (Smithies, 1999). Smithies (1999) has assigned units north of the Mallina Shear Zone and in the far-western part of the district to the Mallina Formation, which consists of interbedded shale, siltstone, and medium- to fine-grained wacke. Elsewhere, rocks of the De Grey Group have not been assigned at the formational level and consist of turbiditic wacke, shale, and siltstone.

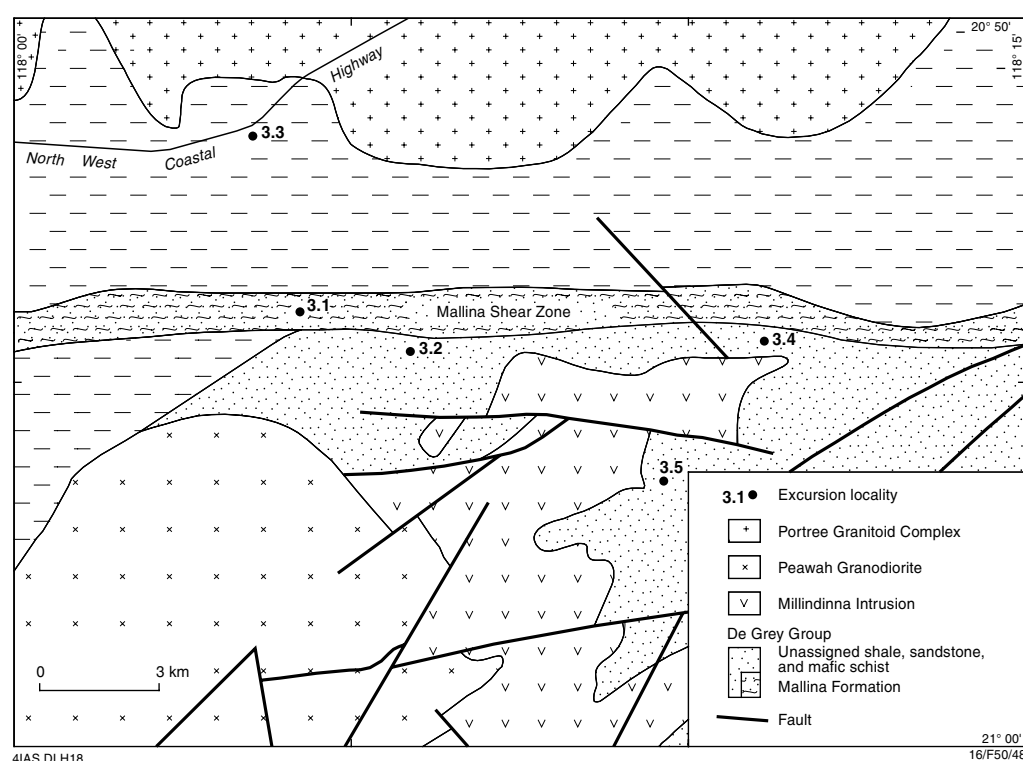


Figure 13. Geology of part of the Central Pilbara Tectonic Zone showing the location of excursion localities (modified from Smithies, 1997, 1998, 1999)

The sedimentary rocks of the De Grey Goup have been intruded by medium- to coarse-grained, equigranular, hornblende–biotite granodiorite with subordinate tonalite of the Peawah Granodiorite (Smithies, 1999). These rocks, which have been dated at c. 2948 Ma, are present in the southwestern part of the district. A second major intrusion, the Portree Granitoid Complex is present in the northern part of the district. Smithies (1998) reported two phases of intrusion, one of which has been dated at c. 2945 Ma (Nelson, 1999). Only the medium-grained leucocratic alkali granite is present in the Indee district. Rocks of the Mallina Formation in this area have been contact metamorphosed by the intrusion of this phase of the Portree Granitoid Complex (Smithies, 1999).

Structural history

aD_1 deformation

The first phase of deformation in the Mallina Basin was the development of regional shortening about an approximately north–south orientation. Upright subhorizontal folds with axes trending east–west were accompanied by an axial-planar slaty cleavage. Regionally, the clearest examples of aF_1 folds outcrop east of Powereena, where they are refolded into type III and type II fold interference patterns by north-trending aF_3 folds. Evidence for aD_1 deformation in the vicinity of the Mallina Shear Zone is restricted to complex fold geometries of aF_1/F_3 fold interference (e.g. Locality 3.4). The main, approximately east–west, penetrative fabric present in the Indee district is interpreted as a composite aS_1/S_3 fabric. The aD_1 deformation is inferred to be progressive and formed at 2950–3000 Ma.

aD_2 deformation

The aD_2 deformation was the result of compression oriented approximately east–west, and resulted in widespread macroscale refolding of the Mallina Basin about north-plunging upright folds. The aF_2 folds are associated with a well-developed crenulation cleavage or pencil-cleavage intersection with the folded aS_1 fabric. The Croydon Anticline and folds of the gabbro sills at Tardarina Hill in the south of the basin are examples of aF_2 folds. Smithies et al. (1999) interpret the intrusion of the Peawah Granodiorite (c. 2948 Ma) as post- to syntectonic with respect to aF_2 folds, dating this event at c. 2950 Ma or older.

aD_3 deformation

The main fabric across much of the Mallina Basin is interpreted to be a composite of aS_1 and aS_3 . The aS_3 fabric is commonly a crenulation cleavage associated with open to tight, upright, east-northeasterly to west-southwesterly plunging aF_3 folds. Macroscale examples of aF_3 folds have been defined by Smithies (1997, 1998) east of Powereena and near the Makuntunah Spring (on SHERLOCK). On the basis of megacryst alignment, Smithies (1998) suggested that the intrusion of the Satirist Granite at c. 2935 Ma was syntectonic with aD_3 .

aD_4 deformation

The aD_4 elements have only been recognized in the northern part of the Mallina Basin, near the Sholl Shear Zone. They consist of conjugate faults suggesting that shortening was oriented north–south.

Extension

A major thermal event at c. 2780 Ma impacted the entire area of the north Pilbara granite–greenstones and resulted in the development of the Hamersley Basin. The effect of early rifting associated with this major basin development was normal fault movement on the Mallina Shear Zone and other linked faults.

aD_5 deformation

Minor crenulations, kink bands, faults, and folds are the result of aD_5 deformation. This event also overprinted the Fortescue Group. Shortening was probably oriented approximately northeast–southwest and resulted in northwest-trending folds. Tourmalinite veins are overprinted by aS_5 crenulations to the east of the Becher gold prospect.

Faults

In addition to the aforementioned folding events, the Indee district is also characterized by a 1 km-wide zone of east–west shearing that Smithies (1999) termed the Mallina Shear Zone. On YULE, this shear zone is characterized by a network of anastomosing faults that forms a low ridge of calcretized and silicified rocks of the De Grey Group (Smithies, 1999). In the western part of the Indee district, the Mallina Shear Zone is intersected by a northeasterly trending fault zone that may be part of the Wohler Shear Zone. Interpretation of kinematic indicators (fold asymmetry) on the Mallina Shear Zone indicate that although a sinistral movement is the latest movement, a dip-slip, south-side-up movement dominates (Smithies, 1999). The Mallina Shear Zone is an important structure in the Indee district as many of the more significant prospects lie just north of it with a similar orientation.

Mineral deposits

There are more than 15 individual gold and antimony–gold deposits within the Indee district, three of which we will visit during this excursion. These deposits can be divided into at least three broad groups:

1. moderate-level gold-only deposits (e.g. Withnell);
2. moderate-level antimony–gold deposits (e.g. Peawah);
3. high-level deposits anomalous in gold (e.g. Becher).

In addition, extensive tourmalinites (Locality 3.3) and quartz–tourmaline veins are also present in the district.

Withnell deposit

The first group of deposits is best exemplified by the Withnell deposit. This deposit is oriented broadly east–west and the ore lenses dip steeply to the south. It lies approximately 1 km north of the Mallina Shear Zone. Based on the logging of oriented drillcore (INDD003 and INDD004), the majority of faults and veins at Withnell dip steeply to the north and south (Figs 14a,b and 15) and are interpreted to be conjugate with σ_1 oriented vertically in an extensional regime.

The highest gold grades are associated with high abundances of locally pyritic, planar quartz–carbonate veins (Fig. 14c), particularly where these veins dip steeply to the south (80–85°). Where the planar quartz–carbonate veins have a lower abundance, or where they dip steeply north, or both, gold grades are not elevated. With the possible

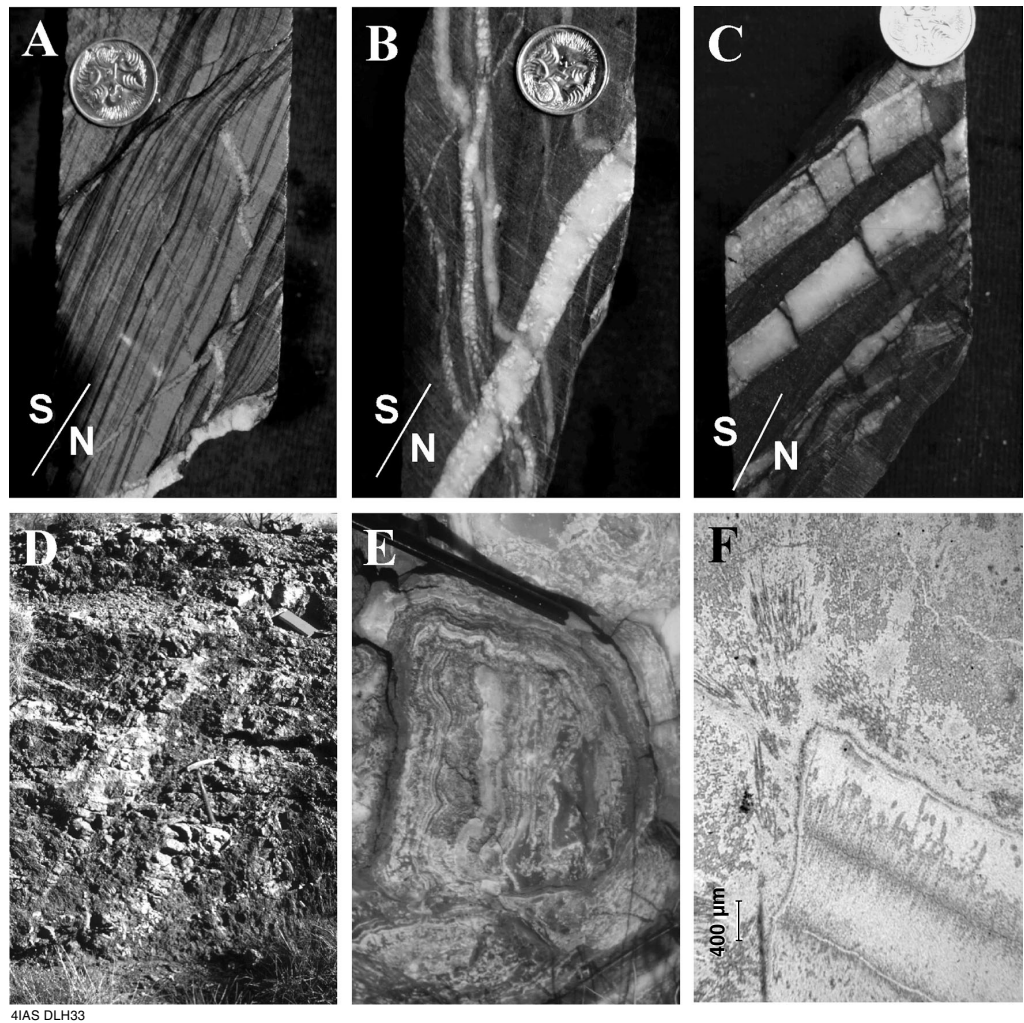


Figure 14. Rocks of the Indee district showing: a) north-dipping vein from the Withnell deposit; b) south-dipping vein from the Withnell deposit; c) south-dipping, pyritic, planar, quartz-carbonate vein from the Withnell deposit; d) south-dipping quartz veins from the Peawah deposit; e) crustiform vein textures from the Becher deposit; f) pseudo-acicular textures in thin section from the Becher deposit

exception of a lone ribbon-quartz vein, which lies along the margin of the high-grade zone, no other quartz-vein types have a relationship to high gold grades. Mutual crosscutting relationships and the local presence of a planar quartz–carbonate vein along south-dipping shears suggest an overlapping temporal relationship between these shears and veins.

Vein textures observed in drillhole INDD003 are characteristic of moderate depths, either in a plutonic or slate belt environment. This inference is supported by the lack of crustiform or colloform textures diagnostic of the epithermal environment, and by the presence of ribbon veins and deformed coarse comb textures that are characteristic of deeper levels (cf. Dowling and Morrison, 1989).

Alteration in drillcore is dominated by carbonate, sericite, and chlorite. The highest gold grades are in silty or shaly parts of the drillcore where high pyrite contents are present. Intervals containing carbonate-altered greywacke with small quantities of pyrite do not have significant gold grades.

In addition to the east–west-trending veins in drillcore, the Withnell deposit also contains north-trending, massive to coarse comb-textured veins, with minor sphalerite, tetrahedrite, and gold.

Peawah deposit

The Peawah deposit (Locality 3.2) lies to the south of the Mallina Shear Zone within weathered, sericitically altered siltstones. This deposit produced 20.4 t of ore grading 55.8% Sb and 9.8 g/t Au (Telford, 1939) up until 1918. The mineralization, which is dominated by stibnite and its oxidized products, is present in steeply southerly dipping, lenticular white quartz veins (Fig. 14d) that trend 110°, have the geometry of tension gashes, and cut a dominant subvertical, east–west-striking foliation (?S₆). The veins are cut by (?S₈) crenulations and kink bands. The workings trend 115°. The stibnite is associated with grey quartz that appears to be paragenetically later than the white quartz. Preliminary fluid-inclusion results indicate homogenization temperatures of around 270°C for three-phase (gaseous CO₂ – liquid CO₂ – aqueous) primary and pseudo-secondary inclusions (Mernagh T., 1999, pers. comm.).

Becher deposit

The Becher deposit (see **Locality 3.5**) differs substantially from the other two deposits in both its orientation and vein textures. The Becher deposit lies 6 km south-southwest of the Withnell deposit. It trends north-northwest (Fig. 16) and is characterized by high-level vein textures dominated by crustiform banding (Fig. 14e) with local brecciated zones. Pseudo-acicular quartz texture, which is common in adularia–sericite epithermal deposits, is present in thin sections from the Becher deposit (Fig. 14f). Dong et al. (1995) inferred that this texture formed by the replacement of calcite by quartz along a set of radial acicular structures within calcite crystals, and suggested that such processes may occur during isoenthalpic boiling.

Excursion localities

At the time of writing, all localities described below were within active exploration leases and permission to enter is therefore required. **WARNING: LOCALITY 3.2 CONTAINS A NUMBER OF COSTEANS AND UNMARKED SHAFTS.**

Locality 3.1: Mallina Shear Zone at Peawah River crossing (YULE, AMG 113887)

From the Whim Creek Hotel, drive east along the Northwest Coastal Highway for 23 km to the turnoff to Mallina Station. Turn right and proceed another 2.4 km to the station. From the station proceed southwest for 4.8 km (initially parallel to the landing strip) until the track crosses the Peawah River.

Although not impressive in outcrop, the Mallina Shear Zone is one of the most important structures in the CPTZ. This fault strikes east–west. Kinematic indicators indicate a south-side-up sinistral motion. To the west, this fault juxtaposes Whim Creek Group against De Grey Group, but at this locality it cuts through lithologically similar units of the De Grey Group. In the Indee district the zone is characterized by a network of anastomosing faults that form a low ridge of calcretized and silicified rocks of the De Grey Group. In the abundant low-strain areas within the shear zone, the replaced rock shows well-preserved sedimentary structures. The Mallina Shear Zone is interpreted as the reactivation of an early growth fault related to the development of

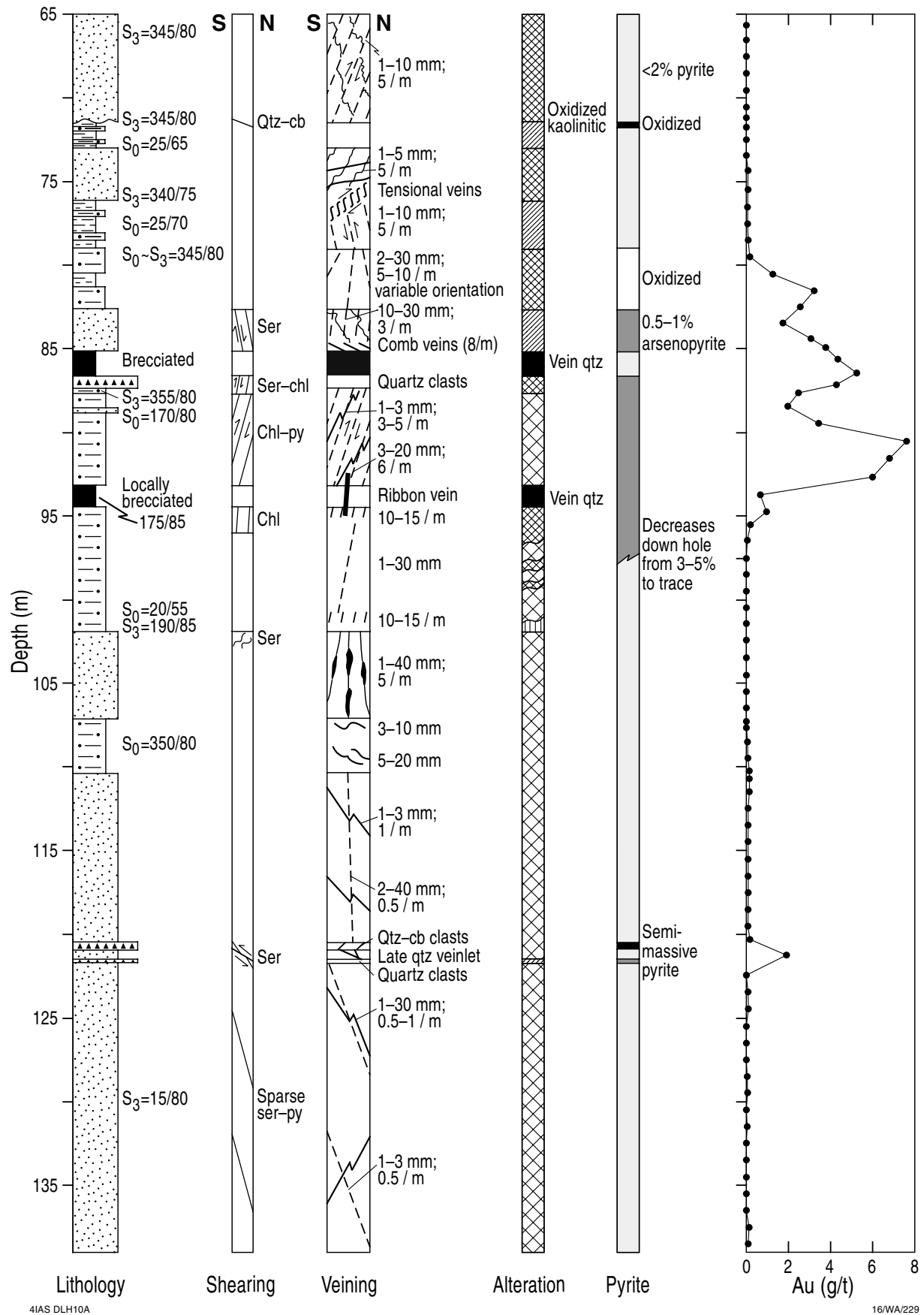
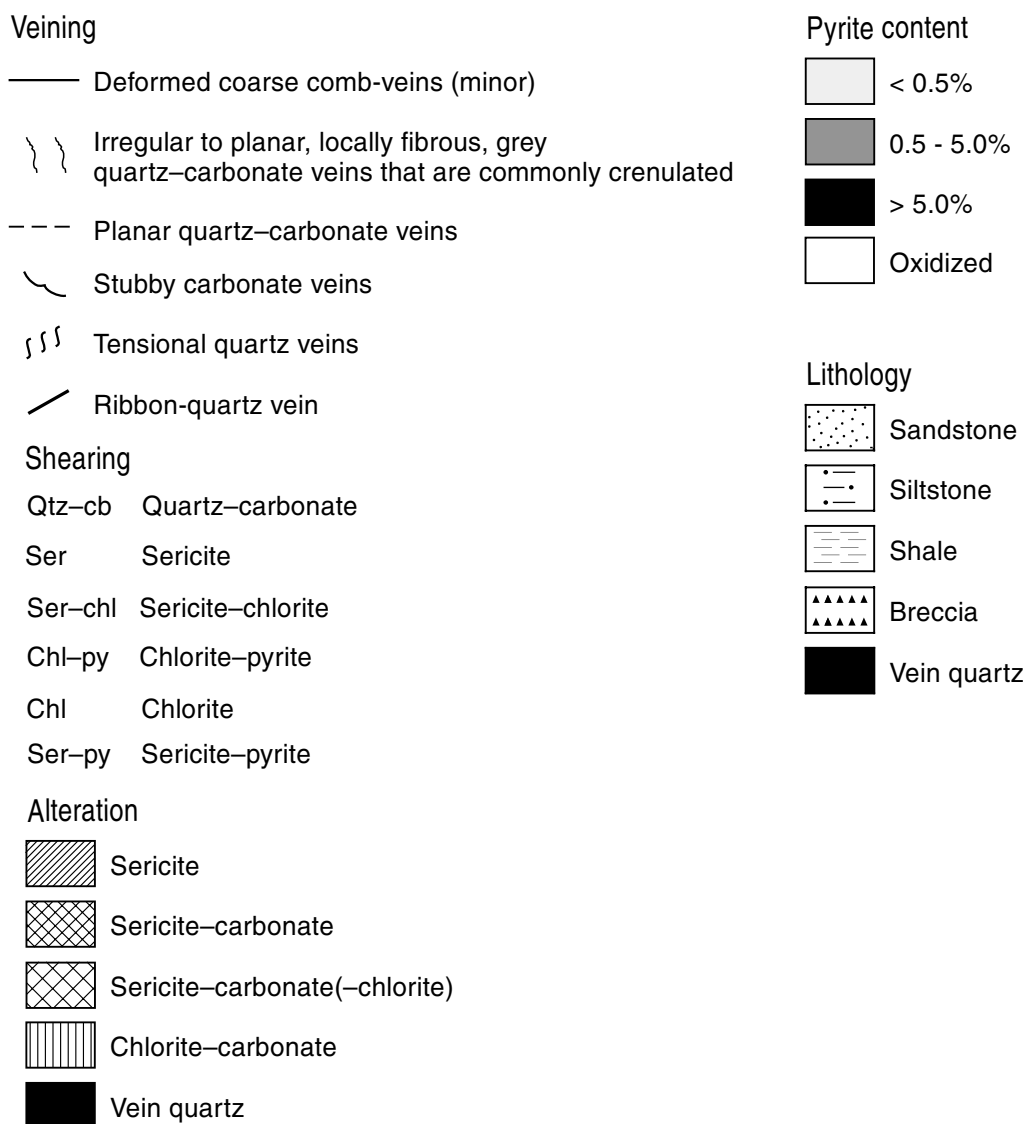


Figure 15. Graphical log of drillhole INDD003, Withnell deposit



4IAS DLH10B 16/WA/229

Figure 15. (continued)

the sedimentary basin in which the rocks of the De Grey Group formed (Smithies, R. H., 1999, pers. comm.).

Locality 3.2: Peawah prospect (YULE, AMG 141876)

Continue across the Peawah River for 0.8 km to a fenceline. Pass through the gate and take the right fork for 2.7 km to the Peawah prospect (visible to the left).

WARNING: UNMARKED OPEN SHAFTS ARE COMMON AT THIS SITE.

The Peawah diggings consist of many costeans and several shafts. In the dumps surrounding the shafts, white quartz veins with stibnite and antimony oxides can be found. In one of the costeans, a white south-dipping quartz vein (Fig. 14e) cuts the main east-trending foliation. These veins appear to fill tension gashes.

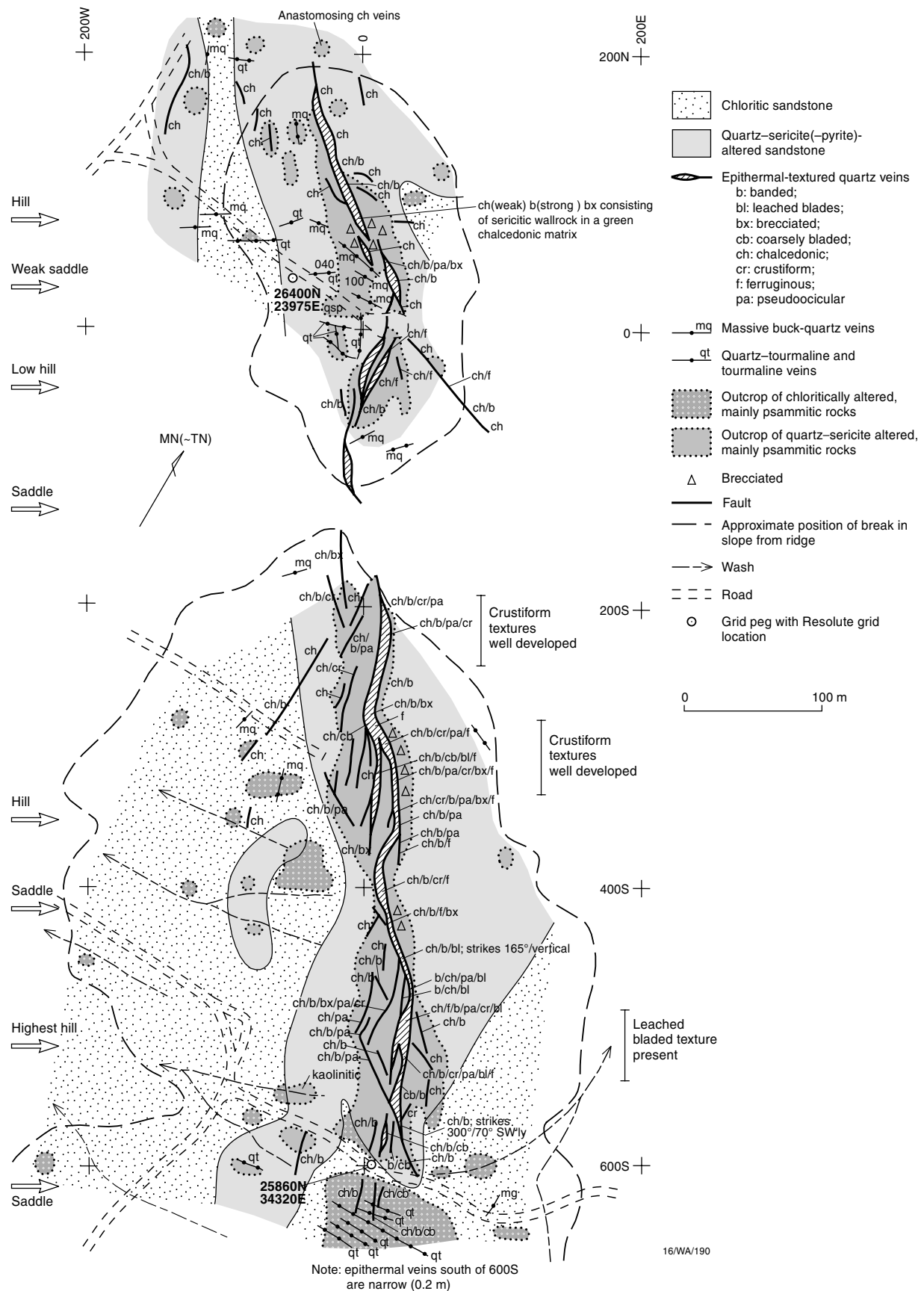


Figure 16. Geology of the Becher deposit

Locality 3.3: Roberts Hill (YULE, AMG 101932)

Return to the Northwest Coastal Highway via the Mallina Homestead. Proceed 3.1 km east along this highway to Roberts Hill, which is located to the south of the highway.

In the Indee district, rocks of the De Grey Group have been affected by intense boron metasomatism, either along zones parallel to bedding or within and adjacent to fault planes. Examples lie within and immediately south of the Mallina Shear Zone, although the most notable example is Roberts Hill, which is north of the shear zone. The tourmaline has iron-rich compositions and is typical of granite-related replacement tourmalinite (Smithies, R. H., 1999, pers. comm.). Both the c. 2935 Ma Satirist Granite and the c. 2765 Ma Opaline Well Granite are locally tourmaline bearing, with the former being a possible source of the metasomatizing fluids.

At this locality, tourmaline–quartz rock has replaced turbidites of unassigned De Grey Group. The rock is mostly massive and locally contains coarse casts after pyrite. Near the top of the hill, quartz veins that cut the tourmaline–quartz rock have been folded, indicating a probable origin during or prior to the last major deformation event.

Locality 3.4: Hill south of Withnell prospect (YULE, AMG 239876)

Continue west along the Northwest Coastal Highway for 6.6 km to a turnoff on the right. Go through the gate and travel for 1.1 km until a junction is reached. Take the left fork and continue for 7.2 km to a second fork. Again take the left fork and drive another 8.6 km to Indee camp (this is where drillcore will be viewed). Continue past the camp for 6.1 km (the road will curve around to the south) until an east–west baseline is reached. Continue south across calcrete to the base of a hill. A poorly formed track follows the base of the hill to the east. Drive east along this track to a saddle in the low range of hills. The best structures are seen along the top of the eastern hill.

At this location, which is about 1.5 km south of the Withnell prospect, many of the structural elements of the Mallina Basin are present in a low ridge of shale and siltstone just south of the Mallina Shear Zone (Fig. 13). Subtle bedding (S_0) can be traced across the width of the ridge and orthogonal to this is the main penetrative fabric — an aS_3 crenulation cleavage associated with mostly tight east–west-oriented upright aF_3 folds. Within the axial hinge of these folds, refolded aF_2 isoclinal folds are preserved, although they are refolded by mesoscale aF_3 folds into type III interference patterns. In the hinge zones to aF_3 folds, the aS_3 axial fabric is demonstrably a crenulation of aS_1/S_3 .

Locality 3.5: Becher prospect (YULE, AMG 209845)

Return to the baseline and travel east along it for 1.1 km until a fenceline is reached. Just before the fence, turn south for 2.6 km until a poorly defined track heads east. Follow this track for 4.3 km to a fork with a track to the south. Turn south for 1.8 km until the Becher ridge is reached.

The Becher prospect is located approximately 6 km south-southeast of the Withnell deposit, along a low north-northwesterly trending ridge. This prospect is characterized by extensive crustiform and chalcedonic vein textures as well as brecciated zones. Epithermal textures, as described in Huston et al. (2000), are well developed for 700 m along this ridge (Fig. 16). The wallrocks adjacent to the vein system are sericitized and contain local (ex-)pyritic zones. The quartz vein cuts a black tourmalinite vein system and the main foliation ($?S_6$), which strikes roughly east–west.

Locality 3.6: Drillcore inspection

Return to the Indee camp where drillcore from Withnell, Becher, and Orange Rock (another epithermal prospect) is laid out.

As the Withnell prospect is poorly exposed, much of the geological data about it has been derived from RC (reverse circulation) drilling. As part of this drilling program, Resolute Ltd drilled four oriented diamond drillholes. Two of these holes are laid out for inspection. Figure 15 is a summary graphical log of drillhole INDD003, which was moderately mineralized. Drillhole INDD004, which was barren, has also been laid out, as well as core from the Becher and Orange Rock prospects.

Return to the Northwest Coastal Highway and travel east for 68 km to the junction with the Great Northern Highway. Turn south and travel 68 km to a crossroad. Turn right and drive 6 km to the Turner River where we will camp.

Part four: The Wodgina tantalum–tin pegmatite district

by M. T. Sweetapple, H. Cornelius, and P. L. F. Collins

Introduction

The Archaean Wodgina pegmatite district is located 130 km south of Port Hedland in the Wodgina greenstone belt, which lies in the centre of the Archaean north Pilbara granite–greenstones (Fig. 17). This pegmatite district contains the world's second-largest tantalum reserve within the Mount Cassiterite pegmatite group (Table 4), and the now-exhausted Wodgina main-lode pegmatite orebody, which supplied up to 80% of the world's tantalum requirements prior to World War II. The Wodgina pegmatite district, centred on the Wodgina openpit mining and processing operation of Sons of Gwalia Ltd (Fig. 18), is probably one of the most tantalum-rich localities exposed on the earth's surface.

Tantalum is primarily used in the electronics industry for the manufacture of capacitors for mobile phones and laptop computers; this use accounts for approximately 50% of production. Other uses include tantalum carbide for cutting tools, pure or alloyed tantalum metal for corrosion or heat-resistant chemical-plant equipment, and in super-alloys for jet engines.

This part of the excursion aims to provide an overview of the geology and mineralogy of these pegmatite orebodies, which are of two distinctly different types: strongly layered pegmatite in the Wodgina North and South pits, and weakly layered to massive pegmatite sheets in the Mount Cassiterite pegmatite group.

The principal units in the strongly layered pegmatites are massive cleavandite (platy variety of albite) and an aplitic–granitic-textured unit. This pegmatite type belongs to Cerny's (1993a) albite pegmatite class. This pegmatite is the largest body of the Wodgina pegmatite group. The weakly layered to massive pegmatite sheets exposed in the Mount Cassiterite opencut belong to Cerny's (1993a) albite–spodumene class, and displays characteristic comb-textured spodumene megacrysts typical of this class. A group of minor pegmatites hosting subeconomic beryl–columbite mineralization is associated with a shear zone on the southern edge of the metasedimentary succession that hosts the Mount Cassiterite pegmatite group (Fig. 18).

Exploration and mining history of the area

Tin and tantalum deposits were first discovered in the Wodgina area in 1901, with a minor 'rush' between 1905 and 1911 when Wodgina was briefly the principal source

Table 4. Tantalum indicated resources and proven and probable reserves within the Mount Cassiterite pegmatite group

<i>Category</i>	<i>Tantalum grade^(a)</i>	<i>Inferred grade of other metals^(b)</i>
Reserve	27 Mt at 420 g/t Ta ₂ O ₅	263 g/t SnO ₂ and 52 g/t Nb ₂ O ₅
Resource	8 Mt at 340 g/t Ta ₂ O ₅	213 g/t SnO ₂ and 42 g/t Nb ₂ O ₅
Total	35 Mt at 402 g/t Ta ₂ O ₅	251 g/t SnO ₂ and 50 g/t Nb ₂ O ₅

SOURCE: (a) Sons of Gwalia data

(b) Inferred from ratios calculated from resource figures and whole-rock geochemistry

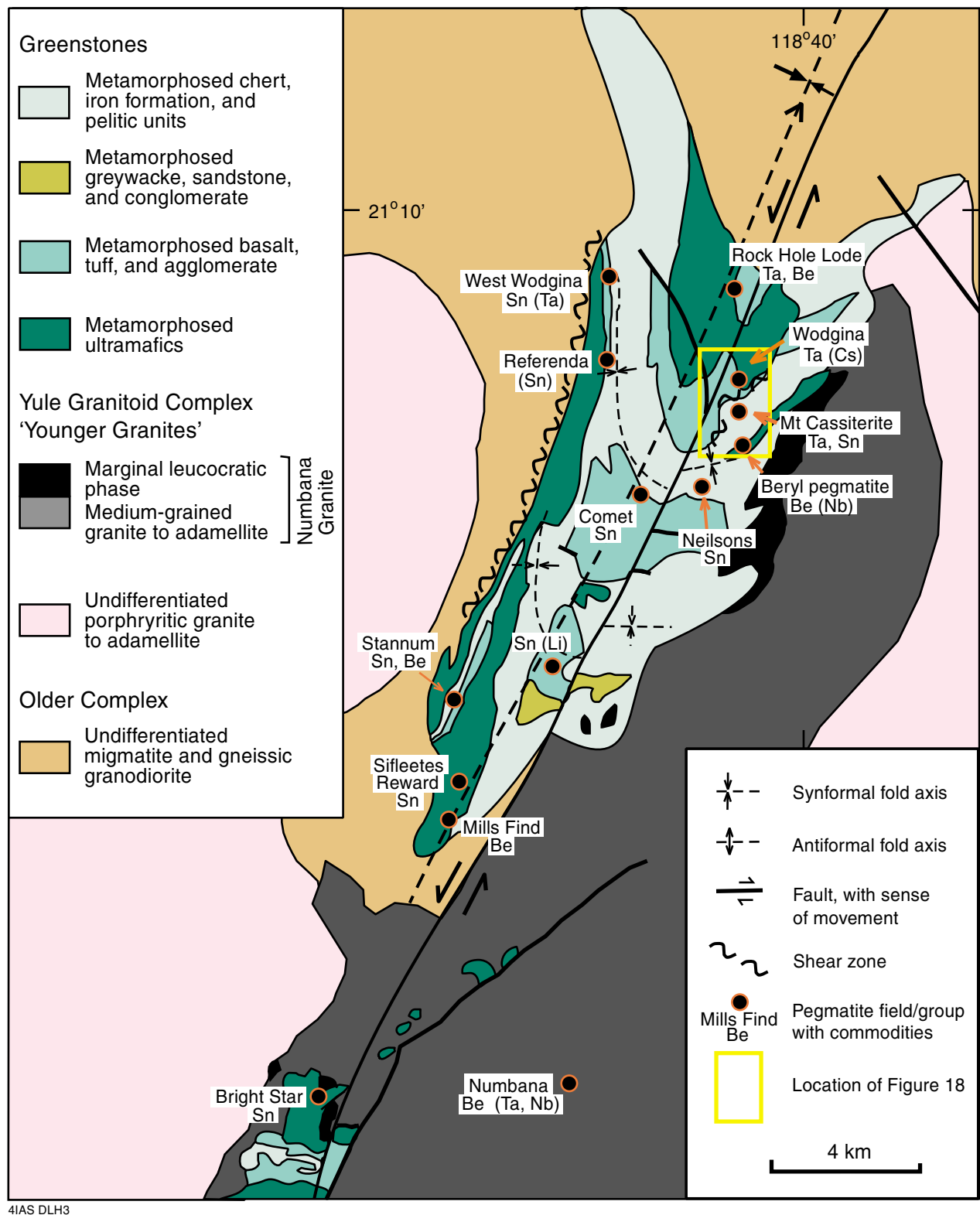
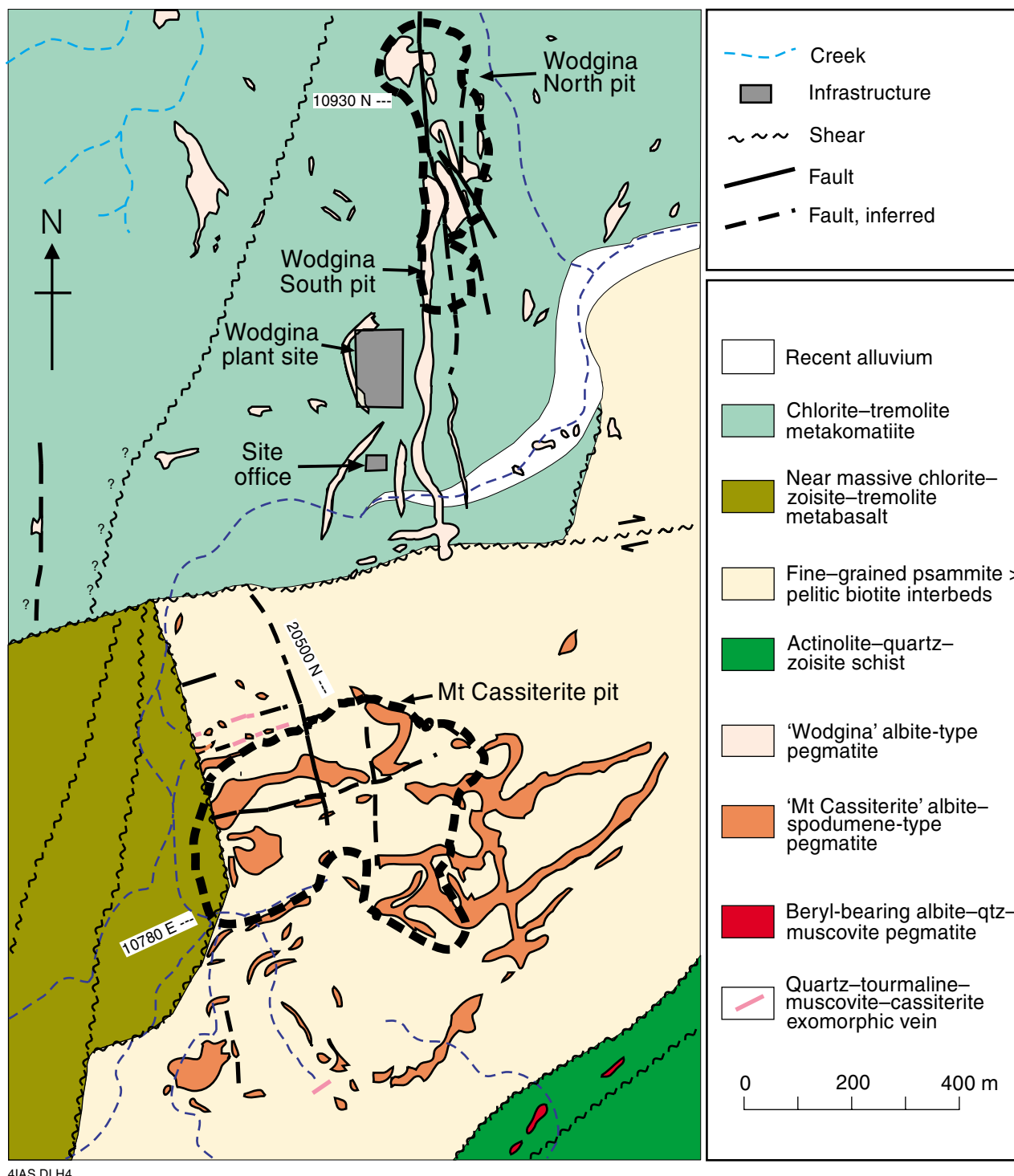


Figure 17. Geological map of the Wodgina greenstone belt showing distribution of pegmatite fields or groups (modified from Blockley, 1980)



4IAS DLH4

Figure 18. Geological plan of the Wodgina pegmatite district showing the location of opencuts

Table 5. Production figures from the Wodgina and Mount Cassiterite orebodies to June 1998

<i>Orebody</i>	<i>Ta–Nb–Sn production^(a)</i>	<i>Other production^(a)</i>
Wodgina main-lode pegmatite	269 t of Ta produced from 1988 to 1994, inferred production of 44 t of Nb ^(b) ; 39.2 t of Ta-bearing concentrates produced from 1905 to 1940 ^(c) negligible	85 t of beryl produced to the end of 1945, including Cs-bearing roosterite beryl ^(e) ; ~51 t of Nb ₂ O ₅ produced as a byproduct of Ta mining; Sn production likely to have been
Mount Cassiterite pegmatite group	308 t of Ta produced to June 1998; inferred production of 193 t of Sn and 39 t of Nb; at least 351 t of Sn-bearing concentrate produced from 1904 to 1918 ^(d)	No known Li (spodumene) production
SOURCES: (a) Historical production records and unpublished data of Sons of Gwalia Ltd (b) Pancontinental Mining unpublished data (c) Records incomplete, Miles et al. (1945) (d) Blockley (1980) (e) Ellis (1950)		

of tantalum for light-globe filaments (Miles et al., 1945). Thereafter, mining of tin and tantalum continued sporadically from the area until 1988, from hard-rock, eluvial, and alluvial sources (Table 5). Initial hard-rock mining was principally for tin, with quartz–mica–tourmaline veins associated with the Mount Cassiterite pegmatite group being the main source of cassiterite. At least 478 t of tin-bearing concentrate was produced from the area between 1902 and the end of World War I (1918), with 369 t coming from hard-rock mining (Blockley, 1980).

Prior to World War II, up to 80% of the world's tantalum requirements was produced from the Wodgina area, principally from alluvial and eluvial workings, with small-scale underground and openpit working of the Wodgina main-lode pegmatite. A total of 150.6 t of tantalite concentrate was produced to 1940, with 39.2 t produced from hard-rock mining (Miles, et al. 1945). A further 11 t of concentrate were believed to have been produced from hard-rock mining from 1941 to 1964 (Hall, 1993). During the latter part of World War II, the Commonwealth Government of Australia undertook production of tantalum as a strategic commodity.

The Wodgina area also has a long-standing reputation as a classic locality for a number of rare mineral species, of scientific as well as economic interest (see Appendix). Wodgina is the type locality for the manganese end-member of the wodginite series (Mn₄Sn₄Ta₈O₃₂), being first recognized by Simpson (1909) as ixiolite. It was then formally identified by Nickel et al. (1963) as wodginite, in conjunction with specimens from Bernic Lake (TANCO), Manitoba, Canada. Simpson (1928) recognized a total of 77 mineral species of scientific interest within a 20-mile radius of Mount Tinstone (Latitude 21°12'S, Longitude 118°40'E). Simpson (1928, 1952) also documented significant occurrences of rare phosphate (lithiophilite) and thorium minerals (thorite, thorogummite) in the Wodgina main-lode pegmatite.

Production and resources since 1988

The Wodgina main-lode pegmatite was mined out (in the area shown in Figure 18), from 1988 to 1994, based on proven reserves averaging 0.402 Mt at 1283 ppm Ta₂O₅ and 211 ppm Nb₂O₅ (Pancontinental Mining Ltd, unpublished data). From July 1994, hard-rock mining has been proceeding at Mount Cassiterite in the area outlined in Figure 18. Sons of Gwalia Ltd have managed the mining operation since 1996. Between July 1997 and June 1998, tantalum production from the Mount Cassiterite operation constituted the world's second-largest source, contributing 7.25% of world tantalum production (170 000 lbs of Ta₂O₅), exceeded only by the giant Greenbushes pegmatite deposit in the Yilgarn Craton. Tin and niobium are obtained as 'credits' in the processing of tantalum concentrate. Table 5 summarizes production in the Wodgina area to June 1998.

Mining operations

The pegmatite is mined by conventional openpit methods from the Mount Cassiterite pit. The earthmoving is carried out by BGC Contracting using a Komatsu PC1100 in a backhoe configuration, which loads Komatsu 785-3 rear dump trucks. Waste and ore is drilled using Tamrock 1100 blasthole drillrigs in 5 m benches and blasted using either ANFO or emulsion depending on ground conditions. The ore and waste is then dug out as two 2.5 m flitches. No conventional grade-control activities are used, as all the grades in the pegmatite (obtained from the reserve model) are currently above the marginal cut-off grade, with efforts instead concentrating on ore spotting. All ore mined is trucked directly to the ROM pad. The processing operations are described in Locality 4.3.

Geological setting

Wodgina greenstone belt

The Wodgina greenstone belt (Fig. 17) is a synformal, north-northeasterly plunging body, approximately 25 km wide north–south and 10 km wide east–west, which is part of the greenstone succession that separates the Yule Granitoid Complex from the Carlindi Granitoid Complex. It is composed principally of interlayered mafic to ultramafic schist to amphibolite, with subordinate komatiite, clastic sedimentary rocks, BIF, and chert (Blewett et al., in press). Metamorphism probably ranges from lower greenschist to lower amphibolite facies, with relatively low pressures (indicated by absence of garnet). Mapping by Hickman (1975) and Blockley (1980) suggests that the broad synformal structure refolds an earlier generation of folds, which had an axial surface roughly perpendicular to the axial surface of the synform.

The stratigraphic succession that comprises this greenstone belt has not been correlated with any certainty with the stratigraphy of other greenstone belts (Blewett et al., in press). However, it is likely that the komatiitic and metasedimentary units in the vicinity of the Wodgina pegmatite district correlate with the Kunagunarrina and Leilira Formations respectively, of Van Kranendonk and Morant (1998).

The Wodgina greenstone belt contains several significant pegmatite fields in addition to those contained in the Wodgina pegmatite district (Fig. 17). These other pegmatite fields were mined on a small scale, primarily for tin, mostly prior to World War I. Details of these latter pegmatite fields may be found in Blockley (1980) and Sweetapple (2000).

Host rocks and structure of the Wodgina pegmatite district

The Wodgina pegmatite district lies on the eastern limb of the synformal structure of the Wodgina greenstone belt, immediately adjacent to the trace of the axial surface of the synform. On a regional scale, the three main pegmatite groups appear to lie on a second-order splay structure related to a major craton-scale northeast-trending lineament.

Each of the major pegmatite groups is hosted within a different lithology and has different structural controls (Fig. 18). The Wodgina and Mount Cassiterite pegmatite groups are separated by a major north-northeasterly trending shear zone with a sinistral sense of movement, which appears to be displaced 750 m in a dextral sense by a east-northeasterly trending shear zone. Pegmatite emplacement postdates movement on these structures, as the Wodgina main-lode pegmatite cuts the dextral shear zone.

The Wodgina main-lode pegmatite

Geological overview

Mining was completed in the Wodgina pit in June 1994 and some of the lower levels of the pit are now flooded. Mining of the Wodgina main lode was undertaken over a 600 m strike length, concentrating mostly on the northern end of the pegmatite where the thickest segments were located. The majority of the pre-1988 hard-rock mining had taken place adjacent to a quartz core just to the south of the Wodgina north pit, and in the southern extension of the lode, immediately next to the modern processing plant and old headframe.

The Wodgina pegmatite group is almost entirely hosted within a succession of variably foliated metakomatiite, with subordinate metabasalt and dolerite (Figs 19 and 20). The metakomatiite has a metamorphic mineralogy of tremolite–magnesium–chlorite(–zoisite–magnetite). This succession shows a broad north- to northeast-trending foliation dipping 25–60° to the west. The northern face of the Wodgina North pit shows evidence of reclined flexural-slip folding with the axial surface lying roughly in the plane of the foliation.

The Wodgina main-lode pegmatite has been emplaced with a reverse sense of movement into a dilational zone within an east-dipping shear zone array in brittle to semibrittle conditions, with subordinate exploitation of west-dipping structures. The Wodgina main-lode pegmatite has a total strike length of 1 km and is 5–40 m thick. The structure of the mined portion broadly comprised an east-dipping sheet intruding into a fault at the south end of the body, which became bulbous and partly saddle shaped at the north end, and centred around an irregular quartz core (up to 50 m wide and 60 m long) that was originally exposed at surface. Emplacement of the northern end of the main-lode pegmatite appears to be partially controlled by pre-existing folding. The northern part of the pegmatite was subsequently disaggregated by a number of later normal and reverse faults. Some evidence exists for an open near-upright folding event that subsequently affected the pegmatite. Intrusion of the pegmatite also produced local contact metamorphism of the host metakomatiite in the form of serpentine hornfels.

Mineralization

The principal tantalum mineral in the Wodgina main-lode pegmatite is manganotantalite, with subordinate manganocolumbite and wodginite and minor amounts of defect microlite and fersmite alteration (Table 6). Sweetapple and Collins (1998) noted a different metallogenic signature between the Wodgina main-lode pegmatite and the Mount Cassiterite pegmatite group, with the Wodgina main-lode pegmatite having a higher Nb:Ta ratio, and the Mount Cassiterite pegmatite having a higher Sn:Ta ratio.

Tantalum mineralization appears to have a primary magmatic origin, co-crystallizing in the cleavandite units with albite, and commonly resulting in an unusual intrafasiculate or graphic texture (Fig. 19). Tantalum minerals are uncommon outside of this unit. Visible tantalum minerals are mostly either at the core of the radial cleavandite aggregates or at the base of the massive cleavandite units. This later observation suggests that some of these tantalum minerals crystallized before the cleavandite and were dense enough to sink to the bottom of this unit. Limited redistribution of tantalum mineralization has taken place with the development of the secondary lepidolite (lithium muscovite) units. The grain size of the tantalum minerals varies considerably, from less than 250 µm diameter to exceptional megacrystic masses

Table 6. Tantalum–tin–niobium mineral assemblages observed in different pegmatite groups (after Sweetapple et al., 2000b)

<i>Pegmatite group</i>	<i>Primary mineralogy</i>	<i>Alteration mineralogy</i>
Wodgina ^(a)	Mn-tantalite, Mn-columbite, wodginite, ?cassiterite	defect microlite (high Ca) ^(b) , ?microlite, fersmite, ?ryersonite
Mount Cassiterite ^(a)	Mn-tantalite, Mn-columbite, wodginite, ?ferrowodginite, cassiterite	microlite, ?defect microlite (high Ca) ^(b) , ?calciotantite
Beryl pegmatite	Mn-columbite	microlite, defect microlite (high Ca) ^(b) , plumbo-microlite

NOTES: (a) High Mn and Ta contents are common, a feature typical of highly fractionated pegmatites
(b) Refers to microlite with a significant amount of A-site vacancies

of up to 250 kg, which were recovered in pre-World War II mining (Simpson, 1928; Ellis, 1950).

Additionally, within the main-lode pegmatite two large masses of translucent clear to grey caesium-bearing ‘rosterite’ beryl were noted (Ellis, 1950). Miles et al. (1945) noted that several hundred tons of this beryl was exported to the USA. This mineral was entirely mined out prior to the period of modern mining (Blockley, J., 2000, pers. comm.).

The Mount Cassiterite pegmatite group

Geological overview

The Mount Cassiterite pegmatite group is hosted in a succession of fine-grained psammites with millimetre- to centimetre-scale pelitic biotite interbeds and subordinate quartzite and chert beds. This host succession is weathered up to 80 m below surface, whereas the pegmatites show variable degrees of kaolinitization to 50 m depth.

The Mount Cassiterite pegmatite group, as exposed in the pit, dominantly comprises two sets (the upper and main sheets; Fig. 21) of 5–80 m-thick stacked sheets that typically dip 20–25° to the southeast, but locally ‘roll-over’ to 15–20° to the southwest. Subordinate near-vertical dykes strike roughly northwest–southeast or northeast–southwest. Most of the major sheets and dykes appear to be interlinked by thin fingers or stringers of pegmatite. Compared with the Wodgina pit, relatively little faulting appears to have affected the pegmatites, although some steeply dipping faulting is noted on some pegmatite contacts. This pegmatite group covers a total surface area of approximately 1.1 × 0.8 km (including all related bodies; Fig. 18). Drilling has identified a third (basal) sheet beneath the upper and main sheets (Fig. 22), which has lower grade mineralization (average 140 ppm Ta₂O₅ across the sheet). The basal sheet is 50 to 200 m thick, the footwall being up to 400 m below the surface.

Two generations of foliations are present in these metasedimentary rocks, each associated with a folding event. An early S₁ foliation is best seen in the biotite schist component, which is overprinted by a later (S₂) foliation that strikes between northeast and east, dipping between 30–80° west, and having an axial-planar relationship with dominantly Z-vergent, tight to isoclinal, north-plunging folding. In the upper part of the north wall of the pit, interference between the two generations of folding produces spectacular refolding patterns (close to type III interference patterns).

The pegmatite sheets appear to be emplaced into a series of thrusts, as evidenced by the reverse sense of movement along the contacts. Other subordinate intrusions are controlled by a range of local structures, including normal faulting and bedding. The

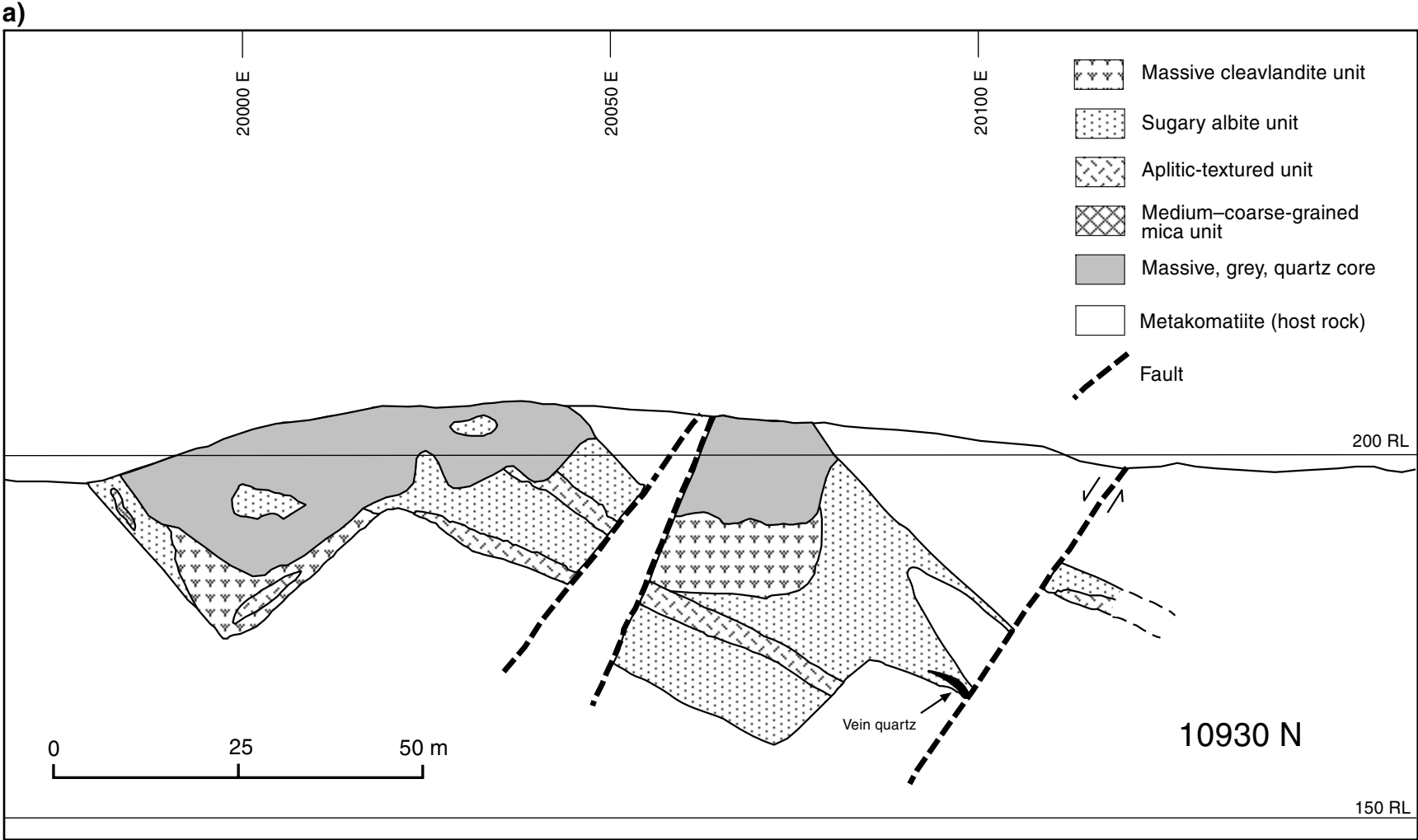
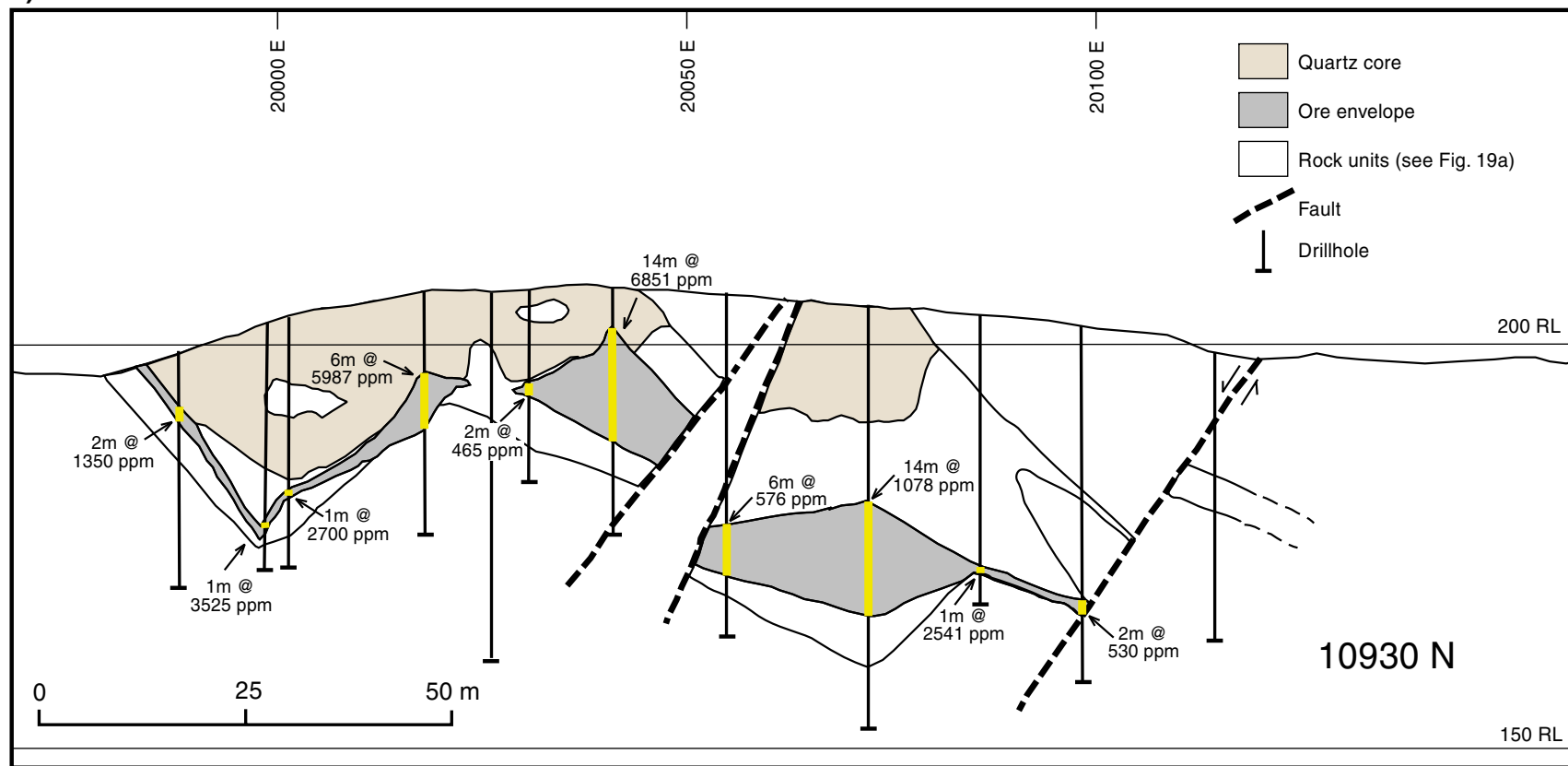


Figure 19a. Cross section 10930N (looking north) at Wodgina pit showing interpreted geological cross section of the internal structure of the Wodgina pegmatite

b)



4IAS DLH13

Figure 19b. Cross section 10930N (looking north) at Wodgina pit showing RC drillhole intercepts and ore envelope within the Wodgina North pit (Pancontinental Mining Ltd, unpublished data; grades in ppm Ta_2O_5)

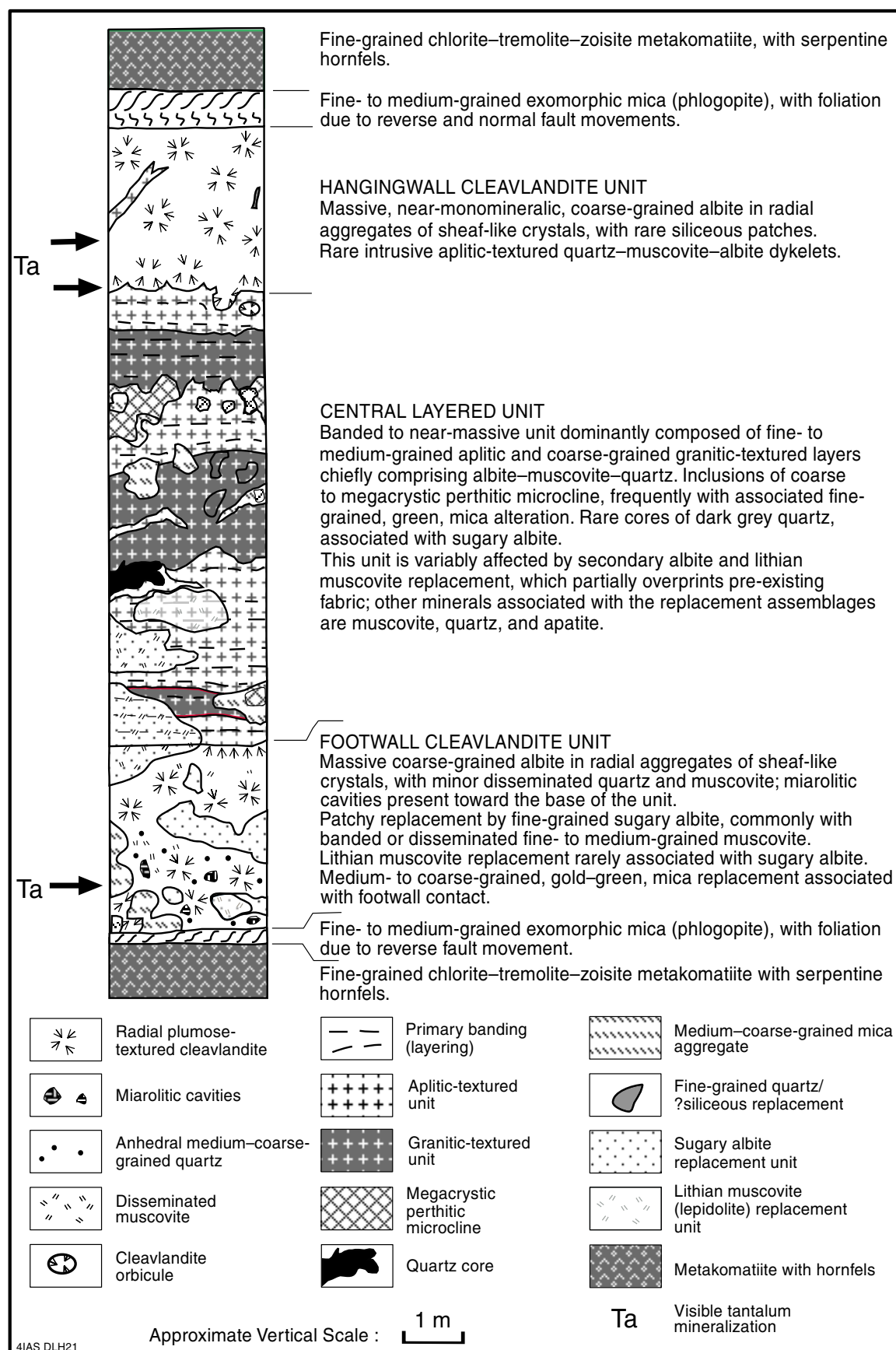


Figure 20. Representative stratigraphic column of rocks exposed in the Wodgina South pit, showing location of visible tantalum mineralization. The pattern of regular layering seen in the south pit progressively decreases northwards within the Wodgina North pit

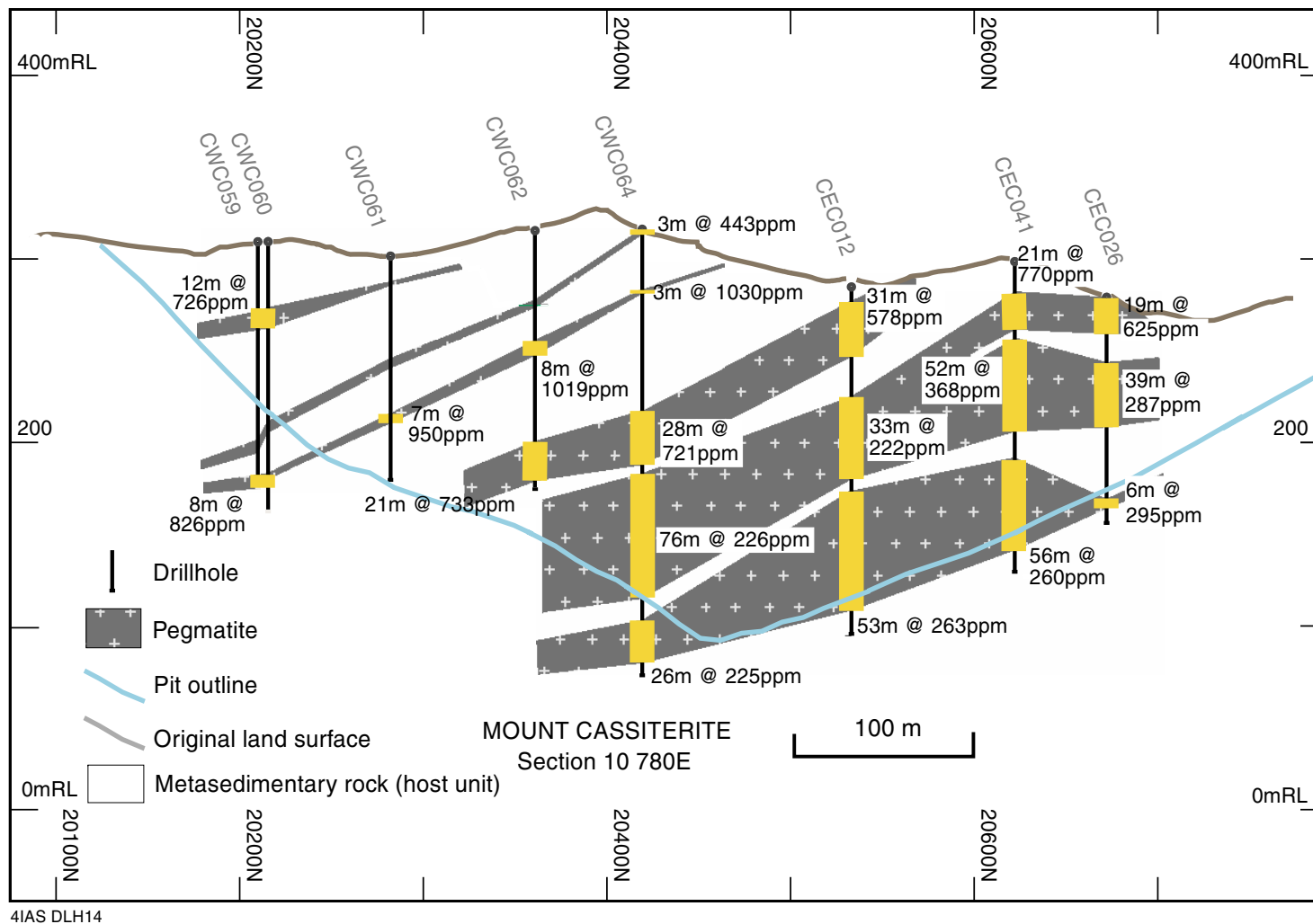


Figure 21. Long section of the upper and main sheets of the Mount Cassiterite pegmatite along 10780E, showing RC drillhole intercepts. Grades shown are ppm Ta_2O_5

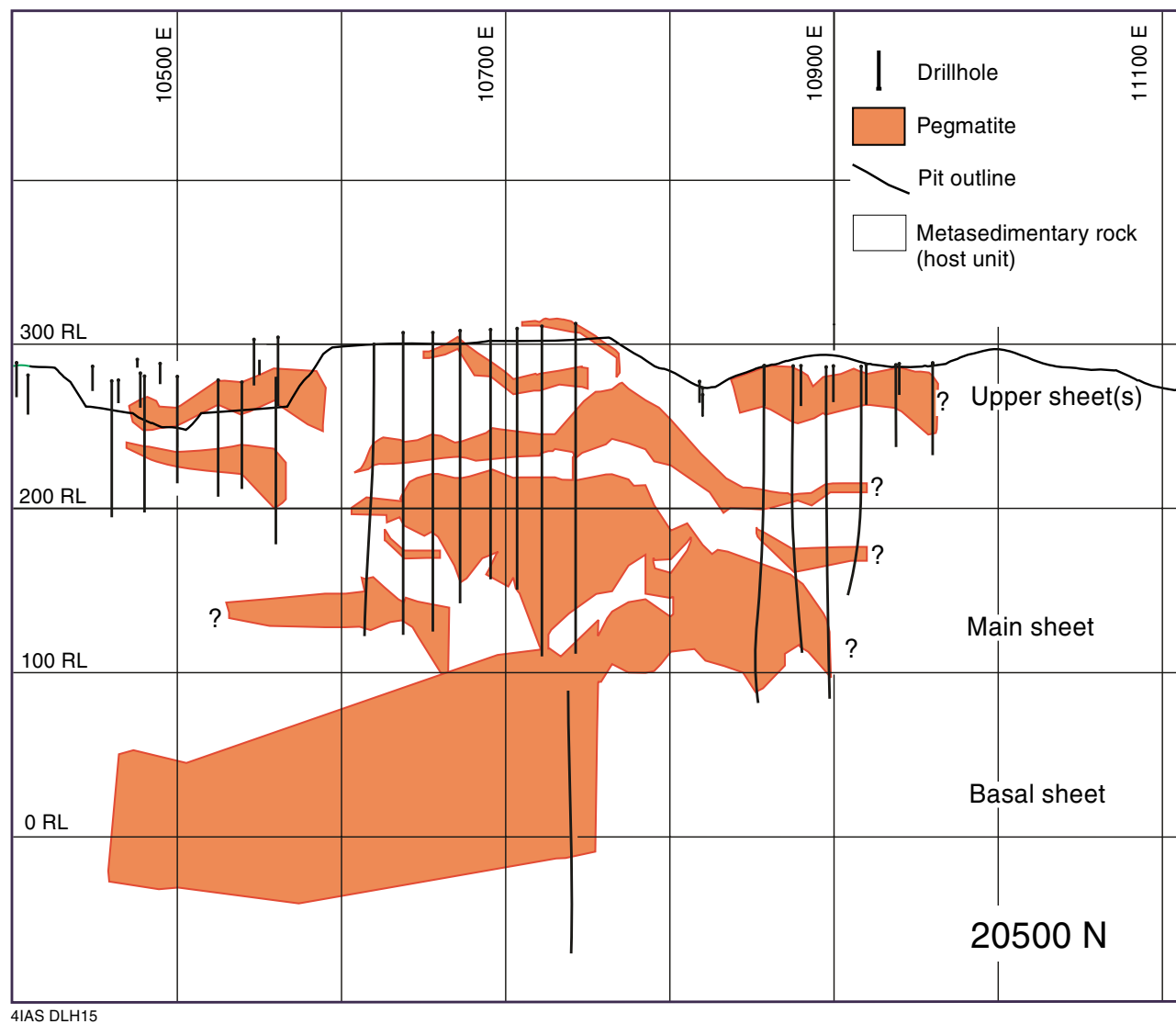


Figure 22. Cross section showing the outline of the upper, main, and basal sheets of the Mount Cassiterite pegmatite group along 20500N, together with drillhole traces

thrusts do not appear to be related to any other structures and it is postulated that they may be due to displacement of the greenstones by an underlying intrusion of the 'younger granite', which may have a similar sheeted morphology typical of this granite suite (Champion, D. C., 2000, pers. comm.).

Whereas the dominant sheeted nature of the main pegmatite bodies is readily apparent in the pit walls, examination of the exposures in the southern pit face shows the development of 'saddle-like' features in both northeast and northwest orientations. In cross section these structures appear as irregular keels and domes (Fig. 22). It is suggested that the nature of this structure has both a magmatic and structural origin, with the northeast orientation partially controlled by S_2 fold limbs. On a large scale, this structure has a flattened 'M' form, with a synformal indentation in the roof (Jankowski, P., 2000, pers. comm.).

Mineralization

The main economic minerals are wodginite and cassiterite (containing wodginite inclusions and development of tapiolite substitution of tantalum and manganese for tin), with subordinate manganocolumbite and manganotantalite, and associated microlite alteration with traces of fibrous calciotantite (Table 6). These minerals appear to be variably distributed throughout the pegmatite sheets at levels above 80 ppm Ta_2O_5 (e.g. Fig. 21). Overall, no internal controls are noted, except for some of the lower sheets where elevated tantalum values are accompanied by elevated caesium and rubidium in association with host-rock contacts and xenoliths. Tantalum mineralization of the deeper pegmatite sheets, however, becomes weaker. The grain size of tantalum–tin minerals rarely exceeds 500 μm , with a range of 100 to 250 μm being more common. A small amount of microlite, 5–10 μm in size, is sometimes associated with altered wodginite. Tantalum–tin minerals appear to be unaffected by syntectonic deformation. However, a minor degree of comminution and fracturing is present, which is consistent with observations made by Cerny et al. (1992) for the Marsikov pegmatite (Czech Republic), when there is no reaction with later fluids.

Discussion

It is now widely accepted that rare-metal pegmatites owe their origin to the migration of hydrous residual magmatic phases of cooling granite bodies, as opposed to metamorphic–anatectic theories of pegmatite genesis (e.g. London, 1996; Cerny, 1992, 1998). These phases are highly enriched in incompatible elements, which accumulate in the apical portions of highly fractionated granite plutons. The relationship between the 2880 Ma 'younger' granite suite and rare-metal pegmatites has been well documented for the north Pilbara granite–greenstones (e.g. Blockley, 1980; Sweetapple, 2000). In the case of the Wodgina pegmatite district, strong field, geochemical, and geochronological evidence provide a link to the Numbana Granite of the 'younger' granite suite (Fig. 17; Blockley, 1980; Sweetapple and Collins, 1998; Kinny, 2000; Sweetapple, et al., 2000a).

Neither pegmatite group displays the classical concentric internal zoning often ascribed to complex, highly fractionated pegmatites (e.g. Cameron et al., 1949; Norton, 1983), which appears to be a pattern that is more the exception than the norm (e.g. Cerny, 1993a). The albite–spodumene pegmatite class as seen at Mount Cassiterite displays little primary internal layering or zoning, but displays the typical comb-textured spodumene crystal array that is characteristic of this pegmatite class (e.g. Cerny, 1989). Experimentally based explanations of internal pegmatite evolution by London (1990, 1996) invoking a magmatic–hydrothermal transition, support the relative rarity of this

type of internal structure. Many of the textures seen have been replicated in London's (1990) experiments from supercooled liquids far from equilibrium.

Strong field and geochemical evidence exists to link the two pegmatite groups; both pegmatites show a similar degree of extreme fractionation of lithophile-element ratios. The southernmost end of the Wodgina main-lode pegmatite group contains a pod of albite–spodumene pegmatite, which suggests a direct link between the two pegmatite groups. Cerny (1992) indicates that London's (1990) petrogenetic model supports the generation of such a residual sodic melt from a semiconsolidated complex pegmatite melt, via a mechanism of substantial concentrations of fluxing elements (e.g. boron, phosphorus, fluorene), shifting the residual melt towards a sodic composition. This experimental model appears to be a valid explanation of the relationship between these two pegmatite groups, as part of a larger regional pegmatite-zonation pattern (e.g. Cerny, 1993a,b).

Both pegmatites belong to the LCT (lithium–caesium–tantalum) petrogenetic class of Cerny (1993a), as they are characterized by a strongly peraluminous composition and a strong enrichment in rare alkali-earth elements and tantalum (Sweetapple and Collins, 1998), as well as other geochemical and spatial criteria.

Tantalum mineralization is interpreted to have a primary magmatic origin, being introduced by pegmatite intrusions. Subsequent internal evolution of the pegmatite bodies has had relatively little influence on the distribution of tantalum mineralization. Both pegmatites display an extreme degree of fractionation consistent with the presence of high-grade tantalum mineralization. The Mount Cassiterite pegmatite group is particularly significant in this regard, as it displays K/Rb and Nb/Ta values markedly lower than those listed for this pegmatite type by Cerny (1989, 1993b).

Excursion localities

Both deposits lie within the infrastructure of the Wodgina mining operation and permission is required from the mine manager to obtain access. **Safety regulations and directions must be complied with at all times.**

From the Turner River campsite proceed back to the Great Northern Highway. Cross this highway and travel 7 km until the mine office is reached. Sons of Gwalia Ltd personnel will guide the excursion to the various localities.

Locality 4.1A: Wodgina South pit (WODGINA, AMG 738570)

The Wodgina main-lode pegmatite as exposed in the south pit shows a distinctive layered structure with discordant replacement units (Table 7). The relationship between the different units is shown schematically in Figure 20. The primary units are hangingwall and footwall massive cleavandite units of coarse platy albite, and a central partly banded aplitic–granitic-textured unit containing megacrystic perthitic microcline. The massive cleavandite unit is virtually monomineralic and has an internal radial crystallization pattern. A dark-coloured metasomatized gabbroic xenolith is present roughly in the centre of the pegmatite. Where the host metakomatiite is in contact with the pegmatite, there is an exomorphic zone of phlogopite approximately 5–30 cm thick. Petrographic examination of these different units almost invariably shows some degree of recrystallization. This is interpreted as principally being a primary magmatic feature due to the presence of late-stage primary pegmatite minerals such as apatite and fluorite, which are associated with the latest stages of recrystallization.

Table 7. Mineralogical units within the Wodgina main-lode pegmatite (after Sweetapple, 2000)

<i>Unit^(a)</i>	<i>Description of assemblage</i>
Cleavlandite unit	Massive coarse cleavlandite with rare quartz, spessartine, and muscovite; contains visible tantalite mineralization
Micaceous unit	Fine- to coarse-grained, layered, aplitic to granitic textured, muscovite–albite–quartz(– megacrystic perthitic microcline) with or without patches of interstitial fine-grained green-mica alteration of microcline
Quartz Core	Massive dark-grey quartz (poorly represented in existing exposure)
Albite replacement unit	Fine-grained saccharoidal-textured albite with minor quartz and muscovite; trace fine-grained blue apatite at some locations
Lithium alteration unit	Fine-grained lithian muscovite(lepidolite)–albite alteration of the micaceous unit; typically patchy and localized; occasionally associated with the albite replacement unit

NOTE: (a) Units typically bear no constant relationship to each other in terms of sequence and thickness, which may be related to syntectonic disturbance

A sharp lobate to cusate internal contact is present between the massive cleavlandite and aplitic–granitic-textured units (forming ‘loadcasts’). In the uppermost bench, orbicules of the cleavlandite unit are present within the hangingwall surface of the aplitic unit. The nature of these textures suggests the co-existence of both units, at least as partial melts of a gel-like or plastic nature.

Locality 4.1B: Wodgina North pit, east wall of ramp (WODGINA, AMG 738570)

Exposure of the Wodgina main-lode pegmatite in this section of the pit contains broadly the same units as found in the south pit. The principal difference is the change in relative position of the granitic–aplitic-textured unit, which appears to lose some of its regular structure and position within the pegmatite closer to the hangingwall surface. The massive cleavlandite units appear to be less pure at this location than in the Wodgina South pit, having internal zones with disseminated very fine green muscovite, as well as discontinuous bands and patches of fine- to medium-grained muscovite. Much of the massive cleavlandite unit has been recrystallized or subjected to replacement by the sugary textured albite unit. Crystallization of the banded granitic–aplitic units appears to have taken place more or less in the current structural position, as evidenced by the orientation of the 20–50 cm-thick aplitic bands in the footwall at this location.

The north end of this pegmatite is affected by a pre-intrusion fault and associated drag folding, which may be an accentuation of pre-existing folding. Notably, the upper part of the pegmatite terminates in sharply tapered irregular sills, probably due to the pegmatite intrusion being able to effectively exploit the reverse structure at the base of the northern end of the intrusion.

Locality 4.2A: Mount Cassiterite pit lookout (WODGINA, AMG 737559)

An effective overview of the dominant sheeted form is provided in the pit walls. Particular features of note are near flat-lying primary layering in the south wall. This primary layering is composed of fine-grained, equigranular, aplitic and quartz-rich layers, typically parallel to pegmatite contacts. Such layering appears to be similar in nature to the layered structure developed in the Wodgina pit, and often is interspersed with bands of the comb-textured columnar spodumene unit.

In the north wall, two unusual intrusive features are notable: an ‘escape structure’ on the upper surface of the uppermost pegmatite sheet, and a blunt-ended dyke segment

below the upper pegmatite sheet. The former structure may have formed as a response to a local failure in the hangingwall of the upper sheet where pegmatite magma pressure has significantly exceeded the tensile strength of the wallrock. The latter feature is related to dyke propagation, where magma pressure, inducing dilation of the dyke, has been taken up by either adjacent shears or local offshoots intruding shear fractures (i.e. the ‘horns’ at the termination of the dyke), or both.

Locality 4.2B: Mount Cassiterite pit floor (WODGINA, AMG 737559)

The exposed mine faces of the pegmatite display the massive to weakly layered textural units typical of albite–spodumene pegmatites documented elsewhere (e.g. Kings Mountain, USA, Kunasz, 1982; Koralpe, Austria, Göd, 1989; Afghan examples, Shmakin, 1992). The dominant textural unit is the primary comb-textured megacrystic spodumene(–perthitic) microcline in a fine-grained quartz–albite–muscovite matrix (Fig. 23). Spodumene crystals are aligned roughly perpendicular to pegmatite contacts exhibiting distinctive ‘pull-apart’ structures, which is a common feature of many pegmatite bodies (e.g. New Mexico examples, Jahns, 1953; Greenbushes pegmatite, Han, 1990). Weak primary layering is observed chiefly in the development of aplitic layers, fine-grained albite–mica border units, and indistinct bands with concentrations of megacrystic microcline. Rare small quartz cores (<3 m long) are locally present. Marginal exocontact mica (probably a rare alkali muscovite), usually of 10–30 cm thickness, is developed along host-rock contacts.

Commonly, the primary elements are overprinted by sugary-textured albite of a secondary (i.e. late pegmatitic) origin, usually accompanied by fine-grained muscovite, which forms a pseudo-gneissic fabric. This fabric probably has a syntectonic deformational origin associated with pegmatite emplacement. Notably, the micas in this fabric do not show a true foliation, suggesting that final crystallization took place under hydrostatic conditions after the termination of shearing associated with emplacement. Cerny and Novak (1997) noted that albite–spodumene pegmatites subjected to subsequent metamorphic events still maintain a phase composition similar to the protolith, so significant changes in mineralogy need not be expected.

Locality 4.2C: Core shed

A wide range of textures are present in the diamond drillcore. They may be subdivided according to the varying influence of three criteria: primary pegmatite crystallization, late-stage pegmatite alteration, and syntectonic deformational features.

A significant cause of textural variation within the pegmatite sheets is due to alteration of primary spodumene. This alteration is associated with late-stage pegmatitic crystallization of albite, quartz, and micropertthite. Spodumene is readily destabilized by low-temperature hydrothermal alteration (e.g. Cerny et al., 1981), which produces fine-grained green mica or a buff-coloured albite–mica mass. It is likely that lithium liberated in hydrothermal reactions concentrates in lepidolite and in exomorphic lithium minerals. Interstitial quartz is the most resistant component to alteration and leaves relicts of ‘amoeboid’ texture. Megacrystic perthitic microcline appears to have undergone significantly less alteration, sometimes only featuring in situ fracturing.

Many of the primary minerals (particularly quartz) display varying degrees of recrystallization and subgrain development on the microscale, which may be recognized in hand specimen as lighter or darker ‘coronas’ to coarse mineral grains. Notably, the strongest alteration of the original fabric, which is increasingly developed in the deeper sheets, but also includes some of the high-grade mineralized zones, is that of a massive to strongly foliated (micro)granitic-like texture, as opposed to pegmatitic textures. This

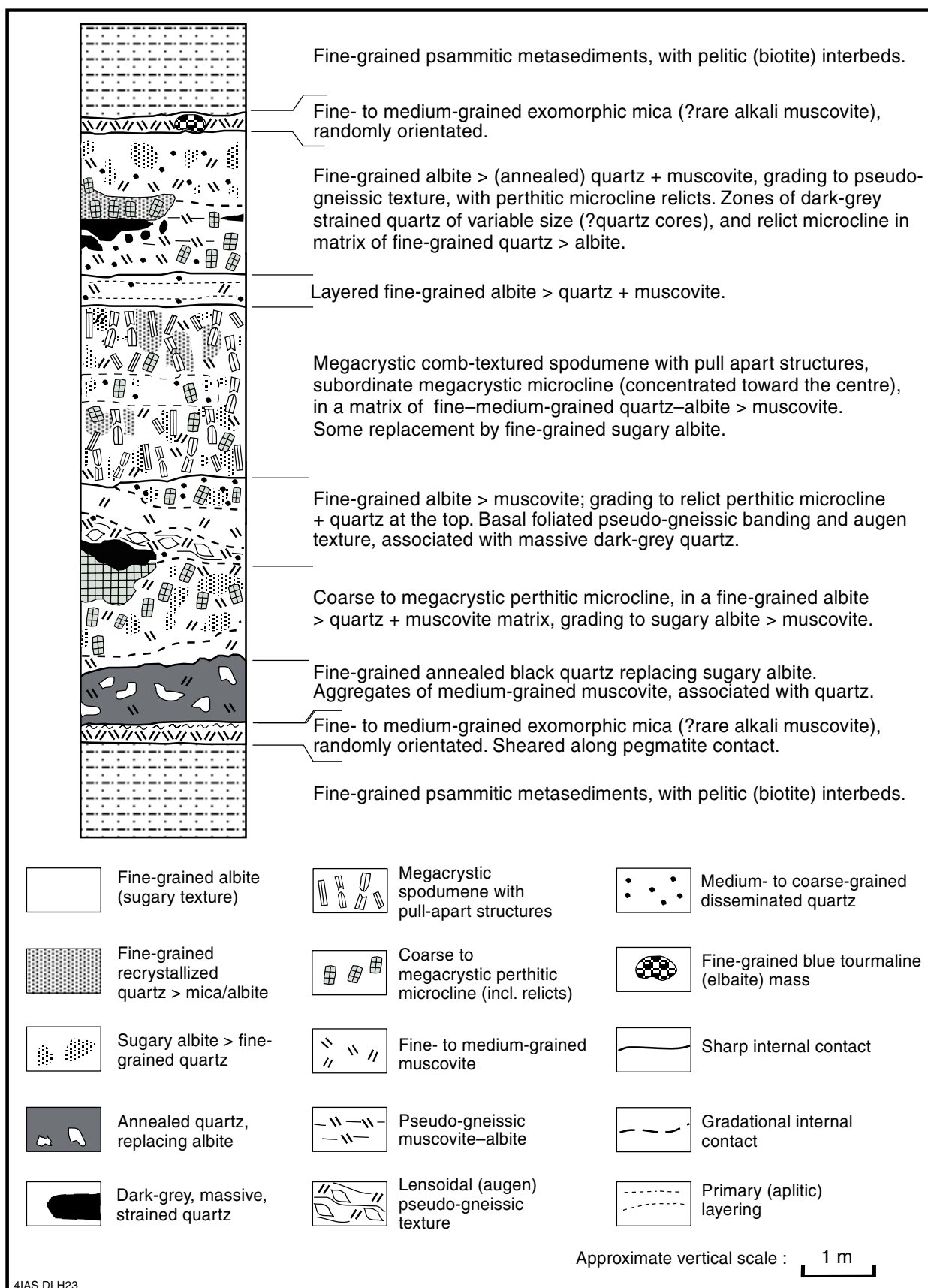


Figure 23. Schematic stratigraphic column showing the textural and compositional nature of the uppermost pegmatite sheet in the west wall of the Mount Cassiterite pit (~260 RL). This column is intended as a general guide to the relationships and nature of mineralogical and textural components within the upper sheets, as considerable lateral variations may be observed within a given pegmatite sheet

unit is characterized by the (almost) complete alteration of spodumene, and the appearance of fine lepidolite and zinnwaldite. This texture is interpreted to have developed after destruction of the primary pegmatitic fabric, associated with secondary fluid movement after the termination of shearing. In some of the lower sheets strong syntectonic deformational fabrics are well developed, including ‘winged’ microcline porphyroclasts and local mylonitization.

Accessory minerals associated with the exomorphic mica include the development of fine-grained aggregates of holmquistite on the outer margins of exomorphic zones, and rare pockets of fine-grained blue elbaite (tourmaline) within the exocontact zone. Coarse pink garnet has also developed in association with veining related to exomorphic activity, following structures in the host rock (i.e. associated with the historically mined ‘tin veins’).

Locality 4.3: Processing plant

Ore from the ROM stockpile is fed directly to the crushing circuit via a front-end loader. The contractors have a three-stage crushing plant on site, with the plant capable of operating at approximately 1.5 Mtpa (or 180 tph) to produce a product of 100%, passing 12 mm final product. The fine ore is then treated in the gravity plant, which has recently been upgraded from a 800 000 tpa capacity to a designed 2.5 Mtpa capacity. The plant uses a gravity separation technique involving a sequence of screening, oversize grinding, spiral, and scavenging circuits. A final concentrate is produced from Falcon concentrators and Holman tables. The product is a filter cake of about 8% moisture, which is drummed and despatched from site as a tantalite concentrate.

Return to and cross the Great Northern Highway. Drive for another 8.6 km, past last night’s campsite, to the Newman railway road. Turn right and continue for about 4 km to the 105.5 km post on the railway. Turn left off the main road and cross the railway. Drive 17.5 km towards the east to a turn-off to the south (you will pass two other turn-offs prior to this). Turn right and continue southeast and then east for 26 km to Strelley Pool where we will camp (after looking at the last locality of the day). To get to the pool, turn right just after crossing Six Mile Creek.

Locality 4.4: Unconformity at Strelley Pool (NORTH SHAW, AMG 221630)

At Strelley Pool the oldest known unconformity in the world is exposed. This unconformity separates the c. 3515 Ma Coonterunnah Group (Buick et al., 1995) from the c. 3430 Ma Strelley Pool Chert of the Warrawoona Group. The upper Coonterunnah Group (Double Bar Formation) is characterized by silicified basalt with well-developed pillows. This unit is unconformably overlain to the south by a silicified sandstone, which forms the base of the Warrawoona Group at this location. The sandstone is overlain by banded chert, which is interpreted as silicified carbonate. This unit, in turn, is overlain by silicified volcanoclastic rocks. Locally, the silicified base of the Warrawoona Group is called the Strelley Pool Chert and can be traced along much of the Pilgangoora Syncline. Elsewhere in the EPGGT, the Strelley Pool Chert is in the upper part of the Warrawoona Group. A succession of relatively unaltered pillow basalt overlies the Strelley Pool Chert.

Part five: The Panorama volcanic-hosted massive sulfide district

by C. Brauhart

Introduction

A brief summary of the regional hydrothermal alteration system and the geology of the Sulphur Springs deposit is given below as background to the excursion localities.

Regional hydrothermal alteration system

The following section summarizes work presented in Brauhart et al. (1998, 2000), and Brauhart (1999). Outstanding exposure across the Panorama district reveals a cross section through a c. 3240 Ma VHMS-bearing volcanic pile and underlying coeval subvolcanic intrusion, in an area of low metamorphic grade and very low strain. This has provided a rare opportunity to map a complete regional-scale hydrothermal alteration system associated with VHMS mineralization, and assess the role of a subvolcanic intrusion in driving such a system.

Volcanic rocks of the Kangaroo Caves Formation range from andesite–basalt to rhyolite in composition, and were extruded in a submarine arc-related extensional tectonic environment. The Strelley Granite was emplaced as a concordant high-level synvolcanic I-type intrusion at the base of the Kangaroo Caves Formation (Fig. 24). SHRIMP U–Pb zircon dating shows that the Kangaroo Caves Formation and Strelley Granite are essentially coeval at 3238 Ma.

Four major alteration facies can be defined in the Panorama district. These are: feldspar-bearing background alteration; feldspar–sericite–quartz alteration; complete feldspar-destructive sericite–quartz alteration; and chlorite–quartz alteration (Fig. 25). These facies affect all of the volcanic pile and the upper parts of the underlying subvolcanic intrusion. Feldspar–sericite–quartz alteration affects the top of the volcanic pile, overlying background alteration, whereas semiconformable chlorite–quartz alteration, towards the base of the volcanic pile, overprints background alteration. Zones of feldspar-destructive alteration extend from the zone of semiconformable chlorite–quartz alteration up to the top of the volcanic pile. These zones crosscut the semiconformable alteration zones, and include transgressive alteration zones that underlie the major VHMS prospects and deposits. Feldspar-destructive alteration centres in the Strelley Granite are spatially coincident with overlying transgressive feldspar-destructive alteration zones in the volcanic pile.

Feldspar-bearing rocks at the top of the volcanic pile are enriched in potassium and silicon, but depleted in sodium, and contrast those at the bottom of the volcanic pile, which are enriched in sodium and depleted in potassium. Sericite–quartz-altered rocks are typically enriched in silicon and depleted in calcium, sodium, and iron, whereas chlorite–quartz-altered rocks, which dominate transgressive feldspar-destructive alteration zones, are marked by potassium–calcium–sodium depletion and magnesium–iron enrichment. Copper and zinc are strongly depleted in rocks at the base of the volcanic pile and, to a lesser extent, in transgressive feldspar-destructive alteration zones (Fig. 26). The amount of metal leached from the volcanic pile is far greater than that contained in known deposits, and thus a magmatic metal source is not necessary to explain the formation of the Panorama VHMS deposits.

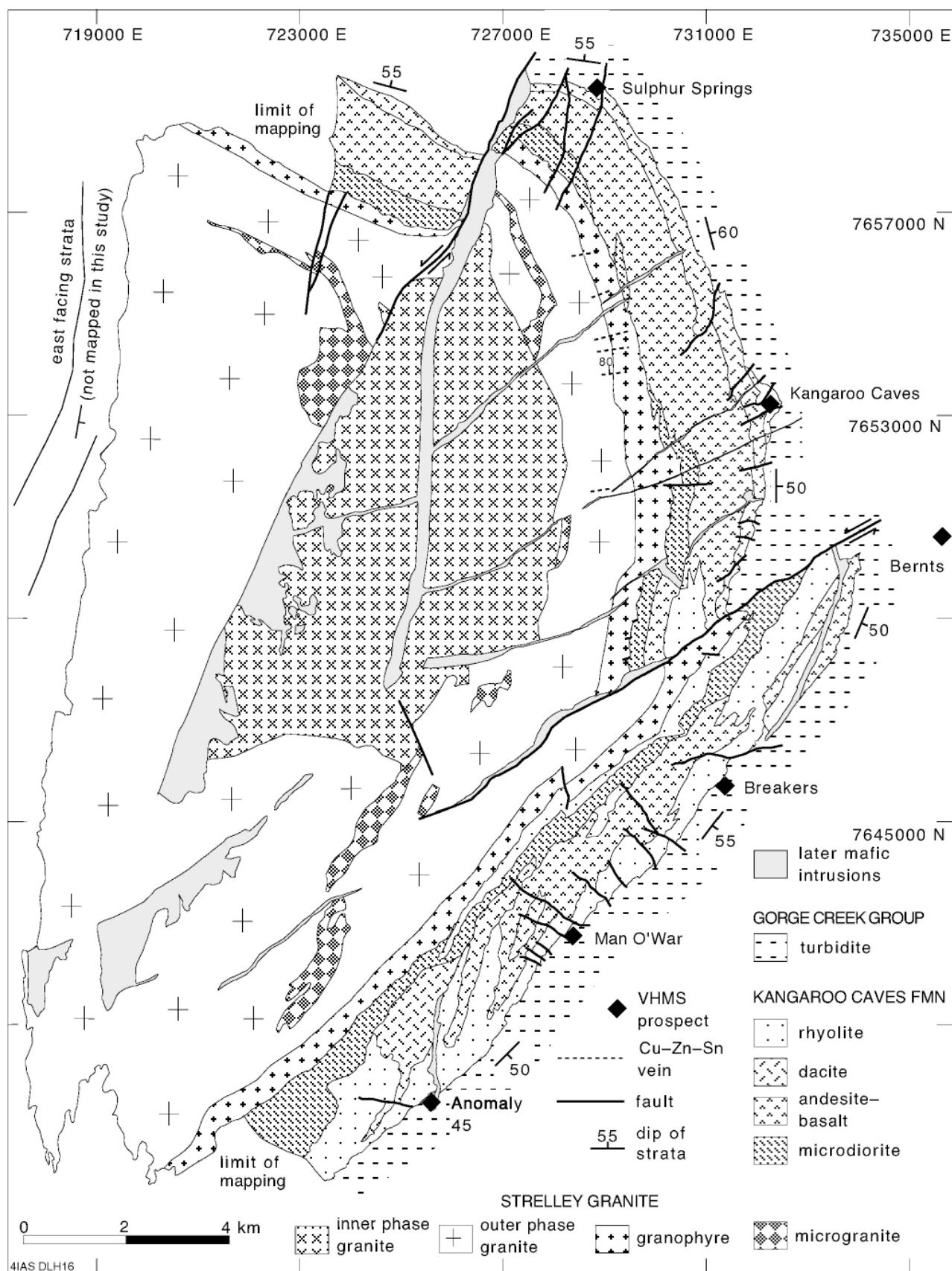


Figure 24. Geology of the Panorama volcanic-hosted massive sulfide district (after Brauhart et al., 1998, 2000)

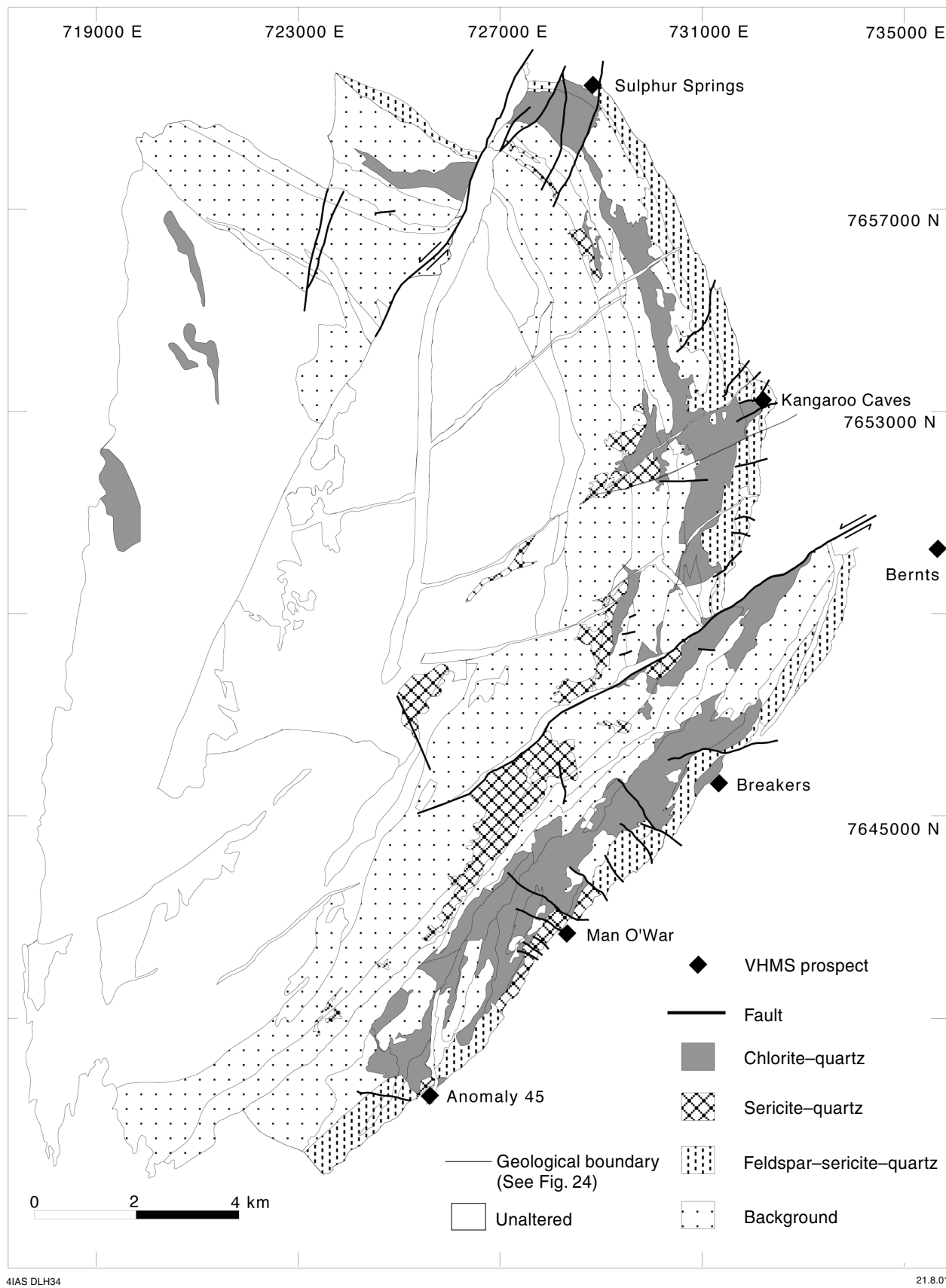


Figure 25. Distribution of alteration facies at the Panorama volcanic-hosted massive sulfide district (after Brauhart et al., 1998, 2000)

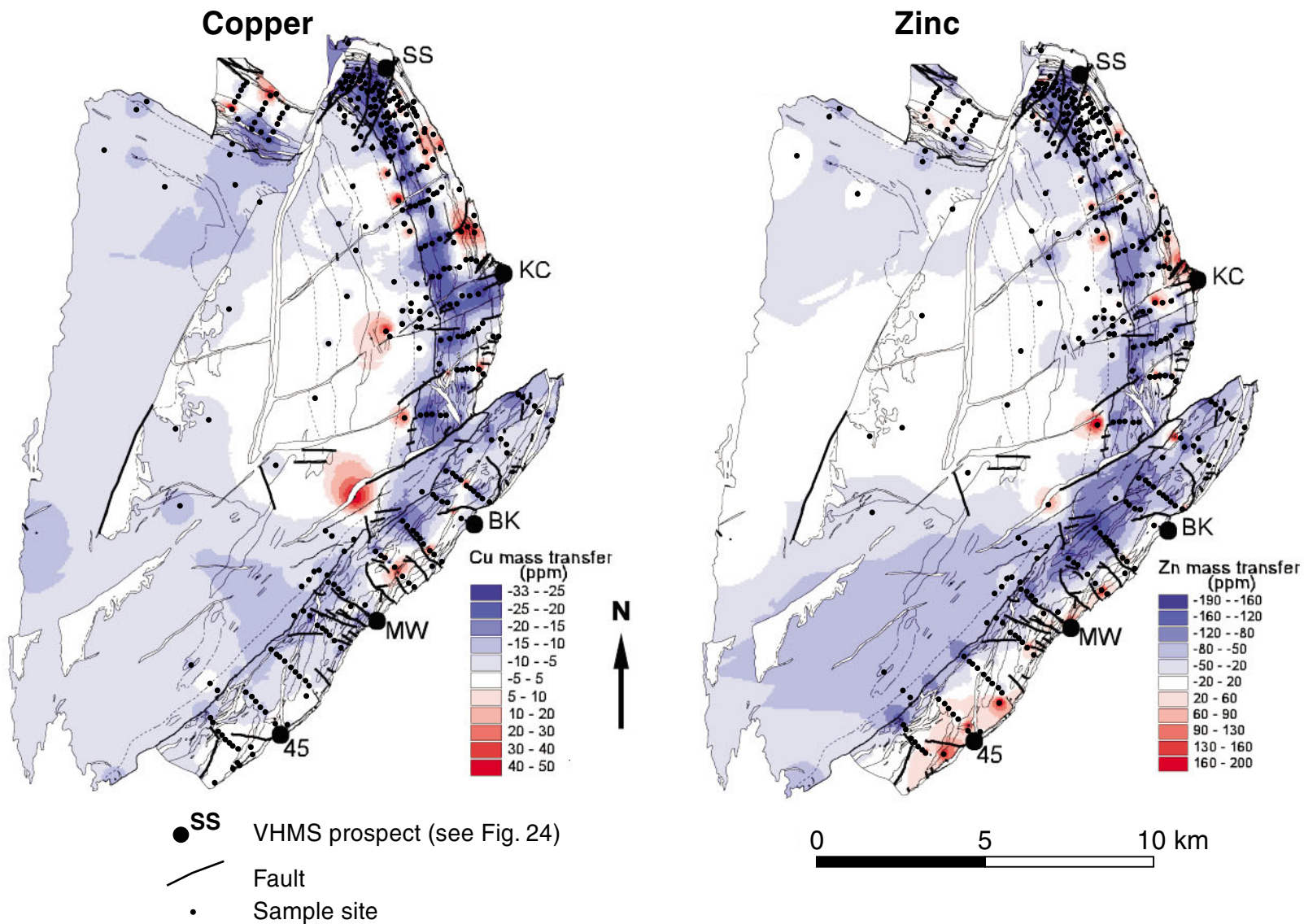


Figure 26. Variations in mass changes of copper and zinc in the Panorama volcanic-hosted massive sulfide district (after Brauhart, 1999)

Whole-rock oxygen isotope data are consistent with a hydrothermal system dominated by seawater, in which low-temperature alteration took place in semiconformable alteration zones at the top of the volcanic pile (high $\delta^{18}\text{O}$ values), and high-temperature alteration took place at the base of the volcanic pile and in transgressive feldspar-destructive alteration zones (low $\delta^{18}\text{O}$ values; Fig. 27). However, $\delta^{18}\text{O}$ values for sericite-quartz-altered granite are more consistent with a dominant magmatic fluid. Fluid exsolution textures, semi-massive copper-zinc-tin veins, and greisen-style alteration in the Strelley Granite provides supporting evidence for a contribution of magmatic fluids at the base of the Panorama VHMS hydrothermal system.

A convective hydrothermal model is invoked to explain this distribution of alteration facies, whole-rock geochemical values, and oxygen-isotope data. In this model, semiconformable alteration zones represent seawater recharge, and transgressive feldspar-destructive alteration zones mark the path of evolved seawater discharging back to the seafloor. The interpreted discharge sites are coincident with base-metal sulfide deposits at the top of the volcanic pile.

Volcanic-hosted massive sulfide deposits

Volcanogenic massive-sulfide mineralization is developed at the top of the volcanic pile immediately below, or within, the marker chert (a regionally extensive unit of silicified volcanoclastic and turbiditic rocks). Drilling has defined measured resources at the Sulphur Springs (estimated at 5.3 Mt at 6.1% Zn and 2.2% Cu), Kangaroo Caves (estimated at 1.7 Mt at 9.8% Zn and 0.6% Cu), and Bernts prospects (estimated at 0.6 Mt at 7.8% Zn and 0.3% Cu). In addition to the potentially economic sulfide body, a comparable tonnage of subeconomic massive sulfide is present at Sulphur Springs. A detailed study of the Sulphur Springs and Kangaroo Caves VHMS orebodies was the basis of a PhD study by Vearncombe (1995a), and the following section is a brief summary of this work (see also Vearncombe et al., 1995).

Drilling and surface mapping has defined two stratiform ore lenses at Sulphur Springs and an elongate stratiform sulfide lens at Kangaroo Caves (Figs 28 and 29). The main ore minerals are pyrite, sphalerite, and chalcopyrite, with minor or trace galena, tennantite, barite, arsenopyrite, and pyrrhotite. Secondary copper sulfides include bornite, covellite, and digenite. There is a strong metal zonation from copper rich at the base of the deposits to zinc rich at the top. Lead (commonly less than 0.5%), gold (commonly <0.2 ppm), and silver (commonly <40 ppm) values are low, but these values are highest in zinc-rich zones. This metal distribution is typical of many VHMS deposits around the world, where the copper-rich zones at the base of the massive sulfide body are interpreted as higher temperature mineralization. The abundance of barite (and quartz pseudomorphs of barite) is unusual amongst Archaean VHMS deposits and more typical of Phanerozoic deposits. This feature was used by Vearncombe (1995a) to argue that ambient seawater at the time of mineralization was sufficiently oxygenated to oxidize H_2S to SO_4 . Minor pyrrhotite and arsenopyrite in the ore demonstrate that the initial ore fluid was reduced below the $\text{SO}_4\text{:H}_2\text{S}$ buffer (Vearncombe, 1995a).

These primary textures are extremely well preserved and therefore allowed detailed study. As such, Vearncombe (1995a) documented a zonation from massive, granular, honeycomb, and filigree textures at the base of the Sulphur Springs deposit, to dendritic and colloform textures near the top. Volcanic textures, such as coarse plates of leucoxene in semi-massive sulfide towards the base of the Sulphur Springs and Kangaroo Caves deposits, indicate that at least the base of the orebodies are of a replacement style. The textures near the top of the orebodies indicate rapid sulfide

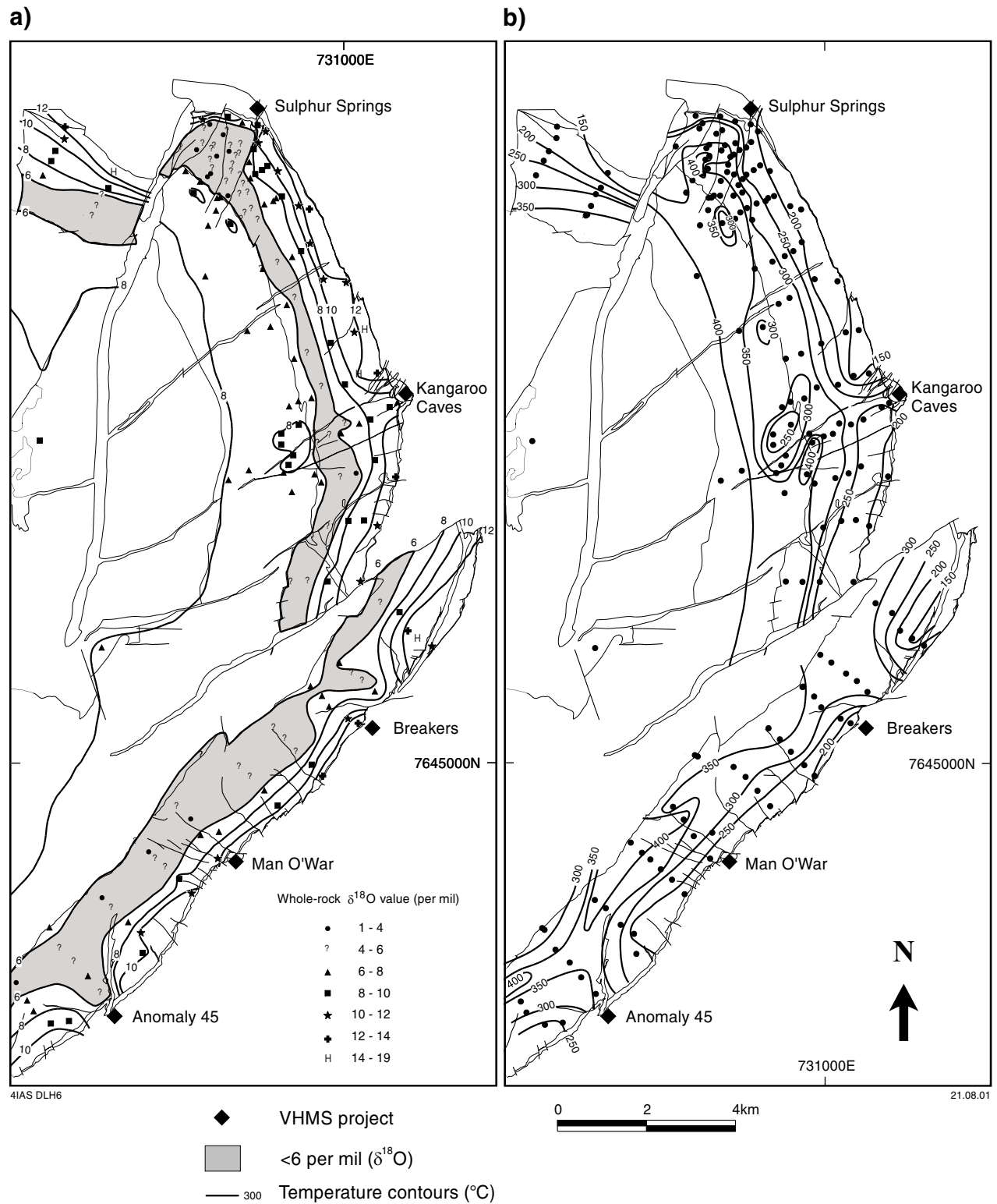


Figure 27. Panorama volcanic-hosted massive sulfide district (after Brauhart et al., 2000): a) variations in $\delta^{18}\text{O}_{\text{whole rock}}$; b) Temperature contours calculated using the $\delta^{18}\text{O}_{\text{whole rock}}$ values and normative mineralogy

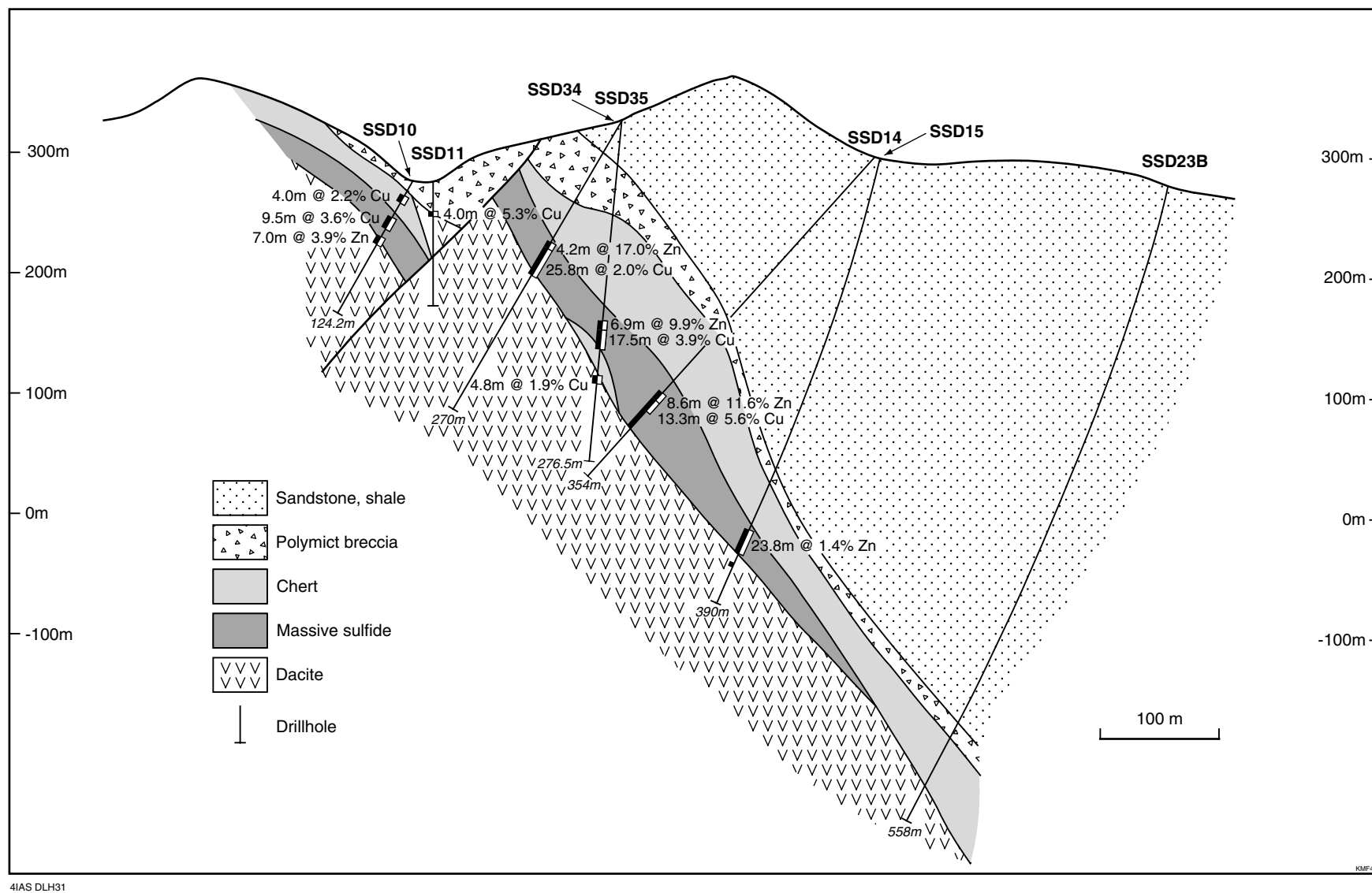


Figure 28. Cross section of the Sulphur Springs volcanic-hosted massive sulfide deposit (after Buick and Doepel, 1999)

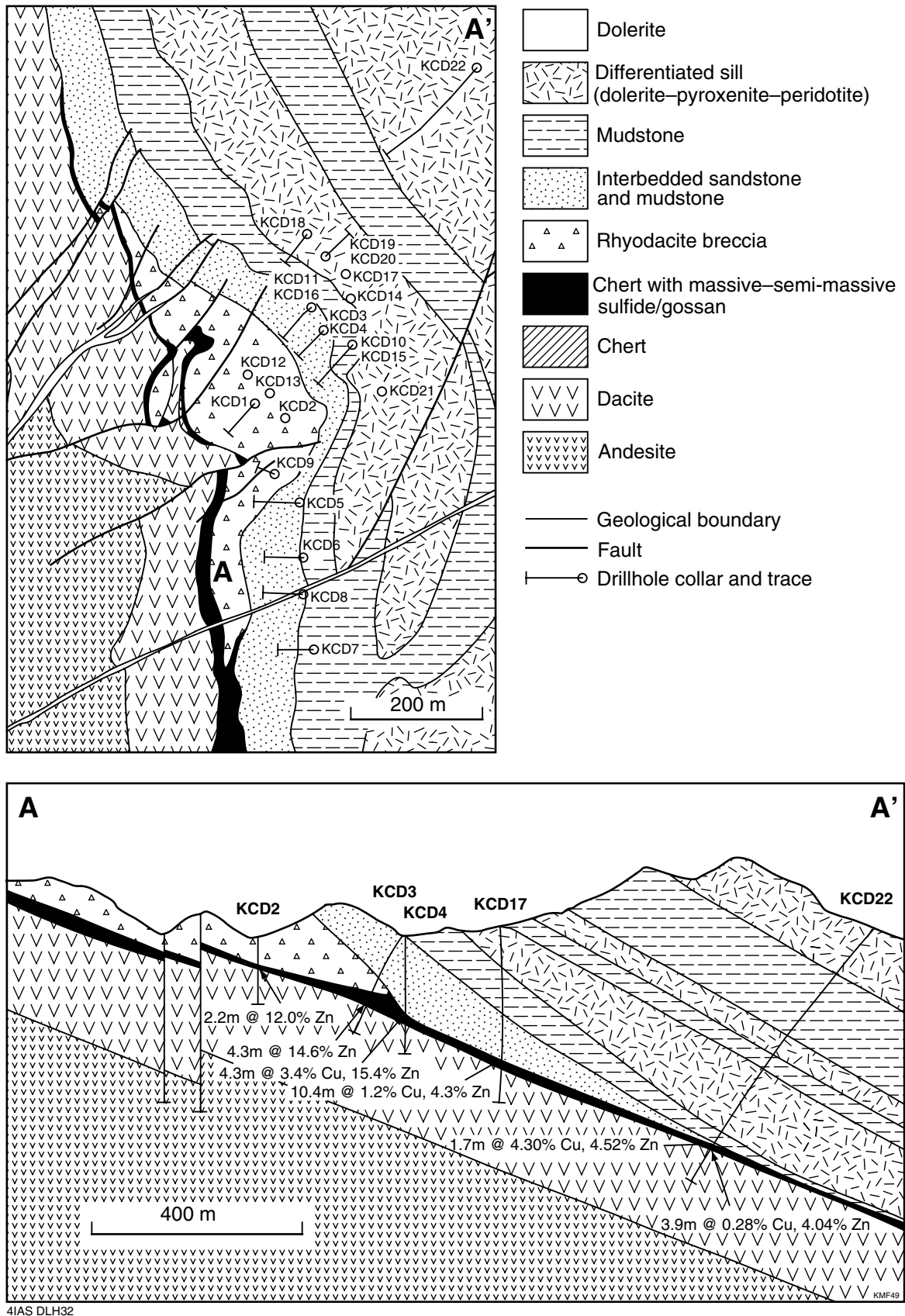


Figure 29. Plan and cross section of the Kangaroo Caves volcanic-hosted massive sulfide deposit (after Morant, 1995)

precipitation into open space, and some of these were interpreted as possible chimney structures (Vearncombe, 1995a). Other workers (Morant, 1998) prefer to interpret the mineralization as subseafloor, based on textures in the ore and the subseafloor emplacement of the host dacite.

Excursion localities

The location of the following excursion localities are shown in Figure 30.

Locality 5.1: Sulphur Springs gossan, footwall dacite, and marker chert (NORTH SHAW, MGA 287594)

From Strelley Pool, drive 5.8 km east along the main track to a junction. Turn south for 5.5 km to another junction. Turn right, follow this track for 5 km and turn left at a crossroad. Drive along this road for about 1.5 km to the Sulphur Springs gossan. Park on moderately weathered chlorite–quartz–altered dacite, 50 m south of the gossan.

This gossan is the surface expression of the Sulphur Springs deposit. Both ferruginous- and siliceous-gossan types are exposed on the hill slope and down in the creek. The marker chert is exposed further down the creek.

Locality 5.2: Feldspar–sericite–quartz–altered andesite–basalt (NORTH SHAW, MGA 290590)

Drive about 500 m back along the track you came in on until it turns sharply to the south (and heads down the discharge-zone bounding fault). Park, and walk about 200 m up the creek to an outcrop of pillowed andesite–basalt.

This exposure is typical of the feldspar–sericite–quartz–altered alteration facies. The andesite basalt here contains 79 wt% SiO₂, 3.0 wt% K₂O, 1.2 wt% Na₂O, and 1.4 wt% TiO₂. Similarly altered andesite–basalt in other places contains up to 6.5 wt% K₂O. Note also the exposure of hyaloclastic andesite–basalt breccia in the floor of the creek immediately down stratigraphy of the pillowed outcrop.

Locality 5.3: Background and chlorite–quartz–altered andesite–basalt (NORTH SHAW, MGA 287584)

Continue back along the track for another 700 m and park adjacent to a creek.

This stop is on the edge of the discordant zone of chlorite–quartz alteration below the Sulphur Springs deposit (Fig. 25). On the eastern side of the creek is background-altered andesite–basalt (rounded blocky outcrop with visible feldspar laths), and on the western side of the creek is chlorite–quartz–altered andesite–basalt (crackled broken outcrop with no feldspar). Note the dull lustre of the chlorite–quartz–altered rock compared to the background-altered rock. The three closest samples of background-altered andesite–basalt contain 2.2–3.1 wt% Na₂O, 150–160 ppm Zn, and 20–50 ppm Cu. The three closest chlorite–quartz–altered samples contain <0.1 wt% Na₂O, 20–50 ppm Zn, and <1–2 ppm Cu. All samples contain between 1.3 and 1.6 wt% TiO₂ and between 54 and 62 wt% SiO₂.

Locality 5.4: Reaction zone (NORTH SHAW, MGA 286577)

Drive down the track you came in on until you come to a junction and turn right. Drive a further 100–200 m and stop by the area of disturbed ground.

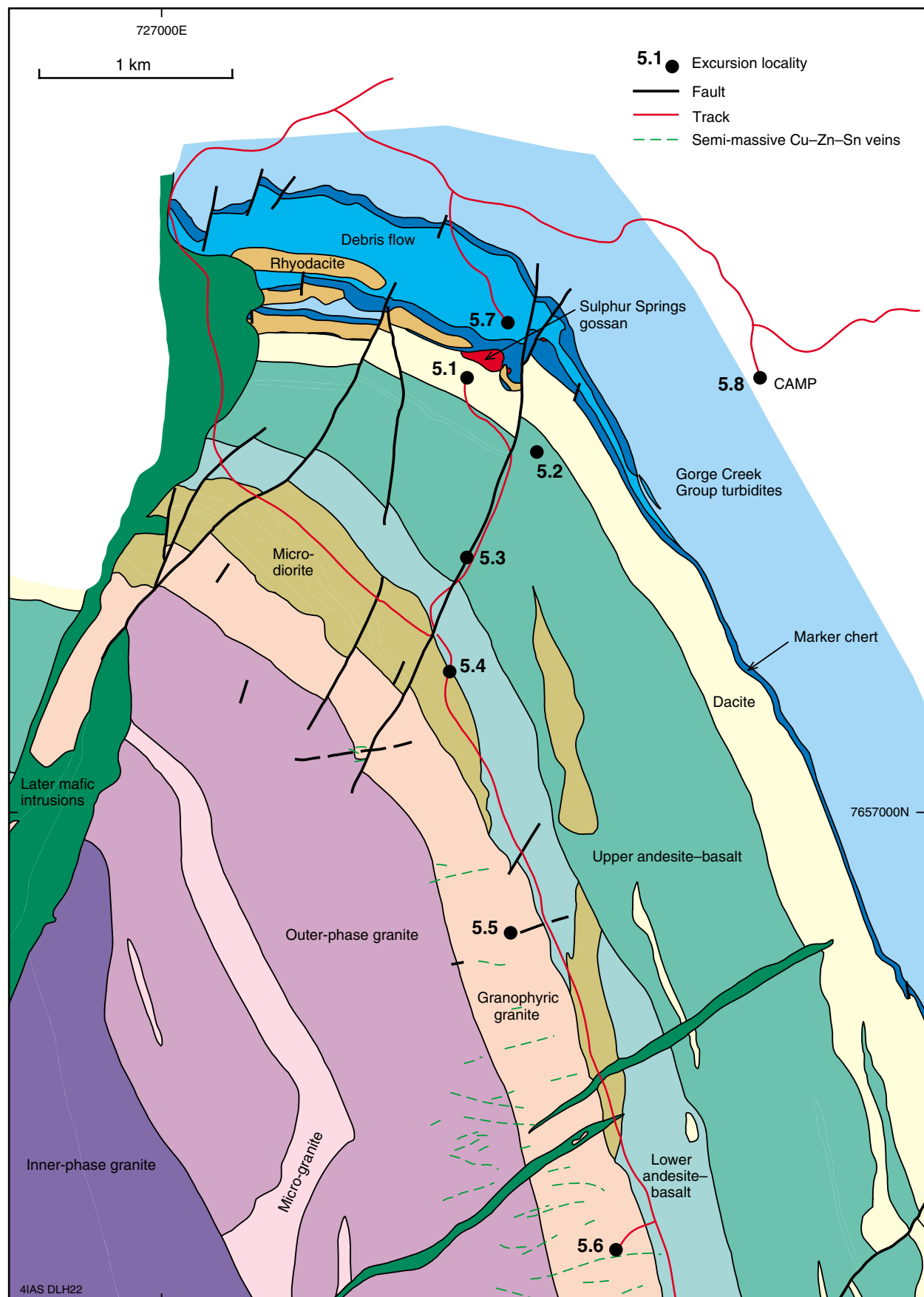


Figure 30. Geological map of the Sulphur Springs area showing excursion localities

Here, outcrops of both andesite and microdiorite are examples of feldspar-bearing rocks at the base of the volcanic pile. They all contain less than 5 ppm copper (most have less than 1 ppm), and typically contain less than 30 ppm zinc. They also contain up to 7 wt% Na₂O and mostly less than 0.2 wt% K₂O. Andesite contains concentrically zoned chlorite–carbonate–hematite spots, whereas microdiorite contains epidote spots. These rocks are substantially depleted in base metals and interpreted as the source rocks for the metal in the VHMS deposits.

Locality 5.5: Subvolcanic intrusion (NORTH SHAW, MGA 288564)

Drive about 1.5 km to the south-southeast along the track, which roughly follows the granite – volcanic rock contact.

Walk west onto the Strelley Granite and look at the quenched granophyric carapace of the intrusion. Walk further west to look at chlorite–quartz-altered and sericite–quartz-altered granite. These rocks define one of a number of feldspar-destructive centres at the top of the Strelley Granite (Fig. 25). If time permits, walk further into the Strelley Granite to see the transition out of granophyric granite into equigranular granite and examples of microgranite sills.

Locality 5.6: Granite-hosted semi-massive sulfide vein (NORTH SHAW, MGA 294545)

Drive a further 2 km until you get to a small track to the right and drive along it to the drillhole collar at the end (don't take the right turn 500 m back down on the flat; this leads into the middle of the granite).

A weathered outcrop of a granite-hosted semi-massive sulfide vein is exposed at this locality. This vein outcrops as a copper-stained gossanous outcrop on the low rise. A hole drilled into this vein intersected 0.5 m at 9.1% Zn, 6.3% Pb, 4.5% Cu, 0.64% Sn, and 68 ppm Ag.

Locality 5.7: Sulphur Springs Creek (NORTH SHAW, MGA 288597)

Drive back to the main road into the exploration camp. Turn right and drive 0.8 km to the first drilling access road, to the right up Sulphur Springs Creek. Look at the yellow sulfate encrustations that give Sulphur Springs its name.

A PhD student, Harry Wilhelmij, found yellow sulfate encrustations in 1984, which led to discovery of the Sulphur Springs gossan after he reported the encrustations to a local prospector. Note also the blocks of chert and felsic volcanic rocks in the debris flow that overlies the marker chert.

Locality 5.8: Drillcore inspection

Go back to the main road and continue on to the exploration camp.

A selection of diamond drillholes from the Sulphur Springs deposit has been laid out. Note the spectacular preservation of delicate sulfide textures, particularly towards the top of the deposit.

Return to the Strelley Pool – Shaw River road, turn right and head east for 19 km to a junction (you will pass the Lalla Rookh gold deposit, which, time permitting, we will visit). At the junction turn left and continue north for 35 km to the Port Hedland – Nullagine road. Turn right and travel southeast for approximately 90 km to the turnoff to Marble Bar. Drive 9 km into town. We will stay at the Marble Bar caravan park.

Part six (Option A): The Warrawoona lode-gold district

by R. S. Blewett

The Warrawoona Belt, or Warrawoona Syncline (Hickman and Lipple, 1978; Hickman, 1983), is located 25 km south of Marble Bar and is a highly attenuated wedge of greenstone between the Mount Edgar and Corunna Downs Granitoid Complexes (Fig. 31). The rocks include felsic volcanic rocks of the Duffer Formation (3470 Ma) and mafic and ultramafic rocks of the younger Salgash Subgroup (Hickman, 1983), and slices of the 3325 Ma Wyman Formation (Thorpe et al., 1992a). The Warrawoona area displays many of the early deformation events seen in the Pilbara, that is, those developed in rocks between 3470 and 3325 Ma.

The Warrawoona district is one of the largest historical mining centres in the Pilbara region. The first production was reported in 1898 from numerous mining leases in the area, with total production up to 1936 of 0.53 t (18 800 oz) of gold at an average grade of 44 g/t Au (Jones, 1938). Recent mining activity resulted in the development of an adit near the Klondyke Queen mine (Locality 6A.1). CRA Exploration recently completed 5078 m of diamond drilling across the main mineralized zone. Based on this drilling program an inferred resource estimated at 9.95 Mt at 1.0 g/t Au (10 t of gold; Register of Australian Mining, 1997–98) was determined.

Structural geology and models of Archaean tectonics

The structural geology of the Warrawoona Belt is controversial, and the area has been considered a classic area to study diapirism (Collins, 1989; Williams and Collins, 1990; Collins et al., 1998). Collins (1989) recognized a four-phase deformation chronology in the Mount Edgar Batholith and adjacent greenstones of the Warrawoona Belt. Collins (1989) suggested that the first fabric (his S_1) in the Mount Edgar Batholith was older than 3450 Ma. This early fabric was folded (his F_2) during a second phase about northwest-trending axes before 3414 Ma. Possible extension faults developed in the adjacent Warrawoona Belt greenstones were interpreted as a response to these two deformation events (his D_1 and D_2) in the Mount Edgar Batholith (Collins, 1989). The third event (his D_3) was only developed in the batholith and was described as northeast-trending folds and axial-plane foliation. No timing was provided. Collins' (1989) D_4 event was interpreted as a batholith-concentric mylonitic foliation, also developed in the greenstones, and related to diapirism between 3314 and 3304 Ma.

Vearncombe (1995b) also identified four phases of deformation in the Warrawoona Belt greenstones, although these are not the same as those of Collins (1989). The first fabric (his S_1) was rotated and transposed into later shear zones (his D_3), the most conspicuous being the Klondyke Fault. Vearncombe (1995b) described fold-interference patterns between his D_2 and D_1 structures, but could not recognize a regional significance to this second phase. Vearncombe's (1995b) D_3 was interpreted as the main shearing fabric, and control on gold mineralization was associated with the development of both intersection and steep stretching lineations. Macroscale folding of his D_3 fabric is found in the Salgash area and in a post- D_3 spaced- to crenulation-cleavage that strikes east-northeast and dips steeply north (Vearncombe, 1995b).

The present and earlier studies (Blewett, 2000a; Blewett and Huston, 1999) largely support the work by Vearncombe (1995b), with the earliest noted fabric in the Warrawoona Belt greenstones (wS_1) as an east-striking foliation in the Q-domains of north-striking wS_2 crenulation cleavages (Fig. 32). Boudins define low-strain zones in

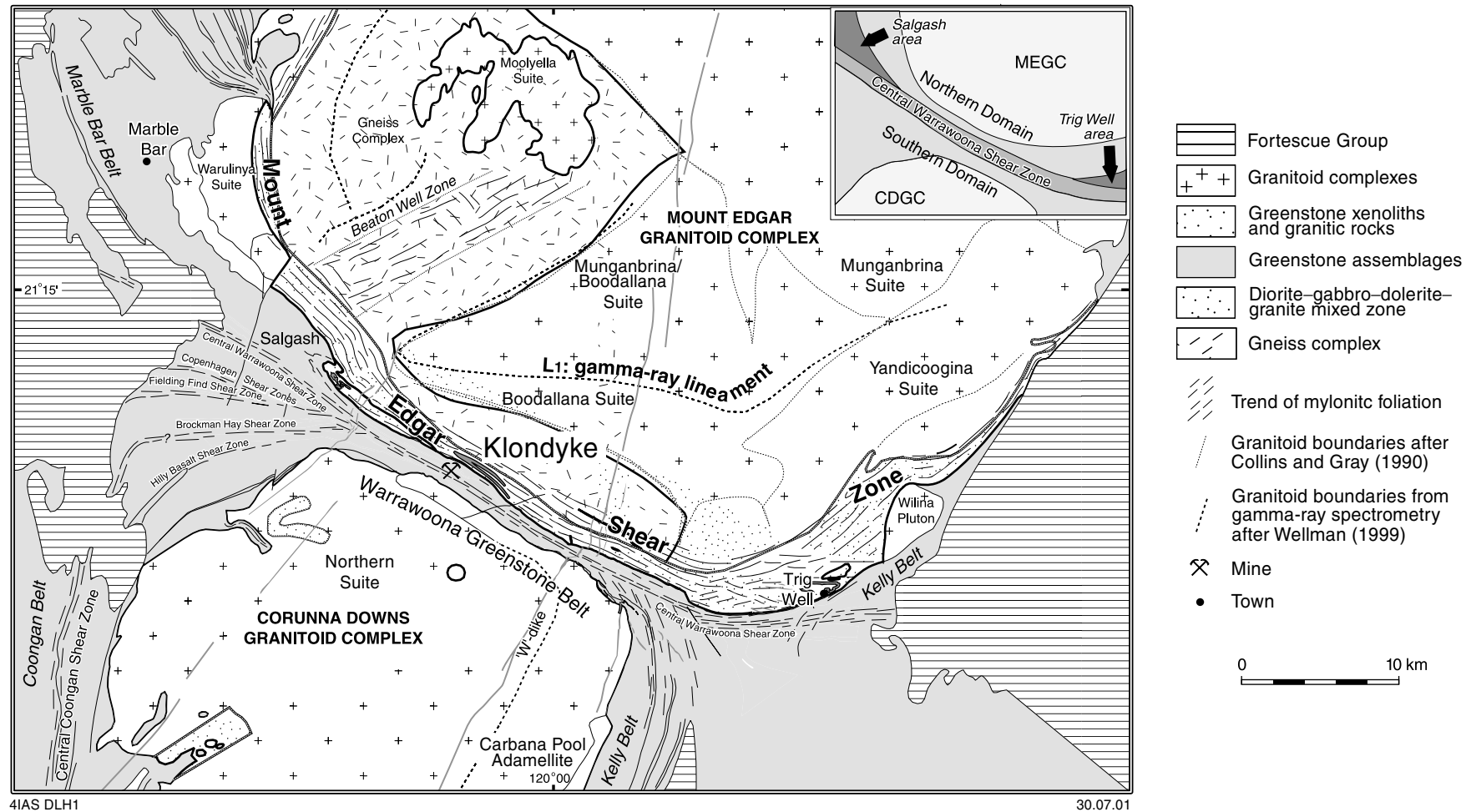
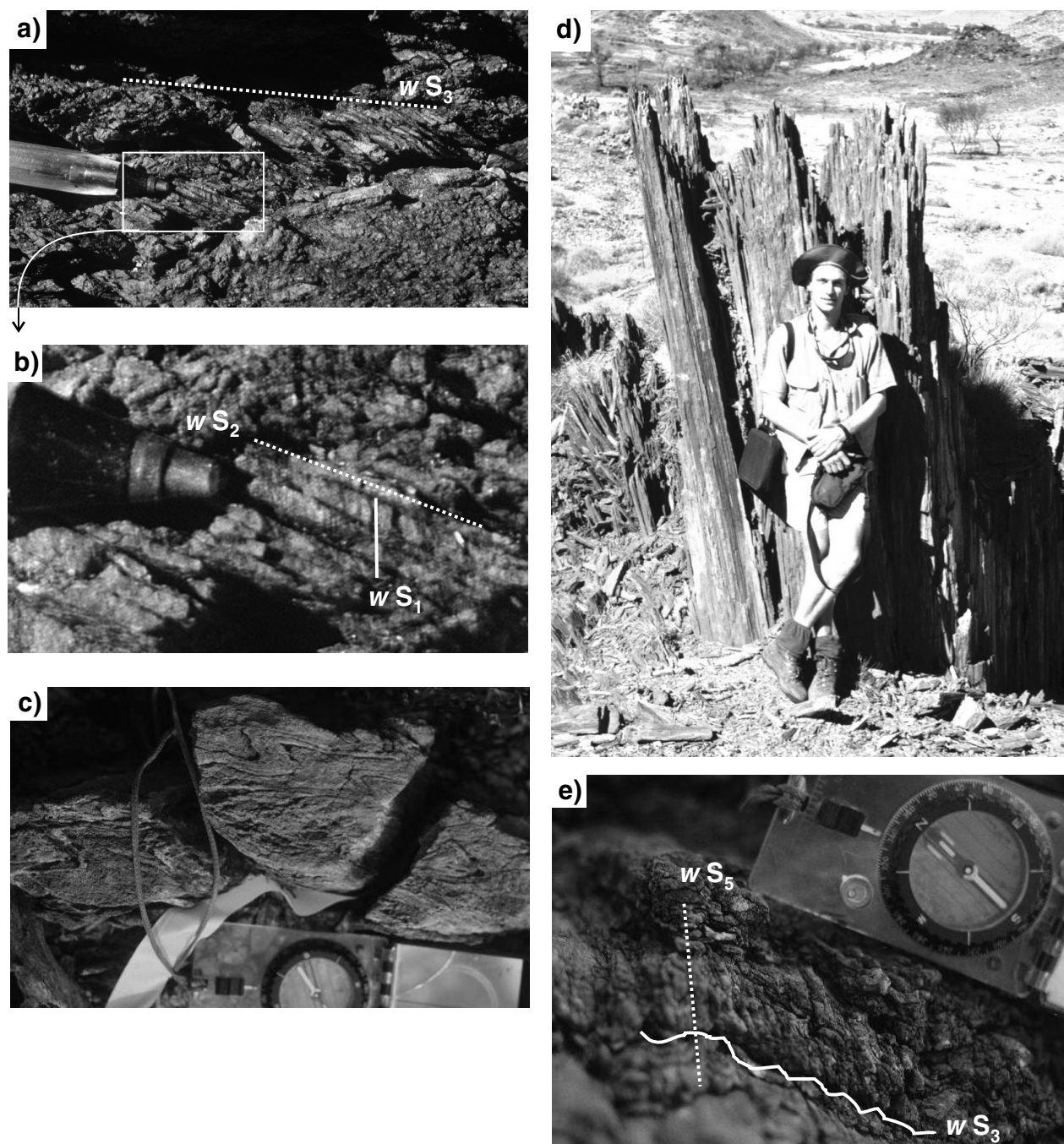


Figure 31. Simplified geological map of the Warrawoona district and location of the Klondyke deposit (after Kloppenburg et al., in press)



4IAS DLH5

28.05.01

Figure 32. Structures developed in the Warrawoona belt:
 a) view north of main shear fabric of Warrawoona Belt (wS_3) overprinting wS_2 crenulation foliation;
 b) detail of wS_2 as a crenulation cleavage of the first fabric (wS_1);
 c) wF_4 folds of the wS_3 shear fabric in the Warrawoona Belt;
 d) view east-southeast of the intense intersection lineation in the Warrawoona Belt; e) detail of wS_5 crenulation of the main wS_3 fabric in the Warrawoona Belt

the Klondyke Shear Zone and preserve multiple crenulation cleavages that do not appear to be described by Collins (1989). The wS_2 crenulation cleavages were overprinted and crenulated by a batholith-concentric wS_3 fabric, equivalent to Collins' (1989) D_4 , which is the main foliation through the Warrawoona Belt (Fig. 32).

The main wS_3 shear fabric is refolded by several generations of mesoscale folds (Fig. 32). Sinistral wF_4 drag folds with an S-shaped asymmetry plunge moderately to steeply to the northwest, and overprint the main wS_3 shear fabric (Fig. 32). These folds may record lateral escape of the greenstones from between Mount Edgar and Corunna Downs Granitoid Complexes. Elsewhere, dextral drag folds of the main wS_3 fabric record a north vergence and greenstone-up sense of shear, which may also be part of the tectonic escape. The Salgash folds may be a macroscale example of this.

The workers that favour diapirism in the Warrawoona Belt (e.g. Collins, 1989; Collins et al., 1998; Van Kranendonk, M., 1999, written comm.) have tended to place great emphasis on a lineation that appears to track the margin of the Mount Edgar Batholith and steepens into the centre of the greenstone belt. One problem with this interpretation is that there are many lineations, including:

1. mineral lineations that plunge subvertically;
2. different mineral lineations that plunge gently to moderately to the west;
3. intersection lineations between the various penetrative fabrics wS_1 to wS_3 ;
4. an intense intersection lineation (L-tectonite) developed by north- to northeast-trending wS_5 crenulation cleavage transecting the main wS_3 fabric (Fig. 32). This last intersection lineation has been interpreted as a stretching lineation related to diapirism (Collins, 1989; Collins et al., 1998; Van Kranendonk, M., 1999, written comm.).

There may be an element of dip-slip stretch in the Warrawoona Belt (e.g. local steep mineral lineation and pressure fringes on pyrite grains). This dip-slip movement was minor in the development of subvertical L-tectonites, as relatively unsheared quartz veins that are crenulated by wS_5 can be mapped across the zones of so-called sinking (cf. Collins et al., 1998). Evidence for vertical and horizontal movements is present in quartz veins in the various mine pits of the Klondyke area. These veins show 'chocolate-tablet' boudinage in both horizontal and vertical sections. In transpressional belts it is not uncommon for strain to be partitioned into strike-slip and dip-slip components, some of this being due to competence contrasts in multilayered systems (e.g. Lin and Williams, 1992; Tickoff and Goodwin, 2000).

The north- to northeast-trending wD_5 structures are the last penetrative structures developed in the Warrawoona Belt, and are at a different orientation to Vearncombe's (1995b) D_4 structures.

An upper age of 3417 Ma for the wD_1 event is provided by the youngest components of the Warrawoona Group that are overprinted by it (Barley and Pickard, 1999). The Warrawoona orogenic gold deposits have Pb–Pb model ages of around 3400 Ma (see above), possibly related to wD_1 or wD_2 . The wS_3 fabric correlates with Collins' et al. (1998) S_4 , which is transected by the 3324 Ma Wilina Pluton of the Mount Edgar Granitoid Complex (Collins et al., 1998). Therefore, the wD_2 event lies between 3417 and 3324 Ma. The wD_4 and wD_5 events are younger than the 3325 Ma Wyman Formation (Thorpe et al., 1992a), which is unconformable on wD_3 -deformed Warrawoona Group rocks (Hickman, 1983).

Alternative tectonic model

Collins et al. (1998) and Collins and Van Kranendonk (1998) presented a crustal overturn model for the development of the Warrawoona Syncline. In this model, a

5–10 km-thick mafic and ultramafic volcanic pile (Warrawoona Group) was initially extruded onto less-dense granitoid rocks of the Corunna Downs and Mount Edgar Batholiths. This instability initiated an overturn of the crust, partly driven by heat input from granitoid intrusions. The D_1 structures therefore represent early foliation development and thrusting, as slices of greenstone shed off rising granitoid domes, consistent with D_1 kinematics. The D_2 folding is a consequence of D_1 deformation, as folding developed during late shearing.

Fourth-generation structures (third generation within the greenstone belt) relate to the latest upward movement of the Mount Edgar Batholith relative to greenstones. This resulted in a wide shear zone at the batholith–greenstone contact, as well as the Klondyke Fault Zone, which is located a few tens of metres south of the Warrawoona mining district. A sharp change in metamorphic grade has been noted across the Klondyke Fault Zone (Collins and Van Kranendonk, 1998). Greenstones north of the Klondyke Fault Zone contain metamorphic kyanite and are therefore of much higher grade than the greenschist-facies rocks to the south. Pressure–temperature calculations indicate that the kyanite-bearing greenstones were buried to 20 km before rebounding as a rim along the outer walls of the Mount Edgar Batholith. This rebound was accommodated by near-vertical uplift on the Klondyke Fault Zone related to late tilting of the Mount Edgar Batholith to the northeast.

Excursion localities

Locality 6A.1: Gauntlet mine (MARBLE BAR, MGA 981388)

Drive east from Marble Bar town centre and turn right after 1 km (signed to Corunna Downs). Drive 19 km south-southeast (at 16 km you pass the large opencut of the Copenhagen mine). Turn left at a green drum and drive east for 4 km, and then turn left towards the large hills, following the minor track around to the left (back on yourself).

WARNING: UNMARKED OPEN SHAFTS ARE COMMON AT THIS SITE.

The Gauntlet mine yielded 4500 oz of gold from 1898 to 1910. Workings consist of two main shafts. Looking east, the line of stopes from the Klondyke Queen mine can be seen trending towards the Gauntlet mine. Locality 6A.1a displays the intense L-tectonite described above. Careful observation will reveal that this lineation is the product of the intersection of two foliations (wS_3 and wS_4).

Jones (1938) reported that the orebody was a small pipe that pitched north at a very steep angle. The orebody was formed at the intersection of an east–west-striking reef and a reef striking 322° . At the surface, the ore shoot was 5 m long, broadening to 10 m at depth, with an average width of 60 cm. Jones (1938) reported little drop-off in grade. Copies of relevant maps are in Blewett (2000b).

Locality 6A.1b shows the brown, weathered, carbonate–chlorite schist, which characterizes the broad wD_3 Klondyke Fault Zone. Locally, boudins acted as wD_3 low-strain zones and preserve evidence of the two earlier fabrics.

At Locality 6A.1c, a shaft shows two stope orientations. One stope is parallel with the main west-northwesterly mineralized zone, as are most workings in this area. However, an oblique, northeast-trending stope was worked parallel to the 10 cm quartz vein visible in the working. Other veins in this area are also northeast trending. This second orientation of veins has not been recognized in other areas.

Locality 6A.2: Mullan zone adit (MARBLE BAR, MGA 993378)

Drive back to the main track, turn left and left again onto a minor track heading towards the hills to the north and the Klondyke Queen mine.

WARNING: UNMARKED OPEN SHAFTS ARE COMMON AT THIS SITE.

Two parallel, northwest-trending mineralized zones have recently been mined. These are connected across a barren zone by an north-trending adit. The southern mineralized zone at the adit entrance consists of subparallel, boudinaged, centimetre-scale quartz veins with sericite–chlorite–pyrite-altered wallrock. Overprinting shallow quartz veins can be seen near the entrance and crosscut the near-vertical foliation. The northern mineralized zone has similar quartz veining to the southern zone, but the alteration assemblage is dominated by fuchsite, a distinct green mica. Pyrite grains record pressure fringes that indicate some vertical stretching.

Locality 6A.3: Klondyke Queen mine (MARBLE BAR, MGA 993379)

Walk up the slope to the northwest to view the mine.

WARNING: UNMARKED OPEN SHAFTS ARE COMMON AT THIS SITE.

This mine produced almost 5000 oz of gold between 1898 and 1936 from extensive underground workings (Jones, 1938). The main shaft is located near the boiler and open stopes extend northwest along the ridge top for approximately 100 m. The mineralized zone, which strikes 290° along the top of this ridge, is the same zone observed in the northern Mullan zone workings and the same fuchsite–pyrite–quartz alteration can be seen. Quartz veins are boudinaged in a ‘chocolate-tablet’ manner (vertical and horizontal); examples are exposed in the western end of the large stope at this locality. A 15 cm-wide black chert band, termed the Kopkes Leader by early miners, is exposed along the southern edge of the fuchsite-altered zone. This chert band is laterally persistent and provided an indication of the location of mineralization.

Return to the Port Hedland – Nullagine road via Marble Bar. Turn left and head north for 156 km to the junction with the Northwest Coastal Highway. Turn left and head west for approximately 25 km to the Port Hedland airport

Part six (Option B): The Lennons Find volcanic-hosted massive sulfide district

by D. L. Huston

Of the VHMS districts of the north Pilbara Craton, the Lennons Find area is one of the more poorly described, despite containing the earliest (c. 3470 Ma; Thorpe et al., 1992b) significant VHMS deposit in the world. Production in the district was 50.8 t of ore. A demonstrated resource estimated at 1.2 Mt grading 7.76% Zn, 1.94% Pb, 0.43% Cu, 100 g/t Ag, and 0.3 g/t Au (Fergusson, 1999) has been outlined for the Hammerhead zone, one of five mineralized zones that are present over a strike length of 5 km.

Local stratigraphy

Volcanic-hosted massive sulfide deposits in the Lennons Find district are located just below the contact between mafic schist of the Apex Basalt and the underlying mainly felsic schist of the Duffer Formation (Fig. 33). The Duffer Formation in this area has been dated at 3465 ± 3 Ma (Thorpe et al., 1992a). In the Lennons Find area, the Duffer Formation contains three laterally persistent units: a basal quartzofeldspathic schist, overlain by a thin unit of metasedimentary rocks, which in turn is overlain by quartz-muscovite schist. This last unit, which is up to 75 m thick, contains all significant gossans and massive sulfide lenses. It thins in unmineralized areas (Fig. 33) and is interpreted as a metamorphosed and hydrothermally altered felsic volcanic rock.

The Apex Basalt in the Lennons Find area consists of strongly foliated mafic schist with lesser talc(–carbonate) schist. One, or possibly two, persistent chert units are present near the base of this unit. Further south, the Apex Basalt is overlain unconformably by the Mount Roe Basalt.

The volcano-sedimentary succession in the Lennons Find area was intruded at its base by foliated leucogranite. Minor pegmatite dykes intrude this granite. Both the granite and the volcano-sedimentary succession are intruded by foliated dolerite.

The rocks hosting the Lennons Find district form a broadly arcuate belt that trends 075° in the west and 045° in the east (Fig. 33). These rocks dip moderately ($40\text{--}70^\circ$) to the south. Although no macroscopic folds are present in the area other than this arching, folds with amplitudes up to 2 m are present in outcrop. Using field relationships and regional relationships, five structural elements were inferred for the Lennons Find area. These can be correlated with regional structural elements of the east Pilbara using the structural chronology of Blewett (2000a).

Mineralization

Five mineralized zones have been defined in the Lennons Find area, based mainly on the location of old workings and on surficial geochemistry (McKeesick, 1996; Fig. 33). These zones lie at two stratigraphic horizons: an upper horizon within the quartz-muscovite schist, and a lower horizon near the upper contact of the underlying metasedimentary rocks.

The upper horizon is more intensely mineralized and contains the Hammerhead zone and three other mineralized zones, two of which (Tiger and Bronze Whaler) have significant (e.g. $>1\%$ Zn) drillhole intersections. The lower horizon contains the Grey Nurse zone, which also has significant drillhole intersection (McKeesick, 1996). A third

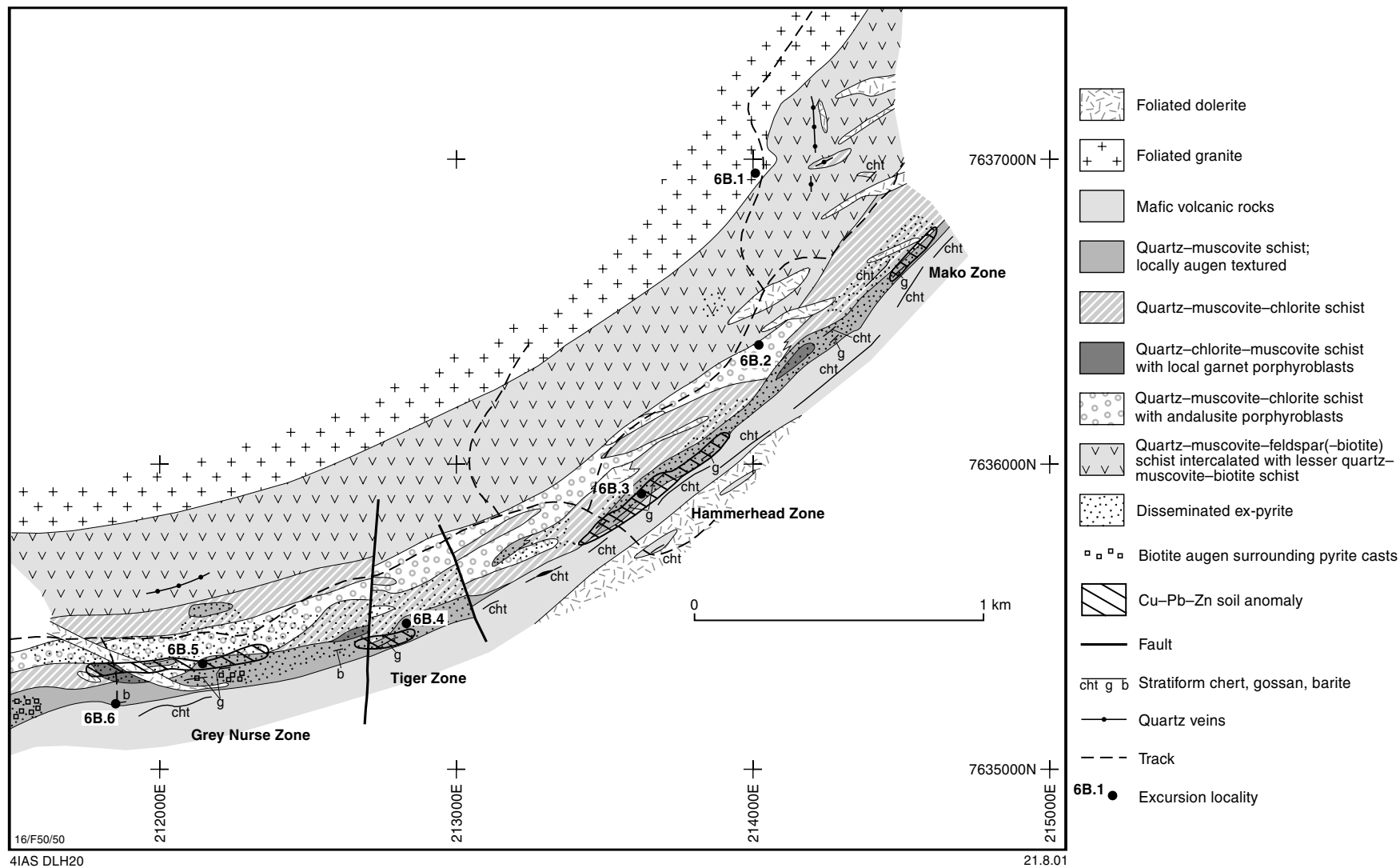


Figure 33. Geology of the Lennons Find area showing excursion localities

horizon, defined by geochemical anomalies and weak pyritic gossan is present below the Grey Nurse zone, near the contact between the psammo-pelitic unit and the underlying quartzofeldspathic schist (Fergusson, 1999; not shown in Fig. 33). A fourth horizon, which contains massive barite, is located at the contact between the Duffer Formation and the Apex Basalt.

The Hammerhead zone

The Hammerhead zone consists of a thin lens (<5 m true thickness) of baritic semi-massive to massive sulfide that dips moderately to the southeast. This lens has a moderate to steep rake to the east, which may be controlled by regional structural elements. Marston (1979) and Sjerp (1983) indicated that this mineralized zone contains sphalerite, chalcopyrite, and galena in association with barite and pyrite. Sjerp (1983) also indicated the presence of three textural styles within the mineralized zone:

- massive banded, which contains 25–80% sulfide with quartz, barite, chlorite, carbonate, tourmaline, muscovite, and biotite gangue;
- thinly banded and disseminated, which contains 5–20% sulfide, mainly pyrite, in 0.1 – 2 cm bands and as disseminated grains;
- disseminated, which contains 1–2% disseminated sulfide, again mainly pyrite.

The massive banded sulfide lies at the top of the mineralized succession, overlying thinly banded and disseminated sulfide.

Alteration

Regional alteration facies in the Lennons Find area are restricted to disseminated pyrite in the upper part of the Duffer Formation and the quartz–sericite schist at the top of the Sharks Formation. The overlying Apex Basalt has not been altered.

Semiconformable zones of disseminated pyrite are present within the quartz–muscovite schist that host the deposits and in the upper part of the underlying metasedimentary unit. The thickest zone of disseminated pyrite is developed in the Grey Nurse and Tiger West zones, where a continuous zone, 50–200 m in true thickness, can be traced over a strike length of 1.5 km. This zone is separated from a second, narrower (25–80 m true thickness) zone of disseminated ex-pyrite that extends more than 1.5 km from the Hammerhead zone to the Mako zone.

Excursion localities

At the time of writing, all localities described below were within active mining leases, and permission to enter is therefore required. The localities and access are shown on Figure 33.

Locality 6B.1: Contact between Mount Edgar Batholith and felsic schists at base of Duffer Formation (MOUNT EDGAR, AMG 140370)

From Marble Bar drive to the Port Hedland – Nullagine road and turn right (south towards Nullagine). Proceed 32 km until you reach the turnoff to the Meentheena Station, then turn left (east). Drive along this road for 3.5 km until you reach the Mount Edgar Station. At the station, take the left fork and proceed for 4.0 km until you reach an unsigned junction. Take the right fork and proceed east for 10.0 km until you reach a second junction near a well. Take the right fork again and proceed 5.0 km to a fenceline. Pass through the fenceline and drive 4.1 km until you reach a low ridge.

At this locality the track crosses the contact between foliated, fine-grained granite of the Mount Edgar Batholith and the felsic schists that form the base of the Duffer Formation. In the Lennons Find area the Duffer Formation is characterized by quartz–muscovite–feldspar(–biotite) schist intercalated with lesser amounts of quartz–muscovite–biotite schist. These rocks are interpreted as metamorphosed felsic volcanic rocks. To the west, along the low ridge, several mafic dykes cut the granite. These mafic rocks also cut the felsic rocks in the Duffer Formation.

Locality 6B.2: Metasedimentary rocks (MOUNT EDGAR, AMG 140364)

Return along the track for 0.45 km until a fork is reached. Take the right fork for 0.15 km and park. Walk down into the creek and then upstream (to the south).

The central part of the Duffer Formation in the Lennons Find area is characterized by metasedimentary rocks that are well exposed in this creek section. At the beginning of the traverse, quartz–muscovite–feldspar(–biotite) schist is exposed, but as you walk further to the south, quartz–muscovite–chlorite schist with andalusite porphyroblasts outcrops. This rock type and the quartz–muscovite–chlorite schist form a unit that can be traced along strike through the Lennons Find area (Fig. 33). The rocks are interpreted as metamorphosed psammo-pelitic rocks.

Locality 6B.3: Hammerhead zone (MOUNT EDGAR, AMG 136359)

Return along the track for another 0.85 km until a fork is reached (just pass a creek crossing) and park. Walk down to the creek and cross it.

A low gossanous exposure is located on the east side of the creek and can be followed discontinuously for 250 m to the east-northeast. This zone is exposed in several costeans, the best of which is located in the east. In this costean a 1.5 – 2.0 m-wide gossan after massive sulfide is exposed, which is the surface exposure of the Hammerhead zone. With a 1.2 Mt resource, this is the oldest significant VHMS deposit known. Baritic zones can be found within the gossanous zone.

Locality 6B.4: Tiger zone and Apex Basalt (MOUNT EDGAR, AMG 129354)

Take the right fork and proceed for 0.50 km to another fork. Turn left off the main track and proceed for 0.45 km and park.

(Ex-)pyritic quartz–muscovite schist forms a stratiform unit that hosts the Mako, Hammerhead, Tiger, and Grey Nurse zones. This unit, which stratigraphically overlies the psammo-pelitic unit (e.g. Locality 6B.2), is interpreted as a quartz–sericite–pyrite-altered felsic volcanic unit. An exposure of this unit in the road contains 1–5% ex-pyrite in 1–5 mm stringers that are commonly transposed into the dominant fabric. However, some of these stringers are deformed, indicating that their formation predated deformation.

Downhill to the east-northeast and along strike, several lenticular gossans are developed. The largest is 3 m long and 1 m wide and appears to be a boudin because the main fabric wraps around it. Several mesoscale folds and crenulations are developed within this zone.

To the south, the overlying Apex Basalt is exposed along relatively high ridges. This is best observed by walking south along the track to a drillpad within a large

exposure of this unit. The Apex Basalt consists of mafic schist intercalated with lesser talc schist. Minor chert bands are also present (Fig. 33)

Locality 6B.5: Grey Nurse zone (MOUNT EDGAR, AMG 122353)

Return to main track and turn left. Proceed 0.9 km and park. Walk 200 m up the ridge to the south, to an adit.

The adit is driven on a baritic gossan that forms a stratiform lens, which is up to 1.5 m thick and can be traced for about 20 m. To the west the lens appears to be cut off by a dolerite dyke. The lens lies within the (ex-)pyritic quartz–muscovite schist about 10 m below the contact with the overlying Apex Basalt. About 150 m to the east-northeast, a thin (10 cm) barite lens can be traced for 10 m at a stratigraphic position several tens of metres below the main Grey Nurse stratigraphic position.

Locality 6B.6: Barite lens at the contact between the Duffer Formation and Apex Basalt (MOUNT EDGAR, AMG 118352)

Continue west along the main track for a further 0.4 km until another track branches off to the left. Follow this track for 0.25 km to a drillpad at the end.

At this locality, three narrow (<15 cm) barite lenses are present in the upper 0.5 m of a knobbly variety of quartz–muscovite schist. The uppermost lens is at the contact with the overlying Apex Basalt. This is the uppermost mineralized position in the Lennons Find area; however, it does not appear to contain significant sulfides as these barite lenses are not gossanous.

Return to the Port Hedland – Nullagine road. Turn left and head north for 188 km to junction with Northwest Coastal Highway. Turn left and head west for approximately 25 km to the Port Hedland airport

Acknowledgements

D. Huston and R. Blewett thank Darcy Baker, David Champion, Arthur Hickman, Brett Keillor, Geoff Pike, Hugh Smithies, Jon Standing, and Martin Van Kranendonk for many stimulating discussions in the field. Arthur Hickman and Terry Mernagh provided many useful comments that improved the manuscript. Armelle Kloppenburg kindly provided Figure 31. D. Huston and R. Blewett publish with permission of the Chief Executive Officer of AGSO – Geoscience Australia.

M. Sweetapple acknowledges financial and logistical support provided by Sons of Gwalia Ltd for research into tantalum mineralization at Wodgina, and for permission to publish this paper. This paper also acknowledges the use of unpublished geochemical data of Sons of Gwalia Ltd from the Greenbushes laboratories. Greg Lumpkin of the Materials Division of the Australian Nuclear Science and Technology Organisation is thanked for collaboration with the mineralogical component of this research. Phil Jankowski (Senior Resource Geologist, Sons of Gwalia Ltd) is acknowledged for discussions regarding the structure of the Mount Cassiterite pegmatite group. The efforts of numerous geologists from companies previously working on this project are also acknowledged.

C. Brauhart acknowledges the Panorama Joint Venture for their financial and logistical support during his PhD studies of the Panorama district.

The authors thank the following companies for allowing access to the ground: Titan Resources NL, Straits Resources Ltd, East Coast Minerals NL, Legend Mining Ltd, Resolute Ltd, Lynas Gold NL, Sons of Gwalia Ltd, Panorama Joint Venture, and Pilbara Mines NL.

References

- ARNDT, N. T., NELSON, D. R., COMPSTON, W., TRENDALL, A. F., and THORNE, A. M., 1991, The age of the Fortescue Group, Hamersley Basin, Western Australia, from ion microprobe zircon U–Pb results: *Australian Journal of Earth Sciences*, v. 38, p. 261–281.
- BARLEY, M. E., and PICKARD, A., 1999, An extensive, crustally derived, 3325 to 3310 Ma silicic volcanoplutonic suite in the eastern Pilbara Craton: evidence from the Kelley Belt, McPhee Dome, and Corunna Downs Batholith: *Precambrian Research*, v. 96, p. 41–62.
- BARLEY, M. E., LOADER, S. E., and McNAUGHTON, N. J., 1998, 3430 to 3417 Ma calc-alkaline volcanism in the McPhee Dome and Kelley Belt, and growth of the eastern Pilbara Craton: *Precambrian Research*, v. 88, p. 3–24.
- BARNES, G. B., 1995, Silver mineralization at Elizabeth Hill, Munni Munni Complex, Western Australia: *Australian Institute of Geoscientists, Bulletin*, v. 16, p. 89–94.
- BLEWETT, R. S., 2000a, North Pilbara ‘virtual’ structural field trip: Australian Geological Survey Organisation, Record 2000/45 (CD).
- BLEWETT, R. S. (compiler), 2000b, Facsimile copy of the aerial, geological and geophysical survey of northern Australia (AGGSNA), Reports (1 to 26, 28, 46, 48, 51 to 59) for Western Australia (Pilbara Goldfield): Australian Geological Survey Organisation, Record 2000/05 (CD).
- BLEWETT, R. S., CHAMPION, D. C., FARRELL, T., and SMITHIES, R. H., in press, Geology of the Wodgina 1:100 000 sheet explanatory notes, North Pilbara National Geoscience Mapping Accord (NGMA) Project: Australian Geological Survey Organisation.
- BLEWETT, R. S., and HUSTON D. L., 1999, Deformation and gold mineralization of the Archaean Pilbara Craton Western Australia: Australian Geological Survey Organisation, Research Newsletter, v. 30, p. 12–15.
- BLEWETT, R. S., WELLMAN, P., RATAJKOSKI, M., and HUSTON, D. L., 2000, Atlas of North Pilbara Geology and Geophysics: Australian Geological Survey Organisation, Record 2000/04, 36 plates.
- BLOCKLEY, J. G., 1980, The tin deposits of Western Australia, with special reference to related granites: *Western Australia Geological Survey, Mineral Resources Bulletin* 12, 184p.
- BRAUHART, C. W., 1999, Regional alteration systems associated with Archean volcanogenic massive sulfide mineralization at Panorama, Pilbara, Western Australia: University of Western Australia, PhD thesis (unpublished).
- BRAUHART, C. W., GROVES, D. I., and MORANT, P., 1998, Regional alteration systems associated with volcanogenic massive sulfide mineralization at Panorama, Pilbara, Western Australia: *Economic Geology*, v. 93, p. 292–302.
- BRAUHART, C. W., HUSTON, D. L., and ANDREW, A. S., 2000, Oxygen isotope mapping in the Panorama VMS district, Pilbara Craton, Western Australia: applications to estimating temperatures of alteration and to exploration: *Mineralium Deposita*, v. 35, p. 727–740.
- BUICK, R., BRAUHART, C. W., MORANT, P., THORNETT, J. R., MANIW, J., ARCHIBALD, N. J., and DOEPEL, M., in press, Geochronology of the Strelley domain: a new tectonostratigraphic province in the Archaean Pilbara Craton, Australia: *Precambrian Research*.
- BUICK, R., and DOEPEL, M. G., 1999, Panorama VMS zinc–copper prospects, *in* Lead, zinc, and silver deposits of Western Australia: Western Australia Geological Survey, Mineral Resources Bulletin 15, p. 80–86.
- BUICK, R., THORNETT, J. R., McNAUGHTON, N. J., SMITH, J. B., BARLEY, M. E., and SAVAGE, M., 1995, Record of emergent continental crust ~3.5 billion years ago in the Pilbara Craton of Australia: *Nature*, v. 375, p. 574–577.
- CAMERON, E. N., JAHNS, R. H., McNAIR, A., and PAGE, L. R., 1949, Internal structure of granitic pegmatites: *Economic Geology, Monograph* 2, 115p.
- CERNY, P., 1989, Characteristics of pegmatite deposits of tantalum, *in* Lanthanides, tantalum and niobium: mineralogy, geochemistry, characteristics of primary ore deposits, prospecting, processing and applications *edited by* P. MOLLER, P. CERNY, and F. SAUPE: Society for Geology Applied to Mineral Deposits, Special Publication, v. 7, p. 195–239.
- CERNY, P., 1992, Geochemical and petrogenetic features of mineralization in rare-element granitic pegmatites in the light of current research: *Applied Geochemistry*, v. 7, p. 393–416.
- CERNY, P., 1993a, Rare-element granitic pegmatites. Part I: anatomy and internal evolution of pegmatite deposits, *in* Ore deposit models, Volume II *edited by* P. A. SHEAHAN and M. A. CHERRY: Geoscience Canada Reprint Series, v. 6, p. 29–47.
- CERNY, P., 1993b, Rare-element granitic pegmatites. Part II: regional to global environments and petrogenesis, *in* Ore deposit models, Volume II *edited by* P. A. SHEAHAN and M. A. CHERRY: Geoscience Canada, v. 6, p. 49–62.
- CERNY, P., 1998, Magmatic vs metamorphic derivation of rare-element granitic pegmatites: *Krystalinum*, v. 24, p. 7–36.
- CERNY, P., and NOVAK, M., 1997, Effects of metamorphism on rare-element granitic pegmatites, *in* Mineral deposits — Research and exploration — Where do they meet? *edited by* H. PAPUNEN: Rotterdam, Balkema, p. 805–807.

- CERNY, P., NOVAK, M., and CHAPMAN, R., 1992, Effects of sillimanite-grade metamorphism and shearing on Nb–Ta oxide minerals in granitic pegmatites: Marsikov, Northern Moravia, Czechoslovakia: *Canadian Mineralogist*, v. 30, p. 699–718.
- CERNY, P., TRUEMAN, D. L., ZIEHLKE, D. V., GOAD, B. E., and PAUL, B. J., 1981, The Cat Lake – Winnipeg River and the Wekusko Lake Pegmatite Fields, Manitoba: Canada, Manitoba Department of Mines and Energy, Economic Geology Report ER80-1, 216p.
- COLLINS, P. L. F., and MARSHALL, A. E., 1999a, Volcanic-hosted massive sulfide deposits at Whundo–Yannery in the Sholl belt, *in* Lead, zinc, and silver deposits of Western Australia: Western Australia Geological Survey, Mineral Resources Bulletin 15, p. 73–79.
- COLLINS, P. L. F., and MARSHALL, A. E., 1999b, Volcanogenic base-metal deposits of the Whim Creek Belt, *in* Lead, zinc, and silver deposits of Western Australia: Western Australia Geological Survey, Mineral Resources Bulletin 15, p. 44–72.
- COLLINS, W. J., 1989, Polydiapirism of the Archaean Mount Edgar Batholith, Pilbara Block, Western Australia: *Precambrian Research*, v. 43, p. 41–62.
- COLLINS, W. J., 1993, Melting of Archaean sialic crust under high H₂O conditions: genesis of 3300 Ma Na-rich granitoids in the Mount Edgar Batholith, Pilbara Block, Western Australia: *Precambrian Research*, v. 60, p. 151–174.
- COLLINS, W. J., and GRAY, C. M., 1990, Rb–Sr isotopic systematics of an Archaean granite–gneiss terrain: the Mount Edgar Batholith, Pilbara Block, Western Australia: *Australian Journal of Earth Sciences*, v. 37, p. 9–22.
- COLLINS, W. J., and VAN KRAENDONK, M. J., 1999, Model for the development of kyanite during partial convective overturn of Archaean granite–greenstone terranes: the Pilbara Craton, Australia: *Journal of Metamorphic Petrology*, v. 17, 145–156.
- COLLINS, W. J., VAN KRAENDONK, M. J., and TEYSSIER, C., 1998, Partial convective overturn of Archaean crust in the east Pilbara Craton, Western Australia: driving mechanisms and tectonic implications: *Journal of Structural Geology*, v. 20, p. 1405–1422.
- de ANGELIS, M., HOYLE, M. W. H., and VOERMANS, F. M., 1988, The Radio Hill Ni–Cu deposit and the Mount Scholl – Munni Munni mafic–ultramafic metallogenic province: a case of integrated explorations technique: Second International Conference on Prospecting in Arid Terrain, Perth, Western Australia, April 1988: Australasian Institute of Mining and Metallurgy, Abstracts, p. 51–57.
- DONG, G., MORRISON, G., and JAIRETH, S., 1995, Quartz textures in epithermal veins, Queensland: classification, origin, and implication: *Economic Geology*, v. 90, p. 1841–1856.
- DOWLING, K., and MORRISON, G. W., 1989, Application of quartz textures to the classification of gold deposits using north Queensland examples: *Economic Geology, Monograph 6*, p. 342–355.
- ELLIS, H. A., 1950, Some economic aspects of the principal tantalum-bearing deposits of the Pilbara Goldfield, North-West Division: Western Australia Geological Survey, Bulletin 104, 93p.
- FINUCANE, K. J., and TELFORD, R. J., 1939, The antimony deposits of the Pilbara goldfield: Aerial, Geological and Geophysical Survey of Northern Australia, Report 47, 6p.
- FERGUSON, K. M., 1999, Lead, zinc, and silver deposits of Western Australia: Western Australia Geological Survey, Mineral Resources Bulletin 15, 314p.
- GIFFORD, A. C., 1990, Blue Spec – Golden Spec gold–antimony deposit: Australian Institute of Mining and Metallurgy, Monograph 14, p. 155–158.
- GÖD, R., 1989, The spodumene deposit at ‘Weinbene’, Koralpe, Austria: *Mineralium Deposita*, v. 24, p. 270–278.
- GOELLNICH, N. M., GROVES, I. M., GROVES, D. I., HO, S. E., and McNAUGHTON, N. J., 1988, A comparison between mesothermal gold deposits of the Yilgarn Block and gold mineralization at Telfer and Miralga Creek, Western Australia: indirect evidence for a non-magmatic origin for greenstone-hosted gold deposits, *in* Advances in understanding Precambrian gold deposits, Volume II *edited by* S. E. HO and D. I. GROVES, University of Western Australia, Geology Department and Extension Service, Publication no. 12, p. 23–40.
- HALL, S. J., 1993, Tantalum ore mining by Pan West Tantalum Pty Ltd at Wodgina, W.A.: Australasian Institute of Mining and Metallurgy, Monograph 19, p. 1113–1114.
- HAN, T., 1990, Evolution of a magmatic–hydrothermal fluid during crystallization of the Greenbushes pegmatite: Curtin University of Technology, MSc thesis (unpublished).
- HICKMAN, A. H., 1975, Precambrian structural geology of part of the Pilbara region: Western Australia Geological Survey, Annual Report 1974, p. 68–73.
- HICKMAN, A. H., 1983, Geology of the Pilbara Block and its environs: Western Australia Geological Survey, Bulletin 127, 268p.
- HICKMAN, A. H., 1984, Archaean diapirism in the Pilbara Block, Western Australia, *in* Precambrian tectonics illustrated *edited by* A. KRÖNER and R. GREILING: E. Schweizerbart’sche Verlagsbuchhandlung, Stuttgart, p. 113–127.
- HICKMAN, A. H., 1996, Dampier, W.A. Sheet 2256: Western Australia Geological Survey, 1:100 000 Geological Series.
- HICKMAN, A. H., 1997, A revision of the stratigraphy of Archaean greenstone successions in the Roebourne–Whundo area, west Pilbara: Western Australia Geological Survey, Annual Review 1996–97, p. 76–82.

- HICKMAN, A. H., 1999, New tectono-stratigraphic interpretations of the Pilbara Craton, Western Australia: Western Australia Geological Survey, Record 1999/6, p. 4–6.
- HICKMAN, A. H., 2001, Geology of the Dampier 1:100 000 Sheet: Western Australia Geological Survey, 1:100 000 Geological Series Explanatory Notes, 39p.
- HICKMAN, A. H., and LIPPLE, S. H., 1978, Marble Bar, W.A. Sheet SF 50-8: Western Australia Geological Survey, 1:250 000 Geological Series.
- HICKMAN, A. H., SMITHIES, R. H., and HUSTON, D. L., 2000, Archaean geology of the West Pilbara Granite–Greenstone Terrane and Mallina Basin, Western Australia: Western Australia Geological Survey, Record 2000/9, 61p.
- HOATSON, D. M., WALLACE, D. A., SUN, S-S., MACIAS, L. F., SIMPSON, C. J., and KEAYS, R. R., 1992, Petrology and platinum-group-element geochemistry of Archaean layered mafic–ultramafic intrusions, west Pilbara Block, Western Australia: Australian Geological Survey Organisation, Bulletin 242, 319p.
- HUSTON, D. L., SMITHIES, R. H., and SUN, S-S., 2000, Correlation of the Archaean Mallina – Whim Creek Basin: implications for base-metal potential of the central part of the Pilbara granite–greenstone terrane: Australian Journal of Earth Sciences, v. 47, p. 217–230.
- JAHNS, R. H., 1953, The genesis of pegmatites — 1. Occurrence and origin of giant crystals: American Mineralogist, v. 38, p. 563–598.
- JONES, F. H., 1938, The Warrawoona area, Pilbara goldfield: Aerial, Geological and Geophysical Survey of Northern Australia, Western Australia, Report 20, 20p.
- KINNY, P. D., 2000, U–Pb dating of rare-metal (Sn–Ta–Li) mineralized pegmatites in Western Australia by SIMS analysis of tin and tantalum-bearing ore minerals, in *Beyond 2000, new frontiers in isotope geoscience*: University of Melbourne, Abstracts and proceedings, p. 113–116.
- KLOPPENBURG, A., WHITE, S. H., and ZEGERS, T. E., in press, Structural evolution of the Warrawoona Greenstone Belt and adjoining granitoid complexes, Pilbara Craton, Australia: implications for Archaean tectonic processes, *Precambrian Research*.
- KOJAN, C. J., and HICKMAN, A. H., 2000, Pindiri Hills, W.A. Sheet 2255: Western Australia Geological Survey, 1:100 000 Geological Series.
- KUNASZ, I. A., 1982, Foote Mineral Company — Kings Mountain Operation, in *Granitic pegmatites in science and industry* edited by P. CERNY: Mineralogical Association of Canada, Short Course Series, v. 8, p. 505–511.
- LIN, S., and WILLIAMS, P. F., 1992, The geometrical relationship between the stretching lineation and the movement direction of shear zones: *Journal of Structural Geology*, v. 14, p. 491–497.
- LONDON, D., 1990, Internal differentiation of rare-element pegmatites: a synthesis of recent research: Geological Society of America, Special Paper 246, p. 35–50.
- LONDON, D., 1996, Granitic pegmatites: *Transactions of the Royal Society of Edinburgh Earth Sciences*, v. 87, p. 305–319.
- MARSHALL, A. E., 2000, Low temperature – low pressure (‘epithermal’) siliceous vein deposits of the North Pilbara granite–greenstone terrane, Western Australia: Australian Geological Survey Organisation, Record 2000/1, 40p.
- MARSTON, R. J., 1979, Copper mineralization in Western Australia: Western Australia Geological Survey, Mineral Resources Bulletin, v. 13, 203p.
- MARSTON, R. J., 1984, Nickel mineralization in Western Australia: Western Australia Geological Survey, Mineral Resources Bulletin, v. 14, 271p.
- McKEESICK, M., 1996, Lennons Find (Mining Lease 45/368), annual report for the period 19 May 1995 to 18 May 1996; Gascoyne Gold Mines NL: Western Australia Geological Survey, Statutory mineral exploration report, (confidential).
- MILES, K. R., CARROLL, D., and ROWLEDGE, H. P., 1945, Tantalum and niobium: Western Australia Geological Survey, Mineral Resources Bulletin 3, 150p.
- MILLER, L. J., and GAIR, H. S., 1975, Mons Cupri copper–lead–zinc–silver deposit: Australasian Institute of Mining and Metallurgy, Monograph 5, p. 195–202.
- MORANT, P., 1995, The Panorama Zn–Cu VMS deposits, Western Australia: Australian Institute of Geoscientists, v. 16, p. 75–84.
- MORANT, P., 1998, Panorama Zn–Cu deposits: Australasian Institute of Mining and Metallurgy, Monograph 22, p. 287–292.
- NELSON, D. R., 1997, Compilation of SHRIMP U–Pb zircon geochronology data, 1996: Western Australia Geological Survey, Record 1997/2, 189p.
- NELSON, D. R., 1998, Compilation of SHRIMP U–Pb zircon geochronology data, 1997: Western Australia Geological Survey, Record 1998/2, 242p.
- NELSON, D. R., 1999, Compilation of SHRIMP U–Pb zircon geochronology data, 1998: Western Australia Geological Survey, Record 1999/2, 222p.
- NELSON, D. R., 2000, Compilation of SHRIMP U–Pb zircon geochronology data, 1999: Western Australia Geological Survey, Record 2000/2, 251p.

- NELSON, D. R., TRENDALL, A. F., and ALTERMANN, W., 1999, Chronological correlations between the Pilbara and Kaapvaal cratons: *Precambrian Research*, v. 97, p. 165–189.
- NEUMAYR, P., RIDLEY, J. R., McNAUGHTON, N. J., KINNY, P. D., BARLEY, M. E., and GROVES, D. I., 1998, Timing of gold mineralization in the Mount York district, Pilgangoora greenstone belt, and implications for the tectonic and metamorphic evolution of an area linking the western and eastern Pilbara Craton: *Precambrian Research*, v. 88, p. 249–265.
- NICKEL, E. H., ROWLAND, J. F., and McADAM, R. C., 1963, Wodginite — A new tin–manganese tantalate from Wodgina, Australia, and Bernic Lake, Manitoba: *Canadian Mineralogist*, v. 7, p. 390–402.
- NORTON, J. J., 1983, Sequence of mineral assemblages in differentiated granitic pegmatites: *Economic Geology*, v. 78, p. 854–874.
- PETERS, W. S., and de ANGELIS, M., 1987, The Radio Hill Ni–Cu massive sulphide deposit: a geophysical case history: *Exploration Geophysics*, v. 18, p. 160–166.
- PIDGEON, R. T., 1984, Geochronological constraints on the early volcanic evolution of the Pilbara Block, Western Australia: *Australian Journal of Earth Sciences*, v. 31, p. 237–242.
- PIKE, G., and CAS, R. A. F., in press, Stratigraphic evolution of Archaean volcanic-rock dominated rift basins from the Whim Creek Belt, west Pilbara Craton, Western Australia: *Sedimentology*.
- PODMORE, D. C., 1990, Shay Gap – Sunrise Hill and Nimingarra iron ore deposits: *Australasian Institute of Mining and Metallurgy, Monograph 14*, p. 137–140.
- REGISTER OF AUSTRALIAN MINING, 1997–98: Perth, Western Australia, Resource Information Unit, 652p.
- REGISTER OF AUSTRALIAN MINING, 1999–2000: Perth, Western Australia, Resource Information Unit, 648p.
- REGISTER OF AUSTRALIAN MINING, 2001–02: Perth, Western Australia, Resource Information Unit, 688p.
- RICHARDS, J. R., 1986, Lead isotope signatures: further examination of comparisons between South Africa and Western Australia: *Transactions of the Geological Society of South Africa*, v. 89, p. 285–304.
- RICHARDS, J. R., and BLOCKLEY, J. G., 1984, The base of the Fortescue Group, Western Australia: further galena lead isotopic evidence of its age: *Australian Journal of Earth Sciences*, v. 31, p. 257–268.
- RICHARDS, J. R., FLETCHER, I. R., and BLOCKLEY, J. G., 1981, Pilbara galenas: precise isotopic assay of the oldest Australian leads; model ages and growth-curve implications: *Mineralium Deposita*, v. 16, p. 7–30.
- SHMAKIN, B. M., 1992, Pegmatite deposits of Australia, Asia, Africa and America: *Indian Bureau of Mines*, 207p.
- SIMPSON, E. S., 1909, Further occurrences of tantalum and niobium in Western Australia: *Australian Association for the Advancement of Science*, v. 12, p. 310–315.
- SIMPSON, E. S., 1928, Famous mineral localities: Wodgina, North West Australia: *American Mineralogist*, v. 13, p. 457–468.
- SIMPSON, E. S., 1952, *Minerals of Western Australia, Volume 3*: Perth, Western Australia, Government Printer, 714p.
- SJERP, N., 1983, Geological report, Lennons Find Prospect, Pilbara Goldfield, Western Australia: Sjerp and Associates report to Centenary International Pty Ltd (unpublished).
- SMITH, J. B., BARLEY, M. E., GROVES, D. I., KRAPEZ, B., McNAUGHTON, N. J., BICKLE, M. J., and CHAPMAN, H. J., 1998, The Sholl Shear Zone, West Pilbara: evidence for a domain boundary structure from integrated tectonic analyses, SHRIMP U–Pb dating and isotopic and geochemical data of granitoids: *Precambrian Research*, v. 88, p. 143–171.
- SMITHIES, R. H., 1997, Geology of the Sherlock 1:100 000 sheet: Western Australia Geological Survey, 1:100 000 Geological Series Explanatory Notes, 29p.
- SMITHIES, R. H., 1998, Geology of the Mount Wohler 1:100 000 sheet: Western Australia Geological Survey, 1:100 000 Geological Series Explanatory Notes, 19p.
- SMITHIES, R. H., 1999, Geology of the Yule 1:100 000 sheet: Western Australia Geological Survey, 1:100 000 Geological Series Explanatory Notes, 15p.
- SMITHIES, R. H., HICKMAN, A. H., and NELSON, D. R., 1999, New constraints on the evolution of the Mallina Basin, and their bearing on relationships between the contrasting eastern and western granite–greenstone terranes of the Archaean Pilbara Craton, Western Australia: *Precambrian Research*, v. 94, p. 11–28.
- SMITHIES, R. H., NELSON, D. R., and PIKE, G., 2001, Development of the Archaean Mallina Basin, Pilbara Craton, northwestern Australia; a study of detrital and inherited zircon ages: *Sedimentary Geology*, v. 141–142, p. 79–94.
- STARKEY, L., 1994, Geophysical signature of the Balla Balla titaniferous magnetite deposit, Western Australia: University of Western Australia, Geology Department and Extension Service, Publication no. 26, p. 385–389.
- SUN, S.-S., and HICKMAN, A. H., 1999, Geochemical characteristics of c. 3.0 Ga Cleaverville greenstones and later mafic dykes West Pilbara: implication for Archaean crustal accretion: *Australian Geological Survey Organisation, Research Newsletter*, v. 31, p. 25–29.
- SWEETAPPLE, M. T., 2000, Characteristics of Sn–Ta–Be–Li-industrial mineral deposits of the Archaean Pilbara Craton, Western Australia: *Australian Geological Survey Organisation, Record 2000/44*, 56p.

- SWEETAPPLE, M. T., and COLLINS, P. L. F., 1998, Tantalum–tin mineralized pegmatites at Wodgina and Mount Cassiterite, Pilbara Craton, Western Australia: Geological Society of Australia, 14th Australian Geological Convention, Townsville, Queensland, 1998, Abstracts no. 43, p. 435.
- SWEETAPPLE, M. T., HICKEY, R. J., and COLLINS, P. L. F., 2000a, Controls on regional distribution of rare metal pegmatites in the Archaean Pilbara Craton, Western Australia, *in* Searching for a sustainable future *edited by* C. G. SKILBECK and T. C. T. HUBBLE: Geological Society of Australia, 15th Australian Geological Convention, Sydney, N.S.W., 2000, Abstracts no. 59, p. 425.
- SWEETAPPLE, M. T., LUMPKIN, G. R., and COLLINS, P. L. F., 2000b, Characteristics of tantalum–niobium–tin oxide minerals from the Wodgina and Mount Cassiterite pegmatites, Pilbara Craton, Western Australia, *in* Searching for a sustainable future *edited by* C. G. SKILBECK and T. C. T. HUBBLE: Geological Society of Australia, 15th Australian Geological Convention, Sydney, N.S.W., 2000, Abstracts no. 59, p. 426.
- TELFORD, R. J., 1939, The Mallina and Peawah mining centres, Pilbara goldfield: Aerial, Geological and Geophysical Survey of Northern Australia, Report 48, 4p.
- THORPE, R. A., HICKMAN, A. H., DAVIS, D. W., MORTENSON, J. K., and TRENDALL, A. F., 1992a, U–Pb zircon geochronology of Archaean felsic units in the Marble Bar region, Pilbara Craton, Western Australia: Precambrian Research, v. 56, p. 169–189.
- THORPE, R. A., HICKMAN, A. H., DAVIS, D. W., MORTENSON, J. K., and TRENDALL, A. F., 1992b, Constraints to models for Archean lead evolution from precise zircon U–Pb geochronology for the Marble Bar Region, Pilbara Craton, Western Australia: University of Western Australia, Geology Department and University Extension, Publication no. 22, p. 395–407.
- TICKOFF, B., and GOODWIN, L., 2000, Competency contrast, kinematics, and development of foliations and lineations, *in* Searching for a sustainable future *edited by* C. G. SKILBECK and T. C. T. HUBBLE: Geological Society of Australia, 15th Australian Geological Convention, Sydney, N.S.W., 2000, Abstracts no. 59, 497.
- VAN KRANENDONK, M. J., 1998, Litho-tectonic and structural components of the North Shaw 1:100 000 sheet, Archaean Pilbara Craton: Western Australia Geological Survey, Annual Review 1997–98, p. 63–70.
- VAN KRANENDONK, M. J., 2000, Geology of the North Shaw 1:100 000 sheet, Western Australia Geological Survey, 1:100 000 Geological Series Explanatory Notes, 86p.
- VAN KRANENDONK, M. J., and MORANT, P., 1998, Revised Archaean stratigraphic nomenclature of the North Shaw 1:100 000 sheet, Pilbara Craton: Western Australia Geological Survey, Annual Review 1997–98, p. 55–62.
- VEARNCOMBE, S. E., 1995a, Volcanogenic massive sulphide-sulphate mineralization at Strelley, Pilbara Craton, Western Australia: University of Western Australia, PhD thesis (unpublished).
- VEARNCOMBE, J. R., 1995b, Structure of the Klondyke Queen gold prospect, Pilbara Craton: CRA Report, October 1995 (unpublished).
- VEARNCOMBE, S. E., BARLEY, M. E., GROVES, D. I., McNAUGHTON, N. J., MIKUCKI, E. J., and VEARNCOMBE, J. R., 1995, 3.26 Ga black smoker type mineralization in the Strelley Belt, Pilbara Craton, Western Australia: Geological Society of London, Journal, v. 152, p. 587–590.
- WELLMAN, P., 1999, Gamma-ray spectrometric data: modelling to map primary lithology: Exploration Geophysics, v. 30, p. 167–172.
- WILLIAMS, I. R., 1999, Geology of the Muccan 1:100 000 sheet: Western Australia Geological Survey, 1:100 000 Geological Series Explanatory Notes, 39p.
- WILLIAMS, I. S., and COLLINS, W. J., 1990, Granite–Greenstone terranes in the Pilbara Block, Australia, as coeval volcano-plutonic complexes; evidence from U–Pb zircon dating of the Mount Edgar batholith: Earth and Planetary Science Letters, v. 97, p. 41–53.
- WITT, W. K., HICKMAN, A. H., TOWNSEND, D., and PRESTON, W. A., 1998, Mineral potential of the Archaean Pilbara and Yilgarn Cratons, Western Australia: Australian Geological Survey Organisation, Journal of Australian Geology and Geophysics, v. 17, p. 201–222.
- WOODALL, R., 1990, Gold in Australia: Australasian Institute of Mining and Metallurgy, v. 16, p. 45–68.
- ZEGERS, T. E., 1996, Structural, kinematic and metallogenic evolution of selected domains of the Pilbara granitoid–greenstone terrain: implications for mid-Archaean tectonic regimes: Geologica Ultraiectina, v. 146, 208p.

Appendix

Rare-metal minerals in pegmatites of the Wodgina district

<i>Mineral name</i>	<i>Composition</i>
Calciotantite	$\text{CaTa}_4\text{O}_{11}$
Columbite-group minerals	$(\text{Fe,Mn})(\text{Ta,Nb})_2\text{O}_6$ (columbite–tantalite mineral group)
Ferrowodginitite	$\text{Fe}_4\text{Sn}_4\text{Ta}_8\text{O}_{32}$
Fersmite	CaNb_2O_6
Holmquistite	$\text{Li}_2(\text{Mg,Fe})_3\text{Al}_2\text{Si}_8\text{O}_{22}(\text{OH})_2$ (Li amphibole)
Ixiolite	$(\text{Ta,Nb,Sn,Fe,Mn,Ti})_4\text{O}_8$
Lithiophilite	LiMnPO_4
Manganocolumbite	MnNb_2O_6
Manganotantalite	MnTa_2O_6
Microlite	$(\text{Na,Ca})_{2-m}(\text{Ta}>2\text{Ti+Nb})_2\text{O}_6(\text{F,OH,O})_{1-n}\cdot p\text{H}_2\text{O}$ (pyrochlore-group mineral, where $m = 0-2$, $n = 0-1$, and $p = 0-?$)
Microlite, defect	$(\text{X,Na,Ca})_{2-m}(\text{Ta}>2\text{Ti+Nb})_2\text{O}_6(\text{F,OH,O})_{1-n}\cdot p\text{H}_2\text{O}$ $\text{X} = \text{site vacancy}$, where X is typically $>20\%$ of A-site; (pyrochlore-group mineral, where $m = 0-2$, $n = 0-1$, and $p = 0-?$)
Microlite, stanniferous	$(\text{Sn,Na,Ca})_{2-m}(\text{Ta}>2\text{Ti+Nb})_2\text{O}_6(\text{F,OH,O})_{1-n}\cdot p\text{H}_2\text{O}$ ($\text{Sn} > 20\%$ of A-site; pyrochlore-group mineral, where $m = 0-2$, $n = 0-1$, and $p = 0-?$)
Rynersonite	CaTa_2O_6
Simpsonite	$\text{Al}_4\text{Ta}_3\text{O}_{13}(\text{OH})$ (hexagonal)
Tapiolite	$(\text{Fe,Mn})\text{Ta}_2\text{O}_6$ (tetragonal)
Thorite	ThSiO_4
Thorogummite	$\text{Th}(\text{SiO}_4)_{1-x}(\text{OH})_{4x}$
Wodginitite	$\text{Mn}_4\text{Sn}_4\text{Ta}_8\text{O}_{32}$

41AS EXCURSION GUIDE

Further details of geological publications and maps produced by the Geological Survey of Western Australia can be obtained by contacting:

**Information Centre
Department of Mineral and Petroleum Resources
100 Plain Street
East Perth WA 6004
Phone: (08) 9222 3459 Fax: (08) 9222 3444
www.dme.wa.gov.au**